Tampere University

Maria Clara Lessa Belone

THERMOGRAVIMETRIC ANALYSIS OF RESIZED GLASS AND CARBON FIBERS

Faculty of Engineering and Natural Sciences
Master of Science
August 2019

ABSTRACT

Maria Clara Lessa Belone: Thermogravimetric analysis of resized glass and carbon fibers
Master of Science
Tampere University
Master's degree programme in Materials Engineering
August 2019

The demand in growth for composite products over the years has as a consequence increased the volume of composite waste, requiring adequate waste management beyond incineration or landfilling practices. Current composite recycling methods cause an unwanted decrease in the mechanical performance of the recovered fibers due to the deterioration in their capacity to effectively interact with the polymeric matrix. Resizing the recycled glass and carbon fibers is a strategy to enable the rescue of their properties and, thus, the reuse of them on a new composite.

This work focuses on the characterization of recycled and resized glass fiber and carbon fiber by Fourier transform infrared analysis (FTIR) and mainly by thermogravimetric analysis (TGA). Fibers were resized with solutions containing different concentrations of coupling agent and film former, in which the coupling agent was added only in the resizing formulation of the recycled glass fibers. Moreover, a study about the extraction of the resizing layer on the fiber's surface by solvent and by burning is performed. The aim of this work is to determine the amount and composition of sizing on the fibers after the resizing process as well as the accuracy of TGA in the sizing characterization. The understanding of the resized fiber's surface is important to the development of a suitable resizing method that could contribute to add value to the recycled and resized fibers and make them attractive to the market.

As a result, the characterization methods have detected the presence of the sizing layer on the fiber's surface in all studied samples. Furthermore, the amount and composition of this layer was determined. The extraction process revealed that the resizing layer had both physisorbed and chemisorbed portion either for recycled glass fibers or recycled carbon fiber. On the TGA technique, the analysis was not greatly affected by varying the heating rate from 10 K/min to 5 K/min, but great change occurred when furnace's atmosphere was changed from nitrogen to air. In addition, TG analysis presented inaccuracies due to the small amount of sizing on the surface comparing to the mass of the fibers that was inserted on the crucible. Then, the use of other characterization methods were important to have better comprehension about the samples.

Keywords: Composite recycling, fiber resizing, thermogravimetric analysis

PREFACE

This thesis was made as a completion of the Master of Science in Materials Science and Engineering. It was conducted in the Plastics and Elastomer Technology research group at the Faculty of Engineering and Natural Sciences, Tampere University, Hervanta campus. The work was done partly in the Horizon 2020 European project “FiberEUse, Large scale demonstration of new circular economy value-chains based on the reuse of end-of-life fiber reinforced composites” (call H2020-CIRC-2016 Two Stage, Project Number 730323), which is acknowledged for the financial support.

Many people have supported me, directly or indirectly, throughout this work. First, I would like to especially thank my thesis instructors Assistant Professor Essi Sarlin and Project Researcher Vsevolod Matrenichev for their time, guidance and advices, they were valuable to achieve this end result.

I would like to thank my co-workers from the Plastics and Elastomer Technology research group for the availability to help and share their knowledge when needed. I sincerely thank Alexandra Shakun for what she taught me on the thermal lab, it made me develop as a researcher. I also thank my White House friends for the memorable moments of joy during this process.

Finally, I express my gratitude for Tomas Lantiainen for his love, support and for being a great partner and for my parents and sisters, that even being far in another continent are my rock and always believed in my potential.

Tampere, 19 August 2019

Maria Clara Lessa Belone

CONTENTS

LIST OF SYMBOLS AND ABBREVIATIONS

APTS	(3-aminopropyl)triethoxysilane
ATR	Attenuated total reflection
CA	Coupling agent
CF	Carbon fiber
CFRP	Carbon fiber reinforced polymer
EuCIA	European Composite Industry Association
IFSS	Interfacial shear strength
IPN	Interpenetrating network
FF	Film former
FTIR	Fourier-transform infrared
GF	Glass fiber
GFRP	Glass fiber reinforced polymer
HCl	Hydrochloric acid
HF	Hydrogen fluoride
HT	Heat treatment
KOH	Potassium hydroxide
LiOH	Lithium hydroxide
MA	Maleic anhydride
MAPP	Maleic anhydride grafted polypropylene
MPS	γ-methacryloxypropyltrimethoxysilane
NaOH	Sodium hydroxide
PBT	Poly(butylene terephthalate)
PTMS	Hydrolyzed propyl trimethoxysilane
PP	Polypropylene
rCF	Recycled carbon fiber
rGF	Recycled glass fiber
SRV	Surface to volume ration
TGA	Thermogravimetric analysis

1. INTRODUCTION

Composites reinforced with glass and carbon fibers are being extensively applied in some industrial sectors, ranging from automotive, aerospace, wind energy, construction and infrastructure to sports and daily life goods. According to European Composite Industry Association (EuCIA), during the past years, the tendency on the usage of composites is successively growing (Sauer & Kühnel 2017; Witten 2017). Figure 1 shows the European production volume of glass fiber reinforced plastics (GFRP) from 2010 to 2018. From 2012 onwards, there is a steady growth in the production volume of it. Figure 2 presents the demand of carbon fibre by region from 2014 to 2025 based on acquired data and estimations. Considering the region of the graph that corresponds to Europe, it is possible to verify that the increase in the volume of demand is also factual for carbon fiber reinforced plastics (CFRP). The reasons behind the increase of GFRP and CFRP consumption are explained by the positive features they offer to the product. These include increased life service combined with low maintenance, corrosion resistance, decreased weight leading to lower energy consumption and lower emissions, freedom of designs and improved mechanical performance (Leroy 2017).

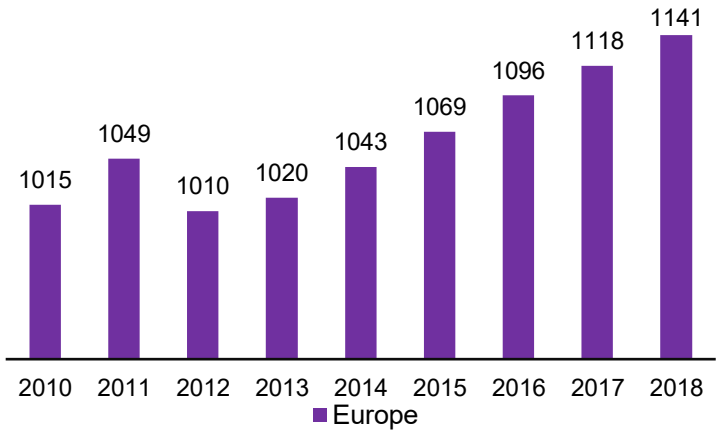

Figure 1. *Production volume of GFRP in Europe in thousand metric tons. (Witten 2017)*

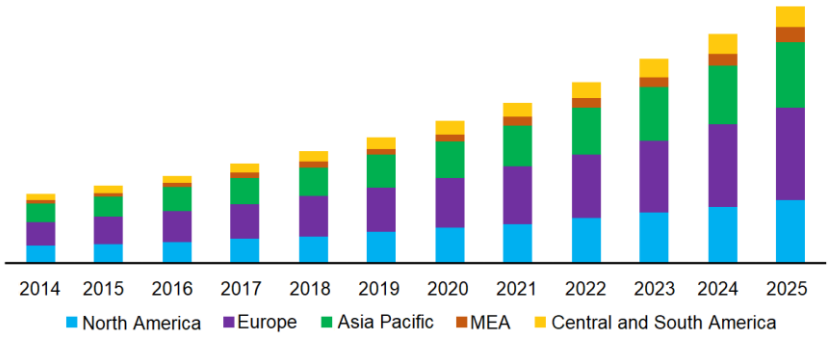

Figure 2. *Global market volume of carbon fiber in tons. (Gran View Research 2017)*

What comes together with higher production is the rise in the amount of composites at the end of their life stage, requiring the development of recycling and reusing strategies in the next few years. Aerospace sector exemplifies the need for proper waste management of composites: older airplanes with 30 to 50% of composites on their structure are being replaced by a generation of more efficient ones.

Currently, the challenges in composite recycling are adding value to the recovered fibers and reusing them in the manufacture of new products (Leroy 2017). Still consumers and industry have a negative perception with regard to products from composite recycling. The main issue being the loss in the recycled fiber's capacity to create an effective interface with a new matrix. It happens due to deterioration of their surface characteristics by the existing recycling methods, leading to a decline in their ability to withstand stress transfer from the matrix. Consequently, the mechanical properties of a probable composite would be compromised (Jenkins et al. 2019). Researches are focused on the rescue of fiber surface properties by fiber surface modification as post recycling treatment (Burn et al. 2016; Feng et al. 2013; Thomason et al. 2016; Wong et al. 2012).

1.1 Aim of the work

This work aims to characterize mainly by thermogravimetric analysis (TGA) the recycled glass and carbon fibers that went through surface treatment known as resizing. Its relevance has the potential to contribute to a field that still requires extensive research. A better understanding of the resized fiber's structure and its properties achieved by characterizing them is a key element to assess the success or failure of the treatment, to advance on its development, and, to tailor desired features on the material.

The work is focused on the following research questions:

a) How to determine the amount of sizing on the fibers that went through the resizing process?

b) What is the composition of the sizing on the fibers after the resizing process and does the sizing composition on the fibers correspond with the composition of the resizing solution?

c) What is the accuracy of thermal methods in sizing characterization?

1.2 Thesis structure

The first part of the work, comprising **chapters 2 to 4**, focuses on the literature review related to the topic. Besides discussing about current composite recycling methods, this work gives greater attention to the following topics: the glass and the carbon fiber sizing process to further understand the resizing process, the science behind interface formation between fiber reinforcement and polymeric matrix to evaluate the importance of fiber surface treatment and, the characterization methods of resized glass and carbon fibers which is the main focus of the work.

The second part of the work is divided into two chapters and is related to the experimental part. **Chapter 5** presents the methodology adopted to prepare and test the samples, while **chapter 6** presents the results of the experiments performed as well as the discussion of the findings based on the literature. The unsized and resized fibers, as well as the film former and coupling agent of the sizing formulation, were analysed with thermogravimetric analysis (TGA) and Fourier transform infrared transmission (FTIR). Furthermore, a study on the amount of physisorbed and chemisorberd sizing on the fiber was performed. Finally, **chapter 7**, the last part of the work, is dedicated to the conclusions and suggestions for the further work.

2. COMPOSITE WASTE MANAGEMENT

Currently, significant amount of composite waste still goes to landfill or incineration. However, legislation against these practices as well as their incapacity to deal with the increasing volume of discarded composites require other routes to treat the waste. According to the European Waste Framework Directive (2008/98/EC), the waste management hierarchy should follow the pyramid presented in figure 3. Recovery and disposal, which comprises, respectively, incineration and landfill, are the last approaches to be adopted in waste management (Job et al. 2016). Therefore, in many European Union countries, composite landfilling, for example, is becoming a banned practice (Leroy 2017).

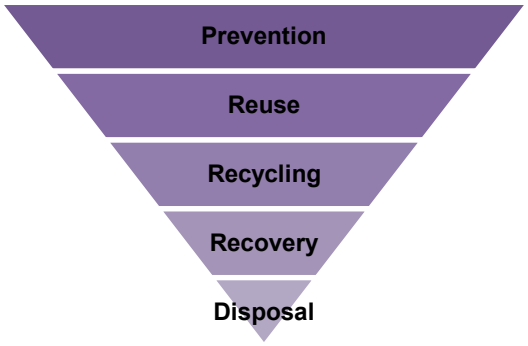

Figure 3. *Waste management hierarchy according to the European Waste Framework Directive (2008/98/EC). Adapted from* http://ec.europa.eu/environment/waste/framework/index.htm

2.1 Composite recycling

This work is done based on fibers obtained from composite recycling. Thus among the European Waste Framework Directive (2008/98/EC) approaches, attention will be given just for recycling.

The existing technologies applied to composite's waste recycling are based on mechanical, thermal and chemical methods. Mainly fibers are the recovered product but it is also possible to obtain components from resin decomposition. The assessment of the most suitable approach will be based on the type of fiber, efficiency, viability, reuse application of the recycled fibers and the environmental aspects, such as, energy consumption, type of chemicals and emissions (Oliveux et al. 2015).

2.1.1 Mechanical recycling

Mechanical recycling consists of grinding the composite waste into smaller pieces by crushing or shredding. Resultant products of grinding operation are resin rich powders as well as fibers of different sizes still embedded by resin. Recovered fibers, after being sorted, can lately be reincorporated as fillers or reinforcements in other materials and in compounds for injection and compression moulding, substituting partially virgin products (Oliveux et al. 2015).

2.1.2 Thermal recycling

Thermal recycling is done by pyrolysis and its variations, such as fluidised-bed pyrolysis and pyrolysis assisted with microwaves. It is probably the most viable route for recycling. Fibers are recovered by matrix degradation, which also produces oil, gasses and char. Because of deposition of char on the fibers surface, it is necessary to have a burning step for decontamination. Operation temperature of the processes varies according to the type of resin on the composite to be recycled, ranging from 450 °C to 700 °C (Oliveux et al. 2015). Lower temperatures are required for polyester resins and higher temperatures for epoxy resins, for example (Job et al. 2016).

2.1.3 Chemical recycling

Solvolysis is the process for chemical recycling of composites and the solvent is responsible for matrix degradation. It admits a wide number of possible systems, once different solvents, catalysts, temperature and pressure can be combined (Oliveux et al. 2015). Comparing to pyrolysis, it requires lower temperatures and results in cleaner fibers without char. More pure fibers contribute to a better capability to adhere to a new resin. On the other hand, reactors can be expensive and the disposal of chemical substances can be a potential source of environmental impacts (Job et al. 2016).

2.1.4 Suitability of the recycling methods

Mechanical grinding is the cheapest among the three methods presented. Moreover, it is more employed on GFRP composites once its production volume is larger and glass fiber (GF) has a lower price (Oliveux et al. 2015). However, the capacity to accommodate the increasing volume of GFRP is limited.

Thermo-chemical processes are not widely applied to GFRP, because virgin GF is still cheaper and more efficient as a composite reinforcement. Furthermore, there is a great loss in mechanical properties with those methods.

According to Oliveux et al. (2015), the tensile strength of GF recycled by fluidised-bed pyrolysis, for example, can be reduced by 50% and 80% at 450 °C and 550 °C, respectively. In the case of solvolysis, the same author presented that GF becomes fragile if exposed to the process conditions, since temperature and acidic and alkali mediums remove the size coating from the surface (Olivieux et al. 2015). However, recycled GF (rGF) can have its properties restored to some extent by post-treatment for their refunctionalisation, which enables extensive research to add value to rGF and make it competitive on the market (Job et al. 2016).

Recycling of CFRP is more suitable for thermo-chemical processes. Firstly, the high value of carbon fibers (CF) justifies the development of more sophisticated techniques instead of only grinding the composites containing them. Secondly, because of the lower deterioration of the resultant recycled CF (rCF). On pyrolysis, there is also a reduction in mechanical properties of rCF. Nevertheless, it is less prominent and in a more acceptable range than in rGF (Oliveux et al. 2015). On solvolysis, CF is not dissolved by the chemicals. Therefore, it is possible to release it from the resin and, depending on process conditions, mechanical properties of rCF is retained in a high degree (Job et al. 2016). According to ELG Carbon Fibre, a company that manufactures recycled carbon fibers products, CF recovery has significantly grown in recent years. A comparison between 2012 and 2015 revealed that it went from under 200 tonnes to nearly 1100 tonnes, respectively (Holmes 2018).

3. FIBER SIZING

Sizing is a kind of surface treatment consisted of coating the fiber's surface during its manufacturing in order to affect the processability and performance of composites. The surface is coated mainly by organic materials (Thomason 2015). Following the fiber's formation and surface treatment (in case of CF), sizing process consists of wetting the fibers with a layer of sizing emulsion or solution on a sizing bath (Moosburger-Will et al. 2018). Then the film is allowed to dry while secondary processes are applied on the fiber, such as winding or chopping (Thomason 2015).

On the composite structure, observed at different length scales as represented in figure 4, the sizing is located at the fiber/matrix interface, a nanoscale region ranging from 30 to 200 nm thickness (Zhang 2014; Petersen 2017). Estimations made by the Michelman, a water-based coating company, indicate that ''in a 1000 Kg composite made from a 30% glass-filled polymer, fiber sizing is typically less than 0.3 Kg''. Although composites contain only a slight amount of sizing, it has significant influence on the short and long term mechanical properties of composites and, therefore, on their performance (Bassetti 2017).

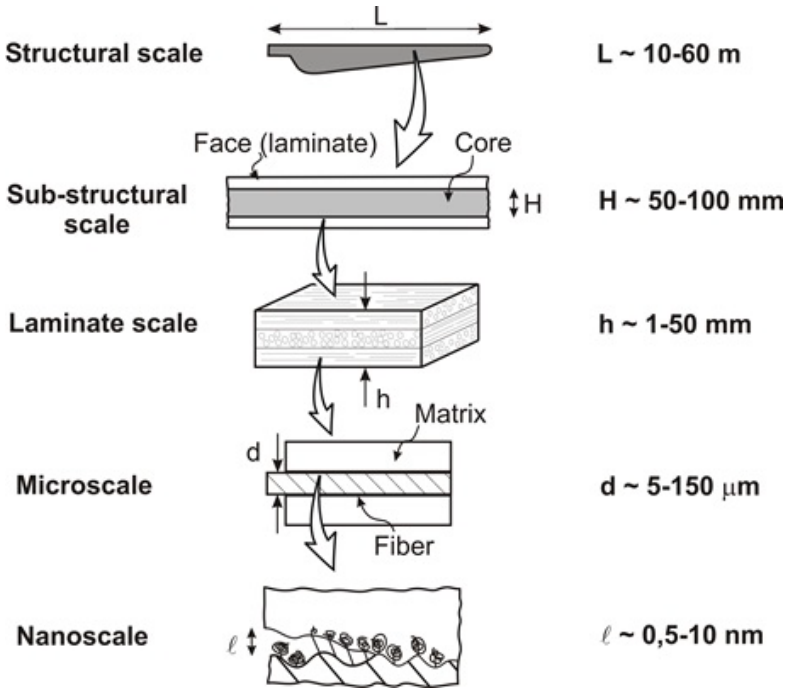

Figure 4. *Details of the composite structure that can be observed in different scale. The interface where the sizing is present is on the nanoscale range. (Petersen 2017).*

Sizing is able to affect the fiber's physical characteristics and composite properties, bringing manufacturing, processing and performance benefits (Bassetti 2017). In terms of fiber protection and fiber/matrix compatibilization, an appropriate size selection provides the advantages presented in table 1.

Table 1. *Effect of sizing on different steps of composite production, from fiber manufacturing to composite testing. Adapted from Thomason & Adzima 2001.*

Stage	**Benefits of sizing**
During manufacturing of the fiber	Protection during transportation and handling; No break in the continuous fiber; Clean chopping; Good package and winding; Lower fuzz.
During composite production	Fiber integrity with low fuzz; Good wetting of the fiber by the polymeric matrix; Low tension.
Considering the performance of the resulting composite	High interaction between fiber and matrix; Better level of stress transfer from the matrix to the fiber; High mechanical performance; Durability and better fatigue resistance; Lower void contents, due to better wet-out.

Due to the impact of sizing on composite's performance, sizing formulation is an area of interest in industry and research, being carefully engineered and optimized (Karger-Kocsis et al. 2015). In the process of choosing the most suitable size, the type of resin, the type of fiber as well as the composite's production method and application also have to be considered (Bassetti 2017).

Sizing formulation is complex, it can contain a high number of components and industries keep their full recipes in secret. Nevertheless, it is known that it contains at least film former and coupling agent in case of GF, and film former in case of CF.

3.1 Fiber/matrix interface

Fiber/matrix interface is the contact region where the chemical and physical interactions between chemical groups on the fiber surface and on the resin occur. It has singular physical and mechanical properties from those on fiber and matrix. It is also a region that chemically differs from the composition of those components. Though, because of interdiffusion, the further the distance from the fibre surface on the radial direction, gradually the more its composition is similar to the bulk matrix (Park & Seo 2011).

Zhang (2014) analysed epoxy/CF composites and obtained the transmission electron microscopy image of the interphase (interface and boundaries of matrix and fibre). In figure 5 it is noticeable the compositional gradient and the differences between the interface and the rest of the composite.

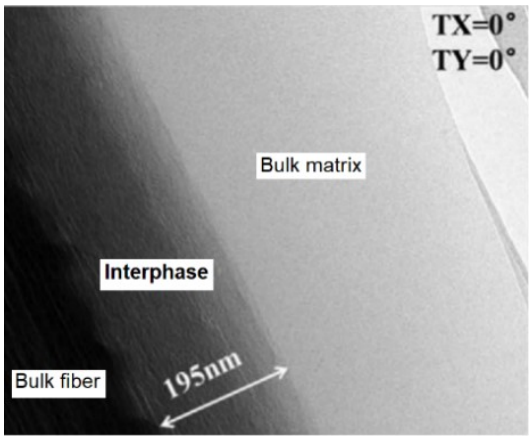

Figure 5. *Interphase region formed on an epoxy/CF composite. Adapted from Zhang (2014)*

The interface is a critical region in a composite. When a force is applied longitudinally on the structure of a unidirectional fibers composite, the deformation of fibers and matrix is different because of the mismatch of stiffness of these components. It then generates shear stresses (τ_s) at the interface (figure 6) and therefore, the interface should be strong enough to withstand the stress transfer that occurs from the matrix to the fiber (Petersen 2017). Efficient stress transfer in an interface with sufficient shear strength acts on preventing the fiber/matrix debonding and avoids premature failure of the composite (Park & Seo 2011).

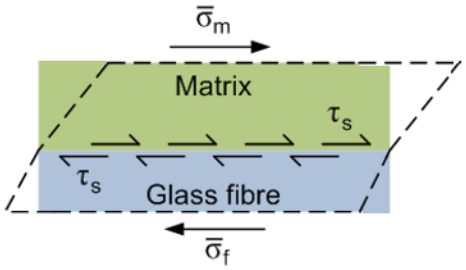

Figure 6. *Stress transfer from the matrix to the fiber due to difference in stiffness of composite components. (Petersen 2017).*

The interface is formed by chemical and physical events. Chemically, there is the establishment of bonds from the interaction between active functional groups on the fiber surface and compatible groups on the resin. The number of chemical bonds as well as their energy influence the stress transfer ability (Zhang 2014). Physically, adhesion mechanisms happen, in which molecular entanglement, interdiffusion, electrostatic attraction

and adsorption are some of the likely ones. Molecular entanglement involves the mechanical interlocking and anchoring of polymeric chains of the matrix and fiber surface. It is affected by the roughness of the latter and the chain's mobility. Interdiffusion mechanism occurs between elements on the not yet cured polymeric resin and components of the coating/sizing layer. Molecules of these phases diffuse across the interface. In electrostatic attraction, electrostatic forces created from the interaction of negative and positive charges lead to interfacial bonding. Charge density and surface treatments influence the intensity of it. Lastly, adsorption involves the formation of secondary forces, such as hydrogen and Van der Waals forces, when constituent atoms are close to each other in a distance of few atomic diameters. Adsorption is important for adequate wetting and full coverage of fibers by the resin (Kim & Mai 1998; Zhang 2014).

Therefore, the characteristics of the fiber surface represent an important role on the interface properties and how well the stress transfer will occur. Its chemical structure, chemical groups, morphology and medium compatibility influence the surface free energy and thus, wetting reactivity and the capability to make bonds with the matrix (Petersen 2017; Tang & Kardos 1997). It is known that a combination of strong fiber and tough matrix alone does not result in a good composite if those two components are not efficiently attached. When the sizing layer, which can be considered as a third component in composites structure, is (1) homogeneous, (2) able to bond chemically and physically to the functional groups of the fiber surface and (3) chemically compatible to the matrix, it will allow an effective interaction between fiber and matrix. Figure 7 visibly demonstrates the quality improvement of the fiber/matrix interface resulted from the selection of appropriate sizing treatment. (Downey & Drzal 2016; Moosburger-Will et al. 2018)

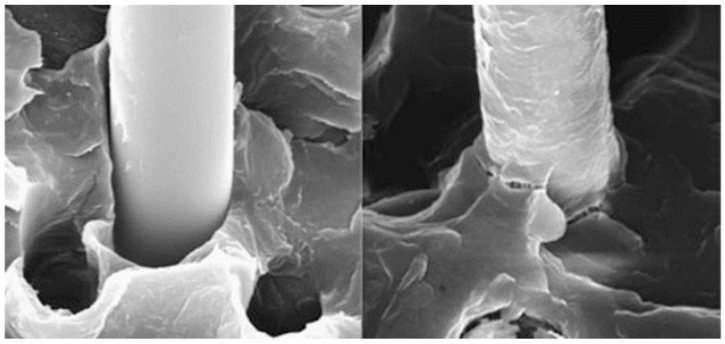

Figure 7. *Sized fiber and matrix interaction resulted by (a) poor coating and (b) good coating. (Peters 2018).*

3.2 Glass fiber sizing

In a simplified way, in glass fiber production, silica sand and other components are melted together at temperatures above 1000 °C until the liquid state. Subsequently, the melt is extruded through bushings and cooled down by a fine water mist, allowing the formation of small diameter strands. Right after the drawing step, fibers get in contact with rollers normally positioned 1 to 2 m below the bushings, as seen in figure 8. The rollers collect the aqueous sizing formulation, containing 3 to 10 wt% of solids, from a reservoir and apply it onto the fiber surface. Applied at this moment of the process, sizing performs its first function: protection against fracture and fiber to fiber damage (Petersen 2017; Thomason 2015). The effects of the initial steps of fiber's production have also an impact on the final properties of the composite.

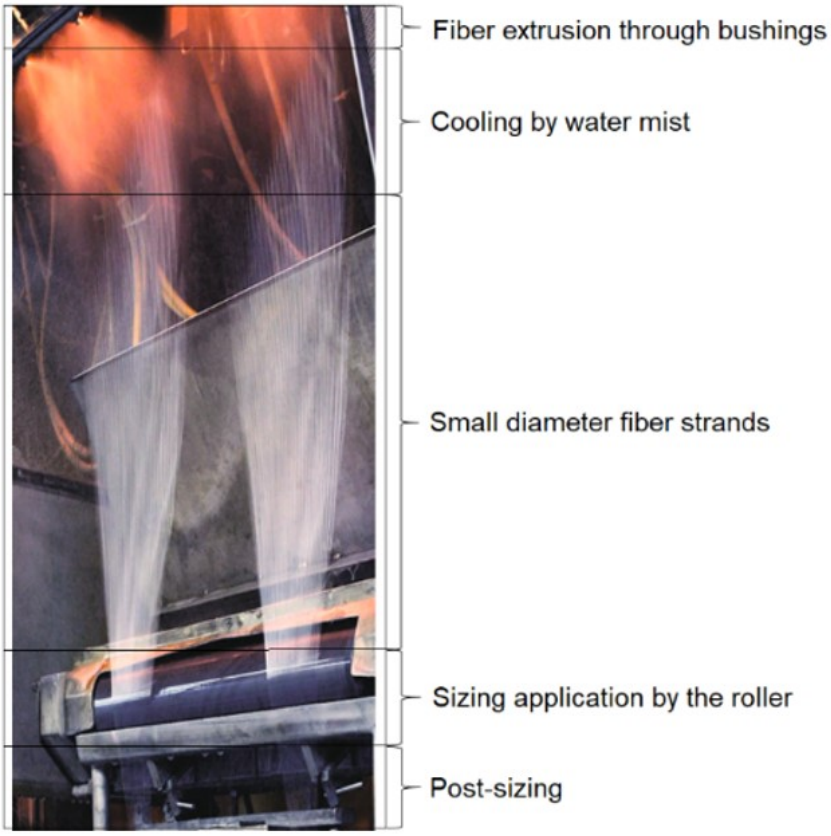

Figure 8. *Glass fibers in contact with the sizing rolls right after molten glass is extruded from the bushings. Adapted from Peters 2018*

Sizing application occurs in a very short time, thus, this moment of sizing/fiber contact has to be as optimum as possible. Better wetting of the fibers by the sizing will occur with lower sizing viscosities according to figure 9(a), which shows the relative number of wetted fibers in relation to sizing viscosity in centipoise. In addition, the medium in which the sizing needs to displace when it is on the fiber's surface affects the wetting as well.

The density of fibers that are in contact with the roller at the same time, should also not be excessive in order to allow the sizing pick up in every fiber surface area as shown in figure 9(b). Following the same idea, the more spread out is the fiber bundle on the roller longitudinal direction, the more efficient is the wetting. In figure 9(c), the curves show that better sizing pick up happens when the number of fibers in the bundle (N) are lower or the fiber's speed (V) is lower. However low N and V are not attractive in a commercial point of view as the efficiency of the process decreases (Thomason & Adzima 2001).

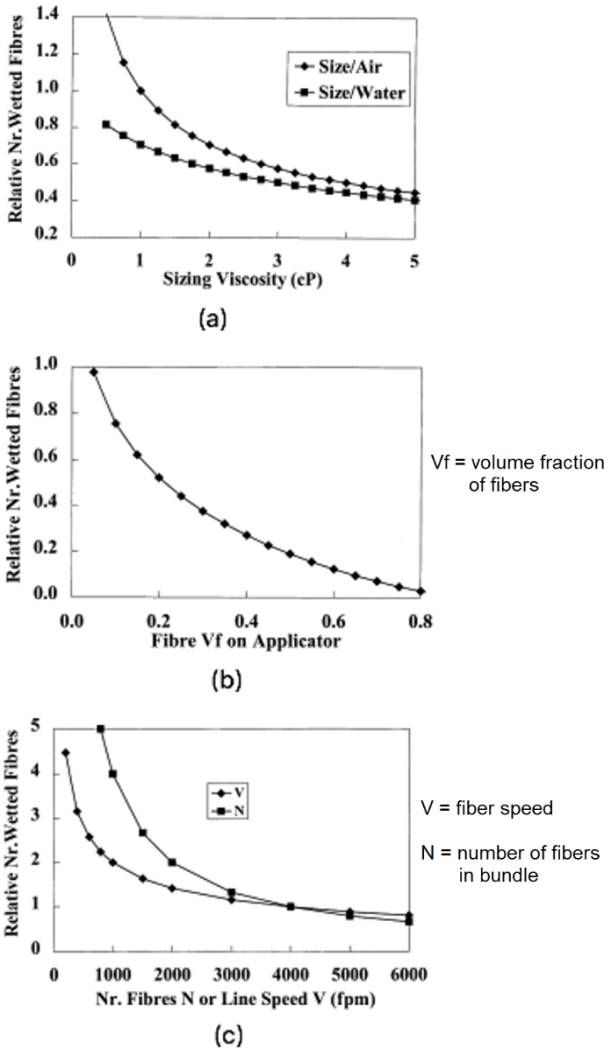

Figure 9. *Efficiency of fiber wetting by sizing in terms of (a) sizing viscosity, (b) fiber volume fraction on the roll and (c) number of fibers in the bundle or line speed. (Thomason & Adzima 2001)*

Water-based sizing coating, the most widely used in GF sizing, contains at least coupling agent, film former and lubricants as main components. Other additives, such as antistatic and anti-foaming can also be added to improve processability and efficiency. The film former promotes the interaction between sizing and matrix and it is selected in a way to be as compatible as possible with the polymeric matrix. Lubricants are responsible for

the filaments lubrication and protection on the process (Peters 2018). The coupling agent is often an organosilane compound. Chemical bonding is known as the main explanation for the use of bifunctional organosilane molecules as coupling agents. They act as a link to enable chemical reactivity between the inorganic reinforcement and the organic substrate (Kim & Mai 1998).

Figure 10 shows, schematically, the chain reaction of a coupling agent, represented as $X_3Si\text{-}R$. Group R reacts with the resin, resulting in the establishment of organofunctional group bonds with it. On the other hand, group X leads to silanol formation (figure 10(a)), that subsequently reacts with hydroxyl groups on the glass fiber surface, establishing siloxane bridges with it (figure 10(b)). It is known that group X must be able to hydrolyze for this process to happen. When the fibers are dried after sizing treatment, a polysiloxane layer is formed and bonded on the top of their surface. It occurs by the condensation between the silanol and M-OH groups on the surface, M can be Si, Fe or Al (figure 10(c)). When contact with the uncured resin occurs, R groups and functional groups in the resin react (figure 10(d)). It explains the necessity of compatibility between these. (Kim & Mai 1998)

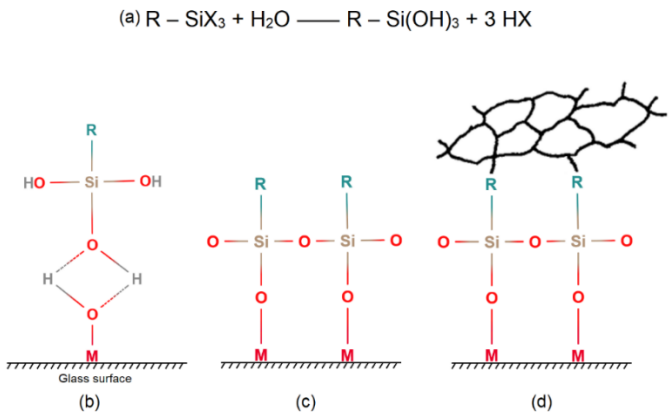

Figure 10. *Coupling agent mechanism of action to form interactions with both fiber and matrix. Adapted from Kim & Mai 1998.*

Interdiffusion is also a major mechanism of interface adhesion on GFRP, an interpenetrating network (IPN) is formed due to it. In figure 11, a scheme of the interface formed after the wetting of the fiber and curing of the matrix is represented. Sizing on the surface is divided in three layers (1) physisorbed region is the outermost layer and is formed mainly by the bulk deposited silane, (2) chemisorbed region consists mainly of higher oligomeric siloxanols and (3) chemically reacted region is the innermost layer with three-dimensional cross-linked siloxane network (Kim & Mai 1998). What results from the IPN formation is the penetration of the resin into the chemisorbed silane layers and the mi-

gration of physisorbed silane molecules into the matrix. Due to the fact that the polysiloxane network (created as discussed previously) is crosslinked but the film former is a linear polymer, the resultant structure formed on the out layer of GF is considered as a semi interpenetration network (semi IPN). A full IPN is formed from the semi IPN if after the curing of the thermoset resin a complete migration of the film former to the bulk resin occurs. The diffusion of the matrix in the semi IPN is dependent on the crosslink density of the polysiloxane network and on the compatibility of the resin with the film former of the sizing. (Karger-Kocsis et al 2015).

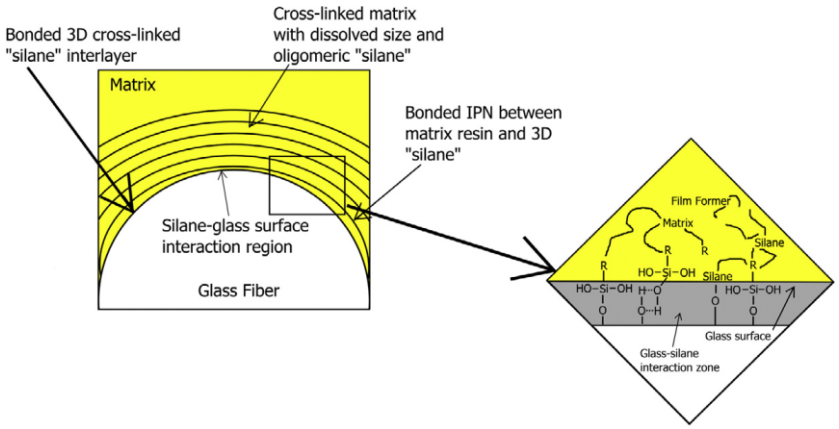

Figure 11. *The formation of the IPN based on the interaction between the sizing and the composite components. (Karger-Kocsis et al 2015)*

Among several similar investigations, a study made by Feresenbet et al. (2003) analyzed the improvement GF/epoxy matrix adhesion achieved by sizing the fiber surface with different sizing compositions. GF were sized in the laboratory with solutions containing (1) hydrolyzed propyl trimethoxysilane (PTMS), which does not bond with an epoxy matrix; (2) (3-aminopropyl)triethoxysilane (APTS), which bonds with an epoxy matrix; and (3) mixture of PTMS and APTS in different proportions to evaluate the effect of the degree of GF/matrix bonding on the interfacial shear strength (IFSS).

Results showed that on the layer with 100% PTMS sizing had no functional groups and it was very hydrophobic. It was determined that interactions between fiber and matrix were due mainly to mechanical interlocking. On the fragmentation test, there was no matrix cracking. It indicates that the debonding between matrix and fiber was a result of absorption of the energy of the fracture on the interface and so, it was a weak region of the composite (figure 12(a)). The coating with 100% APTS sizing, on the other hand, bonded with epoxy by covalent bonds during curing and it was less hydrophobic. In figure 12(b), the failure mode of this system is showed, being possible to notice that the matrix cracked perpendicularly to the fiber and some debonding was also observed.

In this case, stress transfer between matrix and fiber was more effective. By varying the proportion between APTS and PTMS, the level of adhesion changed, the increase of APTS concentration resulted in better interfacial bonding and improvement of IFSS, once the amount of reactive coupling agent and functional groups on the mixture raised (Feresenbet et al. 2003).

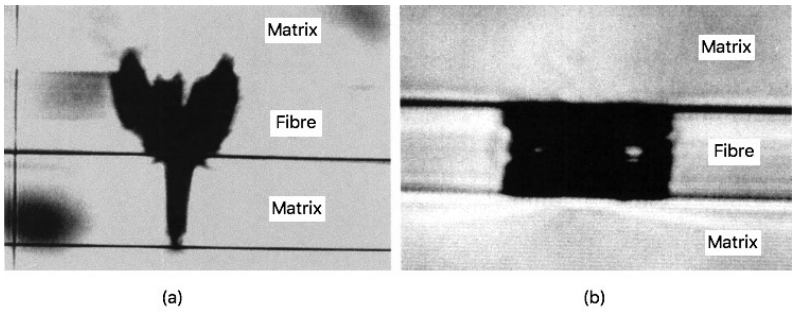

Figure 12. *Failure mode observed on the fragmentation test varying the sizing: (a) 100% PTMS sizing, which does not chemically interact with the matrix and (b) 100% APTS, which is able to make covalent bonds with the matrix. (Feresenbet et al. 2003)*

3.3 Carbon fiber sizing

Carbon fiber sizing consists of the application of a thin layer of some polymer, which is in the same chemical class with the matrix, together with emulsifiers and assistants. The aim is to protect and lubricate the brittle CF during handling (Dai et al. 2011; Park & Hey 2015). Furthermore, the appropriate sizing will bond with functional groups on fiber surface and functional groups of the matrix (Moosburger-Will et al. 2018).

For thermoset matrix, typically polyvinyl alcohol, vinyl acetate polymer, acrylic polymer, polyurethane, epoxy resin or polystyrene are used as sizing (Tang & Kardos 1997). The compatibility between matrix and sizing is desirable to allow their solubility and reactivity as well as the penetration of resin in the fiber bundle (Park & Hey 2015). Considering an epoxy matrix, for example, the use of fibers sized with polyamide and polyurethane would result in a composite with lower interfacial shear strength (IFSS) than the same composite prepared with unsized fibers. What can happen when sizing and matrix lack compatibility is more adsorption of the sizing's functional groups on top of the fiber surface instead of its dissolution through the matrix (Dai et al. 2011; Sharma et al. 2014).

Differently from GF sizing, which occurs right after the formation of the fiber, additional surface treatments are done prior to sizing pick up in the case of CF. Despite being a relevant reinforcing material, because of high specific strength and modulus, its surface has an inert character that limits adhesion with matrices. Thus, surface treatments re-

move weak layers, add functional groups and enable chemical bonding. Moreover, surface roughening resulted from some treatments are favorable for mechanical interlocking. As a consequence, wetting of CF and interface strength, for example, are improved (Zhang 2014). Another difference between GF and CF sizing application is how it is done, CF are immersed in a sizing solution or emulsion bath (Moosburger-Will et al. 2018). PAN-based and pitch-based process are the most important in CF production and in both methods surface treatments, sizing and winding are similar (Park & Hey 2015).

Dry and wet oxidation treatments are typically applied for surface modification and activation. Dry oxidation is carried out in a gaseous atmosphere as oxygen, ozone, carbon dioxide and air. However, it requires high temperatures to treat the extremely inert CF surfaces, once the gasses do not have enough oxidizing power at room temperature. It can cause negative effects in terms of damaging and deterioration of mechanical properties (Zhang 2014). Commercially, anodic oxidation, a type of liquid oxidation, is extensively used since it has lower cost, it is fast and efficient (Park & Hey 2015). It is done with liquid oxidizing agents and the CF is placed as anode in the electrolytic reaction. Oxygen containing functional groups are introduced on the fiber's surface, possible ones are presented in figure 13. The increased concentration of oxygen enhances the surface energy and reactivity with the sizing components, what impacts how well fibers are wetted and covered by sizing. The final result of oxidative treatment is influenced by oxidizing agent, oxidation temperature and process time (Zhang 2014).

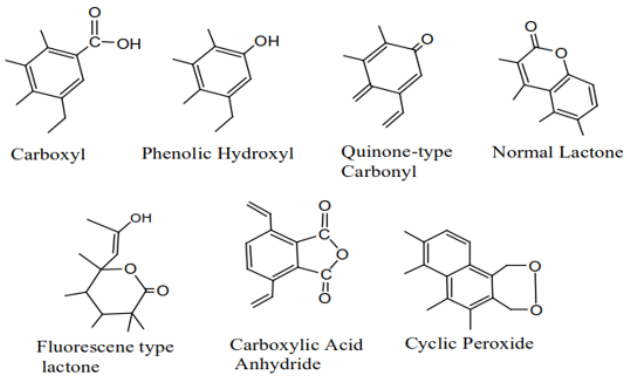

Figure 13. *Possible functional groups containing oxygen introduced on the CF surface after oxidation treatment. (Zhang 2014)*

The effect of fiber surface treatment combined with sizing coating on the enhancement of surface characteristics of CF and the performance of the correspondent composite is a subject explored in many studies. As an example, it was well investigated by Downey & Drzal (2016) on a study about CF/epoxy matrix composites toughening. The surface treatment applied was UV-ozone (UVO), a type of dry oxidation.

Four types of fibers were tested by single-fiber fragmentation test (mechanical test for interface characterization): as received unsized CF, UVO treated unsized CF, UVO treated and aromatic sizing CF and UVO treated and aliphatic sizing CF. In the fiber with neither surface treatment nor sizing, interfacial debonding occurred from the fiber break, characteristic behavior of low adhesion. In the fibers with only UVO-treated and UVO treated combined with aromatic sizing, cracking propagated into the matrix, because the fiber/matrix load transfer was more efficient. The matrix crack on UVO treated combined with aliphatic sizing fibers was a bit more intense, indication once again of an improvement on adhesion when sizing treatment is also added. Fiber with aliphatic sizing presented shear failure at 45° from the interphase, larger matrix cracking and debonding emanating from the tips of fiber fracture. A stronger fiber/matrix adhesion was achieved, with the failure located in the matrix and not at the interface. Figure 14 shows the birefringence patters of each test. (Downey & Drzal 2016)

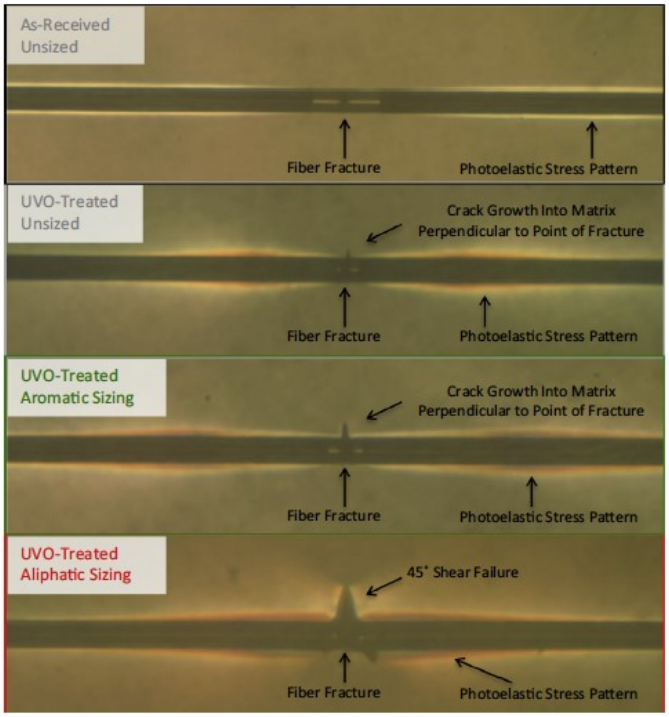

Figure 14. *Birefringence patterns from fragmentation test of different CF. (Downey & Drzal 2016)*

3.4 Sizing of recycled glass and carbon fibers

As discussed in chapter 2, the current recycling methods for composites deteriorate rGF and rCF properties in a certain degree. Especially for rGF, performance reduction is severe and, in some cases, they are unsuitable for reuse as an effective reinforcement. Considering thermal recycling, the method this work focuses, the main reasons behind it are: the degradation of the sizing layer on the fiber surface (Kao & Thomason 2014;

Yang et al. 2015), the damaging of fibers, such as pitting and fractures (Jenkins et al. 2019; Pimenta 2013), and the deposition of contaminants on the fiber surface (Oliveux et al. 2015; Pimenta 2013).

Sizing application on rGF and rCF what is considered a resizing process, has been developed as a strategy to regenerate/improve mechanic and adhesive properties of the fibers. As industrial sizing recipes are kept in secret, the resizing's challenge is to achieve the appropriate/optimum composition and concentration of the components. Thus, in recent years, effort is put on research to develop surface reactivation methods, what can be a significant alternative to add value for the second-life reinforcements (Yang et al. 2015).

Sáez-Rodríguez et al. (2013) proposed a method that first applied hydrochloric acid solution (HCl) and then resized the fibers using two different silanes, APTS and γ-methacryloxypropyltrimethoxysilane (MPS). The rGF samples were obtained from the simulation of the thermal recycling. According to the authors, HCl treatment enables an increase the concentration of hydroxyl groups on the rGF surface. Afterwards, rGF were immersed on silane solutions and allowed to dry. Five different combinations, besides virgin GF and only heat treated (HT) rGF, were tested: HT and HCl treatment, HT and APTS silanisation, HT and MPS silanisation, HT and HCl treatment with APTS silanisation and HT and HCl treatment with MPS silanisation. Results were not satisfactory, in the single fiber tensile testing, all trials gave much lower average strength comparing to virgin fiber. Moreover no significant improvement of properties was achieved comparing to only HT fibers. From the study, however, authors concluded that using only silane treatment cannot recover the strength of rGF. (Sáez-Rodríguez et al. 2013)

Yang et al. (2015) demonstrated that the reinforcement potential of rGF can be significantly improved by a post-treatment that combines chemical etching with hydrogen fluoride (HF) followed by silanisation with APTS. As expected, HT caused pronounced drop on IFSS and tensile strength compared to virgin material, resulted fibers were brittle and difficult to handle without breakage. It shows that recycling not only affects performance but also makes processing on standard composite equipment not possible (Thomason et al. 2016). HF was effective to remove degraded surface layer and regenerate strength of fibers that went through a simulated thermal recycling. As seen in figure 15, resultant strength almost tripled within three minutes of treatment and resizing promoted significant recovery of IFSS. (Yang et al. 2015)

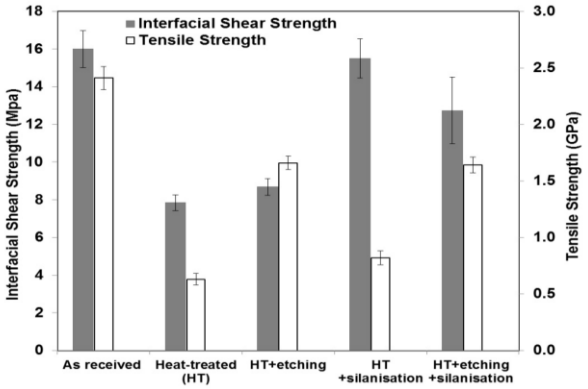

Figure 15. *Effects of HF etching, silanisation and etching combined with silanisation on interfacial shear strength and tensile strength of GF. (Yang et al. 2015)*

Thomason et al. (2016) also proposed a combination of chemical etching, for strength recovery, and resizing, for rGF surface functionalisation. In this study, however, acid solutions were replaced by hot sodium hydroxide (NaOH) alkali solution, HF was considered more aggressive chemical route. Resilanisation solution was APTS and fibers went through a simulated thermal recycling as well. Similarly to previous study, strength was restored at a significant level after NaOH and APTS treatments as seen in figure 16. Comparison with Yang et al. (2015) method was done showing that their method offered even better results. (Thomason et al. 2016)

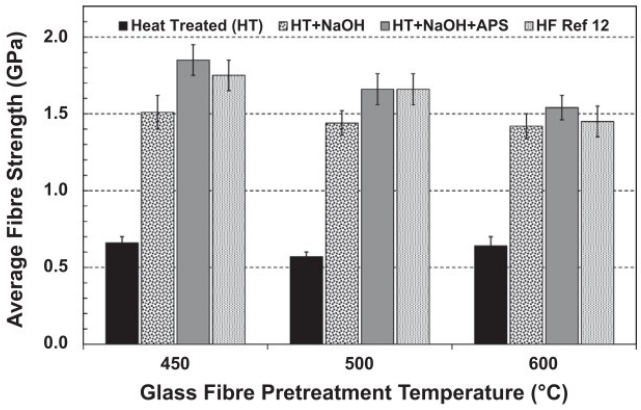

Figure 16. *Changes on the average fiber strength caused by three types of treatment on the GF: NaOH etching, APS silanisation and etching combined with silanisation. Yang et al. (2015) result is referred as 'HF Ref 12' on the graph legend. (Thomason et al. 2016)*

Following the idea to regenerate rGF by alkaline treatment, Bashir et al. (2017) explored different alkaline solutions: sodium hydroxide (NaOH), potassium hydroxide (KOH) and lithium hydroxide (LiOH), at different molarities. Figure 17 shows the results for 10 minutes treatment. Greater increase in fiber tensile strength was achieved with 1.5 M of NaOH. From 2 M onwards, immersion in KOH resulted in strength enhancement, how-

ever similar values were obtained with lower NaOH molarities. LiOH showed a little impact on properties improvement. Based on the results, NaOH was assumed the most effective alkaline solution to improve fiber strength. (Bashir et al. 2017)

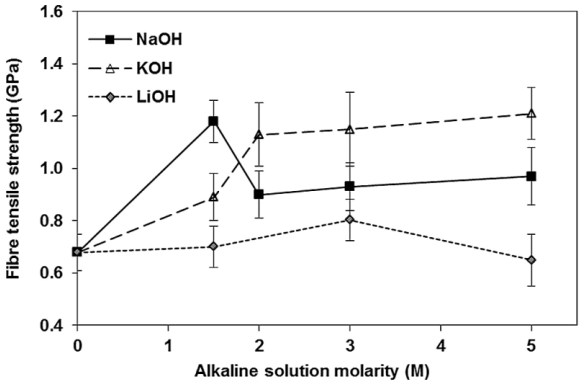

Figure 17. *How different alkaline solutions used for chemical etching affected the GF tensile strength. (Bashir et al. 2017)*

In another part of Bashir et al. (2017) study, treatment time was also changed for NaOH and KOH solutions to analyse its effects on results. Greater rescue of strength was achieved using 1.5 M and 10 minutes treatment. Thus, it suggests that Thomason et al. (2016) method could result an even more significant improvements if NaOH molarity was replaced from 3 M to 1.5 M. Another approach that could possibly improve Thomason et al. (2016) post-treatment results would be keep the 3 M molarity but reduce to half the treatment time. Bashir et al. (2017) results showed that on treatment time of 5 minutes, this is the molarity that results in greater strength.

In a recent work, Durai Prabhakaran et al. (2018) have also concluded that fiber cleaning after thermal recycling and before refunctionalisation plays a key role in improving rGF performance. Their study was focused on the interface of rGF/polyester resin composite. The analysed samples were: pristine fibers, HT fibers, recycled and resized fibers and recycled, washed and resized fibers. For the cleaning step, differently from what was presented previously, water at 70 °C was used instead of chemical solutions. From optical microscope images of the fiber surface before and after water washing in figure 18, it can be considered that the procedure was effective. Authors, however, did not present the composition of the resizing solution, it was only indicated that fibers had the properties regenerated. (Durai Prabhakaran et al. 2018)

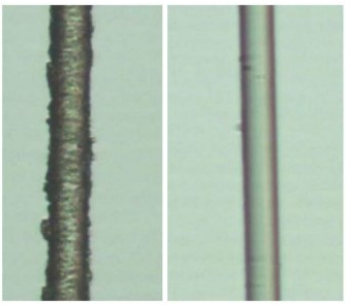

Figure 18. *Before and after hot water cleaning optical microscope images of glass fiber recycled by pyrolysis. (Durai Prabhakaran et al. 2018)*

Based on optimistic outcomes achieved by the rGF resizing routes presented above, an approach this study suggest is that a process with even more efficient results could perhaps be achieved by adding film former together with coupling agent, instead of only using coupling agent on the resizing step.

Wong et al. (2012) studied the improvement of interfacial adhesion between rCF and PP matrix by using maleic anhydride grafted polypropylene (MAPP) as film former on resizing treatment. Wong et al. investigated the effect of three MAPP (designated as E43, G3015 and G3003) in different molecular weights. Shredded CF/epoxy prepreg scrap recycled by fluidised bed process was the source of fluffy and discontinuous rCF that was subsequently converted into pellets. Later, 30 wt% was added on PP matrix for injection moulding. (Wong et al 2012)

Their findings showed greater degree of adhesion between the matrix and rCF with film former. On scanning electron microscopy, the tensile fracture surface appeared rough and fibers were surrounded by a layer of polymer. Moreover, enhancement of mechanical performance of the composite was noticed. For example, as seen in figure 19, significant increase on the tensile strength was achieved by adding 2 wt% of G3015 and E43 and 5 wt% of G3003. For the last one, improvement was around 150% compared to composite with no film former (tensile strength for PP with 30 wt% rCF without coupling agent: 50.62 ± 2.00 MPa). Comparing once more with composite without film former, IFSS had a maximum improvement of approximately 200% by adding 8 wt% of G3015 MAPP and a minimum improvement of 70% by adding 8 wt% of E43 MAPP. (Wong et al. 2012). The influence of maleic anhydride added as a film former to rCF and the significant improvement this post recycling treatment brings to mechanical properties and fiber/matrix adhesion was also documented by other authors later to this study (Burn et al. 2016).

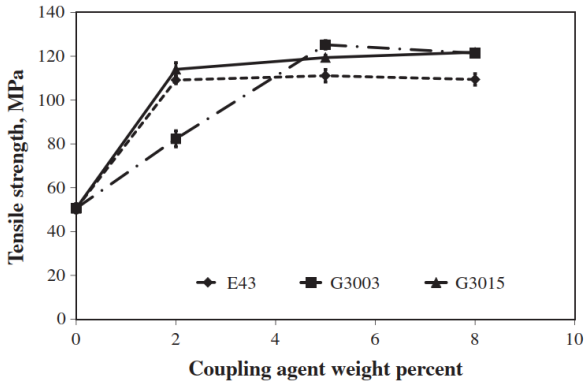

Figure 19. *Tensile strength curves of composites manufactured with CF resized with different MAPP. (Wong et al. 2012)*

Feng et al. (2013) modified the surface of rCF by combining nitric acid treatment and then resizing with epoxy film former to be subsequently used in nylon 6 matrix to produce extruded composite. The rCF source was thermoset composite recycled by fluidised bed process and different reinforcement content on the matrix was tested. The role of the concentrated nitric acid solution was to clean and activate the fiber's surface, because thermo-oxidative recycling results on carbonaceous deposits that can interfere on interfacial bonding capability of rCF. It was noticed that acid treatment did not change surface texture or caused flaws, what was considered positive. Epoxy groups on diglycidyl ether of bisphenol A chemically reacted with functional groups on nylon 6 resulting in better wetting of fibers by the matrix. (Feng et al. 2013)

Comparing to pure nylon 6, addition of 5 wt% surface-modified rCF, tensile and flexural strength were improved, respectively, by around 90% and 200%. Improvement tendency of these properties was observed with addition up to 20 wt%, reaching about 200% tensile strength and 310% flexural strength enhancement. Scanning electron microscopy indicated rough impact fracture surface and fibers well covered with polymer layer, an indication of mechanical interlocking establishment (Feng et al. 2013). Same approach adopted by the same authors was also applied to obtain substantial enhancement on rCF reinforcement potential, interfacial adhesion and mechanical properties of a composite made with poly(butylene terephthalate) (PBT) matrix (Feng et al. 2012).

Some published studies, however, indicates that some recycling methods for CF recovering do not affect significantly the mechanical properties, surface properties and interfacial bond strength (Connor et al. 2006; Jiang et al. 2015; Kanemasu et al. 2018; Yip et al. 2002;). Therefore, some existing researches were focused on the reuse of rCF without prior resizing (Akonda et al. 2012; Stoeffler et al. 2013).

Table 2 summarizes the methods presented on this work to reactivate the rGF and rCF surfaces.

Table 2. *Methods to reactivate the recycled fibers.*

Reinforcement	Matrix	Pre treatment	Resizing solution	Reference
rGF	-	HCl	APTS, MPS	Sáez-Rodríguez et al. 2013
	Epoxy	HF	APTS	Yang et al. 2015
	Polyester	Hot NaOH	APTS	Thomason et al. 2016
	-	Hot NaOH, KOH, LiOH	-	Bashir et al. 2017
	Polyester	Hot water	Not provided	Durai Prab-hakaran et al. 2018
rCF	PP	-	Three different MA	Wong et al. 2012
	PP		MA	Burn et al. 2016
	Nylon 6	HNO_3	Epoxy	Feng et al. 2013
	PBT	HNO_3	Epoxy	Feng et al. 2012

4. TECHNIQUES FOR SIZING CHARACTERIZATION

Characterization methods are necessary to better understand the nature of the sizing layer on the fiber's surface, which is a key element to tailor the sizing process. Moreover, after sizing treatment, surface chemical structure suffers changes. Therefore, the characterization of these changes is an essential practice to investigate the effects of the sizing on the fiber's surface and on the interface formation in the composite. According to Jones (2010), thermomechanical properties of the interface formed between fiber and matrix are critical to the performance of a composite.

4.1 Thermogravimetric analysis

Thermogravimetric analysis (TGA) is a quantitative technique in which the mass of the sample is measured as a function of temperature and time. A thermogravimetric balance is the core of TGA. The measurement occurs under a controlled environment, what means that factors such as heating rate, gas atmosphere, flow rate, sample preparation are defined by the operator (Wagner 2009).

Figure 20 shows the schematic illustration of a TGA device's interior. The sample is placed on a crucible that is positioned inside the furnace in a sample holder. The sample holder is connected to the thermogravimetric balance. The purge gas removes the reaction products away from the furnace and, instead of purge gas, reactive gas can be used in case it is necessary to investigate the interaction between the sample and atmosphere. The protective gas is required to protect the balance from the evolved reaction products (Menczel & Prime 2009).

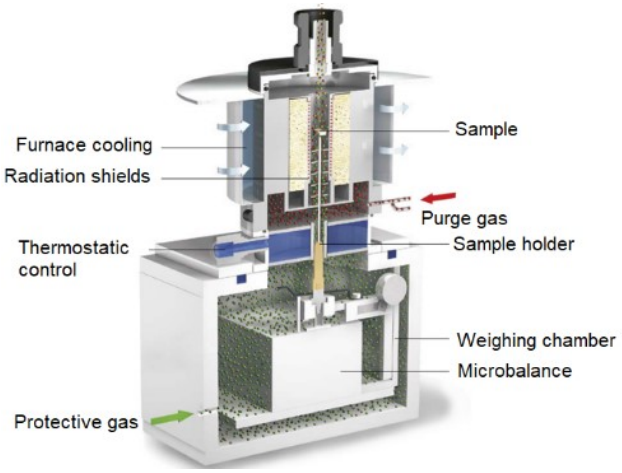

Figure 20. *An inside look on TG 209 F3 Tarsus from Netzsch. (Netzsch n.d.-a)*

Sample mass alterations arise due to different reactions or changes that can possibly occur on the sample during the analysis. TGA is suitable to determine purity, vaporization, sublimation, desorption, thermal decomposition, ageing, depolymerisation, degradation, thermal stability and composition of materials. The mass changes are detected by steps on the resultant TGA curve (Wagner 2009). An example of how results are displayed is presented in figure 21. The analysed material had four mass losses that were represented by percentage values. Residual mass was also given in percentage.

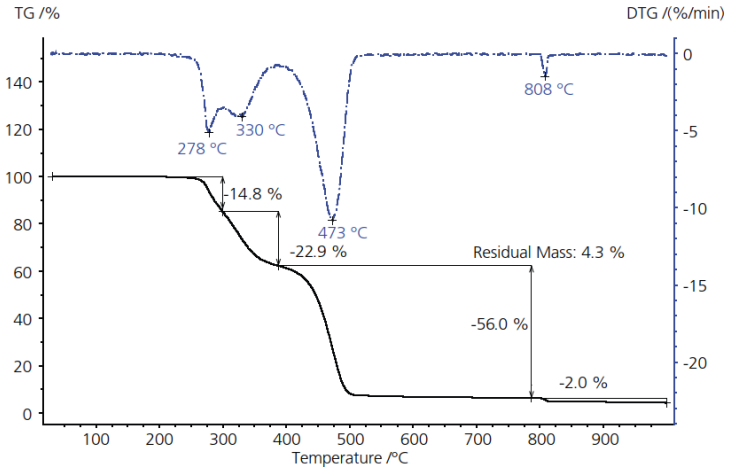

Figure 21. *TGA curve of a hypothetic material. (Netzsch n.d.-a)*

The derivative of the TGA curve (DTG), given on dashed line, is a complementary and useful analysis to obtain more information about the sample. It shows the rate at which the mass changes occur and distinguishes overlapping mass loss events, because each peak on DTG represents a separate event (Menczel & Prime 2009).

For a reproducible and adequate results, the following factors should be considered:

Sample preparation: control the size and geometry of the sample is important since they can affect the results. Sample morphology influences the heat transfer within it as well as the diffusion rate of reaction products formed during the measurement. Moreover, sample mass affects the rate of mass loss and sample homogeneity affects material representativeness (Wagner 2009).

Crucible type: crucible material must not influence on the sample reaction or interact with the sample. Furthermore, it must withstand the experiment's temperature. For polymer analysis, ceramic crucibles made of alumina is usually the suitable option (Menczel & Prime 2009).

Surrounding atmosphere: it is selected according to the experimental purposes and gas switching during the experiment is possible. Nitrogen is normally used when it is important to avoid oxidation. Air or oxygen are used when oxidation or combustion behaviour of the sample is studied. Other possible gases are hydrogen, argon and helium. The purge gas flow rate is an important parameter and normally is set according to the suggestion of the equipment manufacturer (Menczel & Prime 2009)

Temperature program: the start and end temperatures should be sufficiently long to capture the first and last thermal events. Therefore, a baseline at the beginning and end of the experiment should be set.

Heating rate: in case the sample suffers chemical reactions during the measurement, the temperature region which it occurs is dependent on the heating rate. Overlapped or even undetected reactions can be the result of an inappropriate heating hate selection. It is known that lower heating rate gives better temperature resolution, thus better separation of overlapping events. However, measurement takes more time so the need of it should be evaluated according to the experiment objectives (Menczel & Prime 2009; Wagner 2009).

Artifacts: disturbances on the curve that are not directly caused by the sample and, thus, do not have anything to do with the sample properties. The main types of artifacts are fluctuations on the purge gas flow, decreasing of the density of the surrounding gas and sudden mass loss due to sample ejection out of the crucible. Performing multiple measurements is a way to identify artifacts.

TGA assess the thermal stability and thermal desorption behaviour of the sizing layer. The measurement of mass loss, as a function of temperature, caused by desorption provides information about the total amount of sizing on the fiber surface (Moosburger-Will et al. 2018). Moreover, TGA enables the verification of the quantity of residues/char deposited of the fibers after the recycling treatment.

Sizing extraction with appropriate solvent followed by TGA measurement is also an approach to study the sizing portion that strongly interacts with the fiber's surface. The solvent removes the physisorbed sizing components, such as physisorbed organosilanes in GF and film former. Therefore, what remains are the interactions resulted from chemical bonds between fiber and sizing on the surface. (Moosburger-Will et al. 2018; Petersen 2017; Petersen et al. 2013).

Moosburger-Will et al. (2018) have concluded in their study about the influence of fiber surface chemistry and sizing reactivity that the shape of resultant TGA curves depends only on the type of sizing applied. They explained that desorption during TGA characterizes mainly the thermal behaviour of the sizing layer itself since the amount of sizing molecules in direct contact with the fiber surface is much less than the total amount of sizing molecules.

The analysis of sizing on TGA can be challenging because of the small amount of sizing present on the fiber surface. The precision of the method in this case is dependent on the mass of the test specimen and on the percentage of this mass that is in fact the sizing layer. Moreover, the detection of mass loss step coming from the sizing can be impaired by noise of the measurement signals and artifacts. Thus, for more trustworthy analysis, it is highly recommendable to have a reliable baseline curve (Menczel & Prime 2009; Wagner 2009). Another issue is the difficulty to prepare small samples from fibers, the manipulation becomes challenging after they are cut to fit inside the crucible because short length strands are lightweight and scatter easily.

4.2 Fourier–transform infrared spectroscopy

Fourier-transform infrared (FTIR) spectroscopy is an analysis in which chemical bonds of the sample are detected via infrared absorption spectrum. It is quick and reliable as long as the element's concentration is sufficient. FTIR provides information about sample's quality, consistency, composition and it is also useful for identification of unknown materials.

The analysis process is presented in figure 22. It starts with infrared beam emitted from a source. Subsequently, it passes through an aperture that controls its energy and then enters the interferometer. In the interferometer, the infrared beam is separated into two optical beams that are reflected by flat mirrors, one mirror is static while the other is able to move few millimetres. After being reflected, the beams are recombined at the interferometer end. The interferometer output is the interferometer signal, which results from the constructive or destructive interference of the recombined beam. Next, the beam crosses the sample and some specific energy frequencies are absorbed, depending on the sample's structure, and the rest is reflected (Thermo Nicolet Corporation 2001).

Finally, the beam is detected by detectors designed to measure interferogram signals. Individual frequencies are required in the resultant frequency spectrum, therefore, Fourier transformation is performed on the interferogram signals by the computer. The resultant spectrum represents the IR absorption peaks of molecules existent on the sample and the peaks corresponds to the vibrational frequencies of atomic bonds on the molceules. Each molecular structure has its own atomic arrangement and produces a unique IR spectrum, therefore it is considered that FTIR represents the fingerprint of the sample (Thermo Nicolet Corporation 2001).

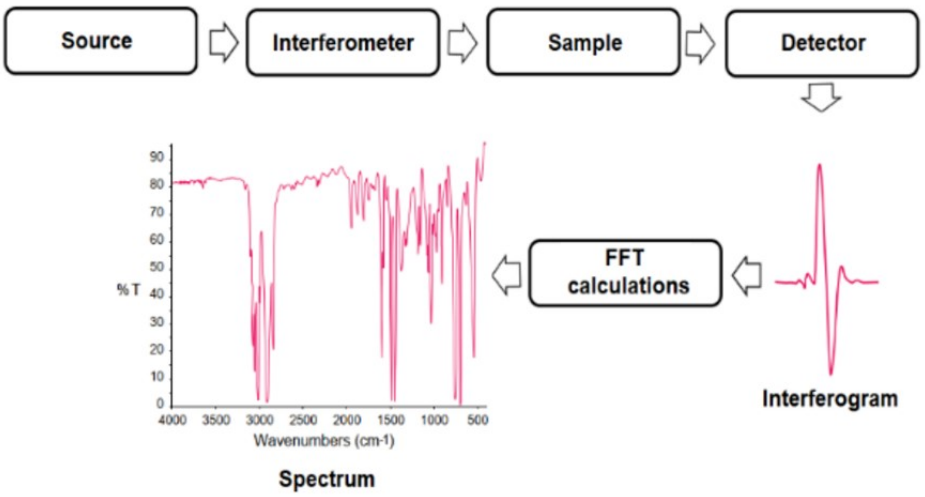

Figure 22. *The analysis on FTIR. Adapted from Thermo Nicolet Corporation 2001.*

Since it enables the identification of the functional groups present on the fiber surface, it is a useful analysis to observe the resultant products of the sizing process on the surface by comparing untreated and treated fibers or different treatments (Bashir et al. 2017; Feng et al. 2013; Wu et al. 2015). The FTIR technique is a valid and quick method to examine what is on the sizing layer. However, the challenge of the technique in this case is to capture intense enough signals from the layer and not only from the bulk fiber, since the first is present in much smaller amount than the second.

4.3 Thermogravimetric–infrared spectroscopy coupled analysis

An advancement of TGA characterization is achieved by using thermogravimetry – infrared spectroscopy coupled analysis (TG-FTIR). TGA is accurate to measure the sample weight loss but no information about the chemical composition of evolved gases is given. FTIR spectroscopy provides the characteristic spectrum of the gases that are released from the test specimen (Robertson & Lawson-Wood 2017).

Figure 23 represents schematically the work principle of this method. Sample is placed in the TGA equipment and measurement is performed as discussed previously in section 4.1. The gases generated during mass loss steps together with the purge gas (inert gas, because it does not exhibit IR-absorption) are transferred to FTIR device through the transfer line. The temperature of the transfer line is an important factor, it should be high enough to prevent condensation but low enough to avoid degradation. Subsequently, the FTIR gas cell detects those gases to provide information about the nature of the material's degradation products (Menczel & Prime 2009). To ensure better detection sensitivity, the gas cell need to have long path length, to enable the passage of more molecules at the same time, and low volume, for higher concentration of evolved gases (Netzsch n.d.-b).

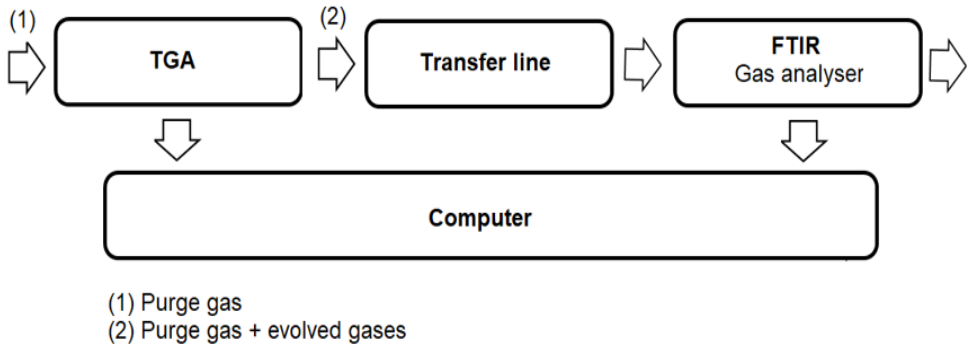

Figure 23. *Scheme of TG-FTIR measurement. Adapted from Wagner 2009*

The evaluation results are given in a 3-dimensional diagram that includes the wavenumber, peak intensity and temperature information of the performed thermal analysis (figure 24). The chemical analysis resolution will depend on the TGA heating rate, FTIR scan time and the gas transfer delay from TGA to FTIR. This last factor is influenced by TGA flow rate and the path length of the transfer line (Menczel & Prime 2009).

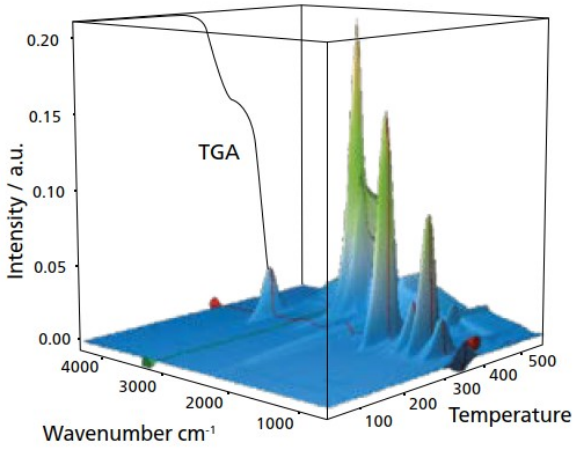

Figure 24. *3-D plot of a TG-FTIR measurement. (Netzsch n.d.-b)*

This coupled technique is useful for sizing characterization, because the information about of evolved gases enables an understanding of the sizing chemistry and then which compounds were in fact deposited on fiber surface during sizing application. Depending on the application process, it may not wet the fibers appropriately and sizing elements may not be found on the fiber surface.

Furthermore, it is possible to analyse how the sizing interacts with the fiber surface, in other words, what are the components that are more weakly bonded to it and the ones that are more strongly bonded to it. The hypothesis that the film former is not bonded to the fiber, for example, could be validated by examining if it decomposes first than the coupling agent, which is bonded to the fiber.

Besides the challenges faced on TGA, another possible one that arises from this coupled technique is to ensure that transferred gas is enough for analysis and does not condensate or degrade on the transfer line.

5. MATERIALS AND METHODS

5.1 Materials

FiberEUse project provided the recycled, unsized and sized rGF and rCF. They were obtained by thermal recycling (pyrolysis) of long GF and CF composites from wind energy industries and aeronautics, respectively. In this work, the unsized samples were used as reference for the study of any modification detected on the fibers after the resizing process. The analysis of resized samples enabled the investigation of the components deposited on the fiber's surface and their quantification.

For rGF, the resizing process was done according to the following procedure. First, the coupling agent (CA), APTS purity 99% from Sigma-Aldrich, distilled water and acetic acid were mixed with a magnetic stirrer for 1 hour to promote the hydrolysis of the organosilane. It enabled the formation of siloxane bridge bonds with the fiber surface, as discussed in section 3.2. Afterwards, PP solution (Hydrosize® PP2-01, Michelman) used as film former (FF) and water were added and the resultant solution was mixed for 1 hour more to obtain a homogeneous solution. Then, acetic acid was added to set the pH solution in a range of 4 – 4.5. Different solutions varying the sizing component concentrations were produced. The absolute concentration of the sizing solution, considering just the CA and FF in the solution, and the relative concentration of CA and FF are presented in table 3. When the sizing solution was ready, rGF were immersed into it for 30 seconds. Subsequently, it was rinsed with distilled water for 30 seconds and dried in oven at 80 °C for 10 hours to reduce fiber moisture.

Table 3. *Absolute and relative concentrations of rGF resizing solution.*

Absolute concentration w%	**Relative concentration w%**	
	Coupling agent	**Film former**
1	5	95
	10	90
	20	80
3	5	95
	10	90
	20	80
5	5	95
	10	90
	20	80

In the case of rCF, first PP solution (Hydrosize® PP2-01, Michelman) used as the FF was allowed to rest for 1 hour at 30 °C. Afterwards, fibers were dipped into it for 30 seconds. Resizing was performed with two different solution concentration, 1 and 5 w% PP. Subsequently, fibres were rinsed with distilled water and then allowed to dry at 80 °C for 10 hours.

To evaluate the effect of surface activation on the received recycled fibers, part of the samples were treated with HNO_3 to promote acidic oxidation on the surface before being resized with 1 and 5 w% PP. For this procedure, unsized fibers were immersed for 20 minutes in 63% HNO_3 and subsequently rinsed with distilled water at 60 °C and dried at 80 °C for 10 hours. After this, resizing process was performed as detailed previously. The types of resizing process, considering the PP solution concentration and HNO_3 pre-treatment are presented in table 4.

Table 4. *Parameters for resizing procedure of rCF.*

	Sizing solution concentration w%	**Pre-treatment with HNO_3 before resizing**
Type of samples	1	No
	1	Yes
	5	No
	5	Yes

For resized rGF, each sample was named according to the absolute and relative concentrations. For example, rGF_1_5/95 represents the rGF resized in a 1 w% absolute concentration solution, which contains relative concentration of 5 w% CA and 95 w% FF. In case of resized rCF, each sample was named according to the concentration and condition before sizing. Fibers resized without HNO_3 pre-treatment were assigned as ‘ar’, meaning ‘as received’, and fibers that went through the pre-treatment, as ‘pt’, meaning ‘pre-treated’. As an example, rCF_1_ar represents the rCF that was resized as received in the 1 w% resizing solution.

5.2 Experimental methods

5.2.1 Resizing extraction

Part of all resized fibers batches were separated for resizing removal process. The process consisted in solvent extraction by the soxhlet extraction followed by fiber's burning. The procedures were based on the methods used by Petersen and Tanoglu and its scheme and real apparatus are illustrated in figures 25 and 26, respectively (Petersen 2017; Tanoglu et al. 2001). The procedure was executed twice for each sample.

Soxhlet extraction was employed to remove sizing components that were loosely bonded to the fiber surface without damaging the fibers. In this method, the vapours generated by heating up an extraction solvent travels to the chamber and then the soluble sizing components are slowly transferred to the solvent. A fiber bundle of approximately 1 gram, for rGF, and 0.1 gram, for rCF, was placed on a filter paper and then positioned on the extraction chamber. Acetone was the extraction solvent and 100 millilitres was added in an Erlenmeyer flask and kept at constant temperature of 120 °C to assure boiling during the procedure. The extraction was performed for 24 hours. It was assumed that the physisorbed fraction that was able to diffuse through the matrix is equal to the fraction that is soluble to acetone and also that the acetone did not react with sizing components (Petersen 2017; Tanoglu et al. 2001).

After extraction and before drying, both fibers and filter paper were washed with acetone to collect any not bonded sizing that eventually could have stayed on them. This additional acetone solution was incorporated to the extracted solution. Afterwards, the acetone containing the sizing extract was concentrated to a volume of 25 millilitres by evaporating acetone at 120 °C and reserved for further analysis.

Extraction was followed by burning to evaluate the amount of bonded sizing on the fibers. Before burning, fibers were dried in oven at 110 °C for 30 minutes in order to remove excess of moisture and solvent. Subsequently, fiber's burning was conducted for 3 hours at 560 °C in air atmosphere, in case of rGF samples, and for 3 hours 500 °C in inert nitrogen atmosphere to avoid fiber's degradation, in case of rCF samples.

The weight of the fibre samples were determined before and after extraction to evaluate the amount of extractable sizing. Fibers were also weighted after the burning process to assess the amount of bonded sizing.

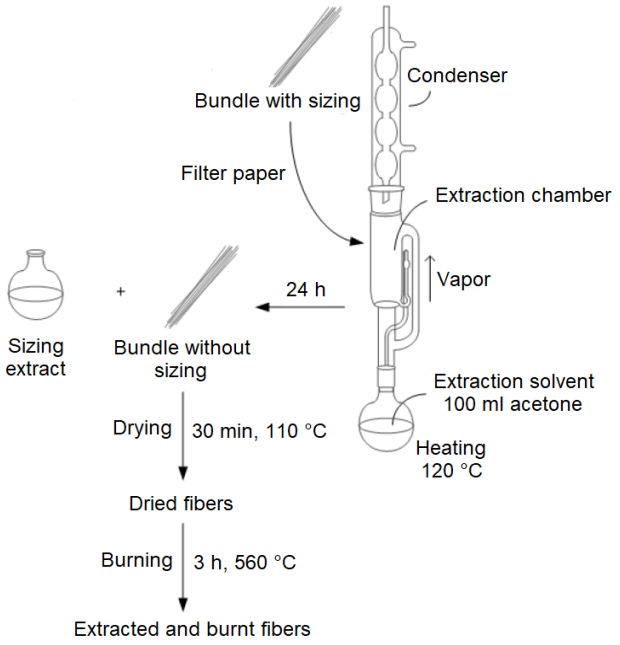

Figure 25. *Schematics of the resizing extraction process. (Petersen 2017)*

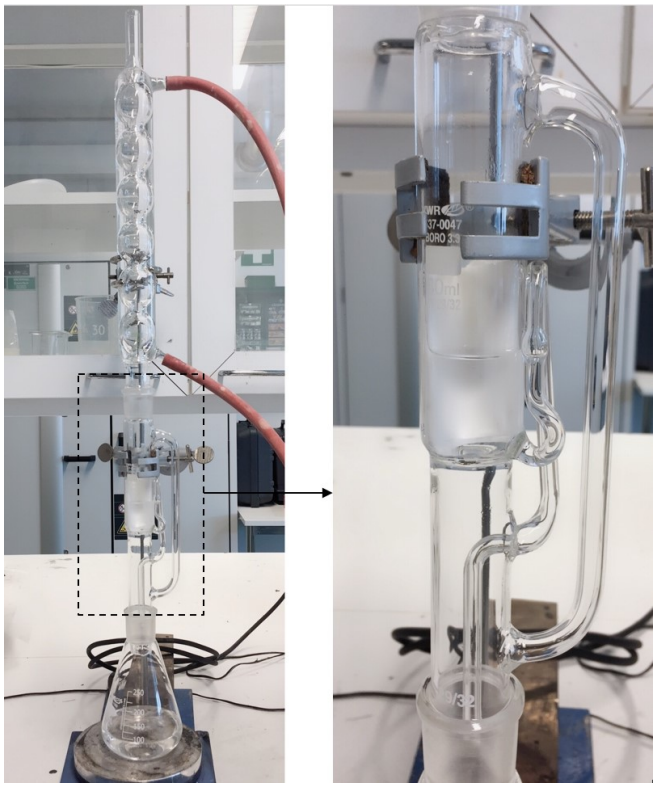

Figure 26. *Soxhlet extraction apparatus and the extraction chamber with a sample wrapped in a filter paper highlighted on the right.*

5.2.2 Thermogravimetric analysis

TGA measurements were performed on rGF and rCF as received and after being submitted to resizing. In addition, rGF and rCF after solvent extraction and after burning were measured. Coupling agent, film former and a 5 w% absolute concentration solution containing 20 w% coupling agent and 80 w% film former (referred as 'mixed solution' henceforward) were also tested. Measurements were conducted with Netzsch TG 209 F3 Tarsus and performed twice for each sample.

For resized fiber samples, to assess the influence of TGA parameters on the detection of sizing's desorption, it was used temperature range from 30 °C to 550 °C, at different heating rates (5 and 10 K/min) and nitrogen and air atmospheres. The samples were prepared by taking a small fiber bundle and continuously folding it and cutting the extremities until a length that could fit on the crucible. The mass of the samples were around 50 mg for rGF and 30 mg for rCF. The intention was to fill the TGA crucible with the maximum amount of material possible to make the signals coming from the sizing as intense as possible.

For fibers submitted to extraction process, the aim was verify the surface content after each process and draw conclusions about the physisorbed and chemisorbed parts of the sizing on the surface. Sample preparation was done similarly to resized fibers, temperature range was 30 °C to 550 °C, heating rate was 10 K/min and nitrogen was the atmosphere applied.

For coupling agent, film former and the 'mixed solution', two different analysis were performed. First one, samples were just added on the crucible in the liquid form. Second one, samples were dried for 24 hours at 105 °C and crushed to powder before the analysis. For the drying, solutions were placed in a borosilicate watch glass. In both situations, temperature range was 30 °C to 550 °C, heating rate was 10 K/min and nitrogen was the atmosphere applied.

Correction measurements were made to obtain the blank curve for curve subtraction in order to eliminate curve effects that do not originate from the sample. In this case, the same experiment parameters were applied.

5.2.3 Attenuated total reflectance Fourier–transform infrared spectroscopy

FTIR-ATR measurements were conducted in order to identify the functional groups on the samples. Unsized and resized fibers as well as dried coupling agent and dried 'mixed solution' were tested. To obtain fiber's spectrum, the fiber bundle was placed in the sample holder and then crushed to a fine powder by compressing the sample screw holder over it. This way it was assured that the whole ATR crystal was covered by the sample, furthermore, inevitably the fibers were crushed under the pressure of the screw due their brittleness. In case of the dried samples, as they were already powder, they were placed on top of the ATR crystal and compressed by the screw.

Measurements were conducted with Bruker Tensor 27 spectrometer with a PIKE Technologies GladiATR Attenuated Total Reflectance (ATR) sample holder. Diamond crystal was the ATR material. The wavenumber range of analysis was 600–4000 cm^{-1}, the resolution was 4 cm^{-1} and the number of scans was 30. Furthermore, detectors were cooled with liquid nitrogen, which provided highest measurement speed, sensitivity and resolution. Each sample was measured three times.

Before sample testing, the background spectrum was also obtained in order to eliminate signals coming from the surroundings. Background signal measurement was done without any sample on the sample holder and following the same experimental conditions of the sample's analysis.

5.2.4 Thermogravimetric–infrared spectroscopy coupled analysis

TGA-FTIR coupled analysis was performed on FF solution in order to evaluate the thermal behaviour of this constituent of the sizing. The measurement was performed on Netzsch TG 209 F3 Tarsus and Bruker Tensor 27 spectrometer with a gas cell. TGA and FTIR were connected by a transfer line kept at 200 °C.

The parameters selected for TGA analysis were heating rate of 10 K/min, temperature range of 30 °C to 550 °C and nitrogen atmosphere. Regarding to sample preparation, drops of the FF was carefully added on the crucibles until it was approximately 50% filled.

For FTIR, the wavenumber range of analysis was 600–4000 cm^{-1}, the resolution was 4 cm^{-1} and liquid nitrogen was also used to cool the detector. Infrared spectra were taken every 30 s during the experiment and they were plotted on top of each other providing information as function of wavenumber and temperature of the nature of the products generated on the desorption of the sample.

6. RESULTS AND DISCUSSION

6.1 Characterization of film former and coupling agent

To evaluate the thermal behaviour of the FF and CA, they were characterized using TG and FTIR. Data was acquired in order to have better understanding of the TGA and FTIR results from sized samples. From the characterization of CA and FF, it was afterwards possible to evaluate the presence or not of FF and CA on the surface of resized rGF or of FF on the surface of resized rCF.

For both rGF and rCF, the FF used in the sizing formulation consisted mainly of maleated polypropylene dispersion (MAPP), a polypropylene modified with maleic anhydride (MA) polar groups. Because exact formulation of the FF is not known, it can be assumed that it can contain other components as well. Figure 27 presents the chemical structure of MAPP.

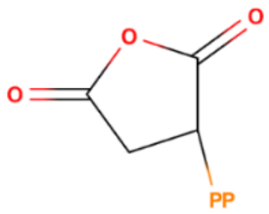

Figure 27. *The chemical structure of MAPP film former.*

As seen in the TGA curve of the dried FF solution (figure 28), under nitrogen atmosphere it presented one degradation step that occurred from 400 to 500 °C. The thermal decomposition of PP can produce many gaseous products, depending on additives present in its composition and the measurement parameters, such as temperature or atmosphere. At inert atmosphere, the decomposition of PP occurs mainly by random chain scission, generating low molecular weight hydrocarbons of various chain lengths. Due to the presence of the MA groups, besides hydrocarbons, different organic compounds containing oxygen are formed, principally CO and CO_2 but also other volatile products (Paabo & Levin 1986).

The FF solution exhibited two degradation steps, one at 80 to 200 °C and the other at the similar position of the mass loss step of the dried FF sample. It indicates that the first one is attributed release of water or solvents present in the solution, therefore not being related to the thermal behaviour of the FF itself. Because no major differences were observed between the TGA curves of dried FF and FF solution, the latter is not displayed.

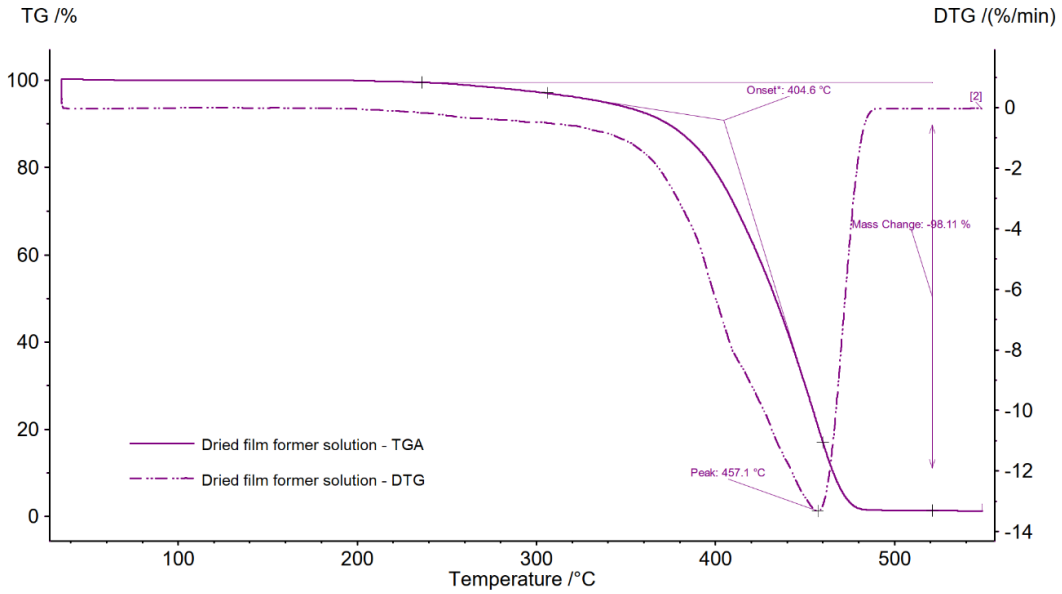

Figure 28. *TGA curve of dried MAPP film former Hydrosize® PP2-01.*

From the 3D plot of the TG-FTIR measurement for FF solution (figure 29), it was possible to evaluate what gases evolved during each of mass loss steps. The series of peaks detected at temperatures below 362 °C on the graph is not associated to the FF, as discussed previously. Peaks above this temperature are related to thermal decomposition of FF itself. It was detected peaks in the ranges of 3000-4000 cm^{-1} associated to O-H stretching vibrations, 2500-3000 cm^{-1} associated to the C-H stretching vibration, 1600-1800 cm^{-1} associated to C=O stretching vibrations, 1300-1600 cm^{-1} associated to the C-H bending vibration and 1000-1100 cm^{-1} associated to the C-O stretching vibration. From figure 29, it is possible to verify that the first peaks to get stronger during temperature increase were the ones located at the wavenumbers associated to hydrocarbon bonds, such as in 2500-3000 cm^{-1} range. Therefore, for the thermal decomposition of MAPP, it can be considered that PP chain started to degrade first. On the other hand, the broad peak related to O-H bond begun to be noticeable afterwards and its stronger intensity was somewhere around 450 °C, indicating the degradation the MA group. (Liu et al. 2015)

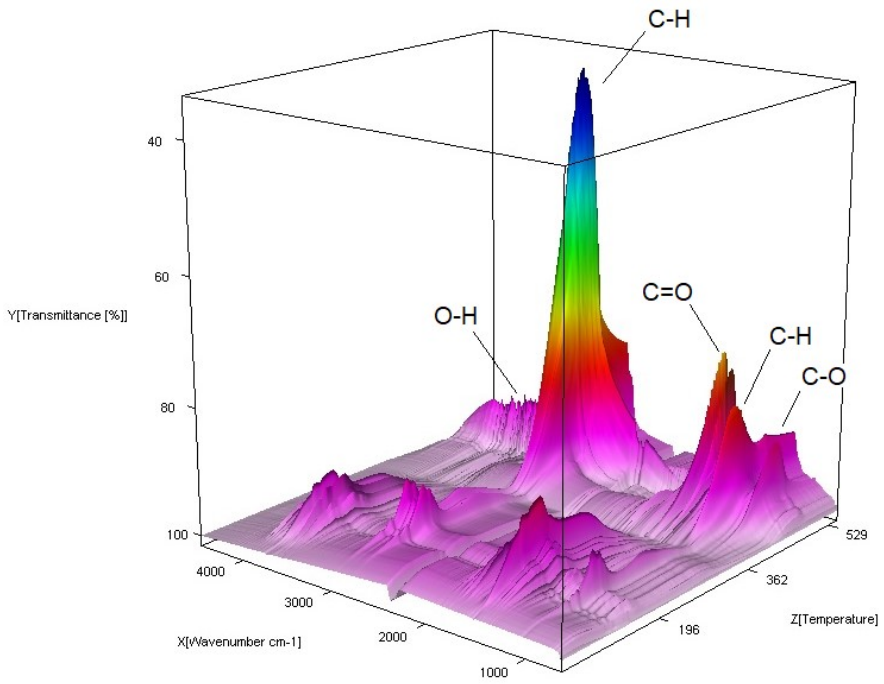

Figure 29. *TG-FTIR diagram of MAPP film former Hydrosize® PP2-01.*

Figure 30 shows the chemical structure of ATPS used as CA to resize the rGF. As seen, the molecule is composed by a silicon atom bonded with three ethoxy groups, which are reactive sites able to interact with the rGF surface, and an amine group functionality, which interacts with the resin during the composite manufacturing.

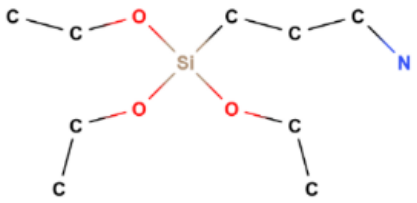

Figure 30. *The chemical structure of ATPS coupling agent.*

The TGA curve of the CA is presented in figure 31 and 32 and they are clearly different depending if CA was dried or not. For the CA solution, thermal decomposition occurred in a single mass loss step starting around 150 °C and before 300 °C the degradation was over. This is due to the fact that APTS has aliphatic and amine functionalities and they are not expected to provide high thermal resistance (Tiefenthaler & Urban 1989).

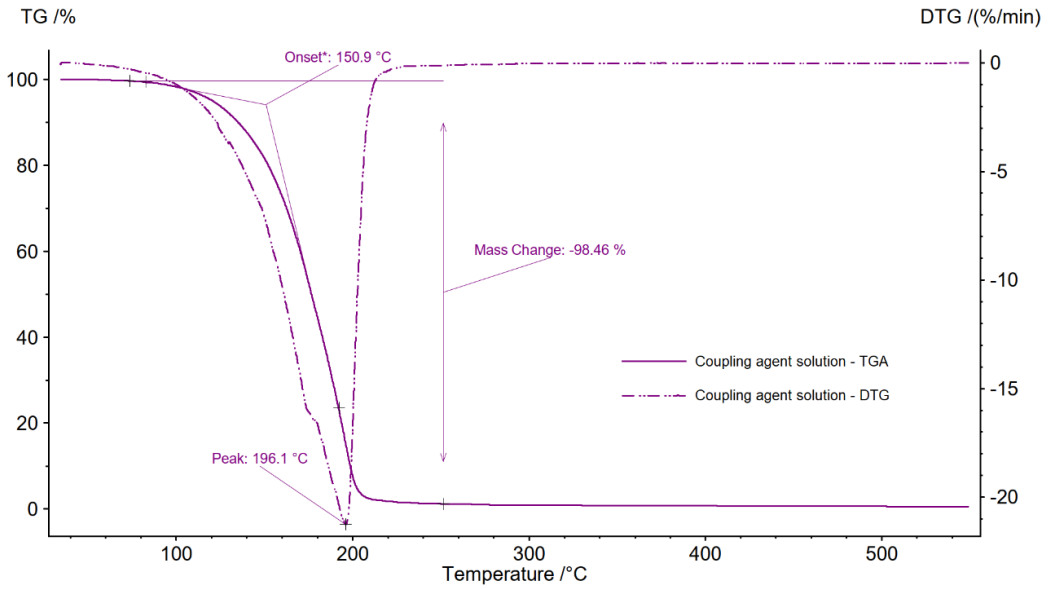

Figure 31. *Figure. TGA curve of APTS coupling agent solution.*

On the other hand, for the dried CA, three mass loss steps were detected. First one below 100 °C corresponds to release of water that is absorbed due to the hydrophilic character of ATPS (Acres et al. 2012). The second mass loss step started around 240 °C and can be associated to the degradation of aminopropyl. According to Sándor et al. (2016), the last temperature range can be associated to the dehydroxylation of Si-OH residual functions that results in the formation of Si-O-Si groups. The authors also indicated that dried APTS exhibits a high content of uncondensed Si-OH functions. At the end of the measurement, what remained was inorganic residue.

The change on the thermal behaviour of the CA could have happened due to the interaction possibly established between the organosilane and the glass substrate during the drying process. It was noticed during the removal of the dried sample from the glass watch that the CA and the ‘mixed solution’ were more attached to it, scraping was successive and required the application of force, while the FF was effortless. This assumption can be further supported by the study conducted by Petersen (2017) about glass fiber’s sizing. In some of the experiments, the author used glass plates coated with organosilane. The objective was to mimic the glass fiber coated with the same component to get indications of how the surface of the glass changes with functionalisation.

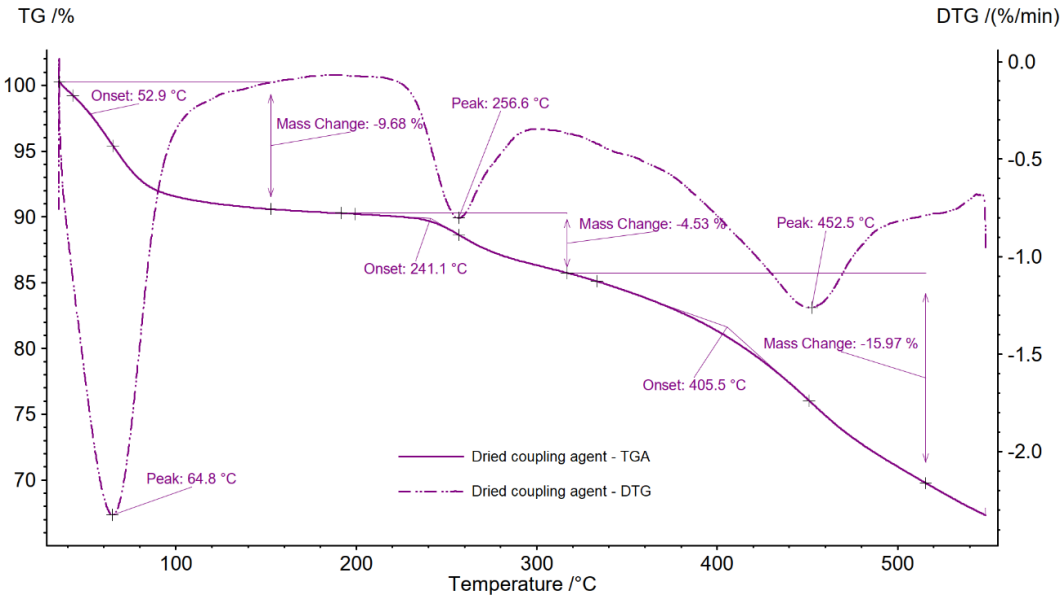

Figure 32. *TGA curve of dried APTS coupling agent.*

Regarding to the FTIR spectrum presented in figure 33, the $(RO)_3Si—CH_2CH_2CH_2NH_2$ have dominating infrared bands in the region of below 1200 cm^{-1} that are related to the $(RO)_3Si$ part of the structure. According to Launer (2013), in polysiloxanes, $Si\text{-}OCH_2CH_3$ has vibrational modes of 1160-1170 cm^{-1}, 1075-1100 cm^{-1} and 940-970 cm^{-1}. Moreover, the spectrum has less intense infrared bands related to the aminopropyl reactive group, in which the one around 3300 cm^{-1} corresponds to N-H stretching vibration of primary amines, the 3000–2800 cm^{-1} region corresponds to the stretching vibrations of CH_2 and from aminopropyl segment and the 1650–1580 cm^{-1} region are characteristic to NH_2 bending mode in amines (Sándor et al. 2016; Petersen 2017).

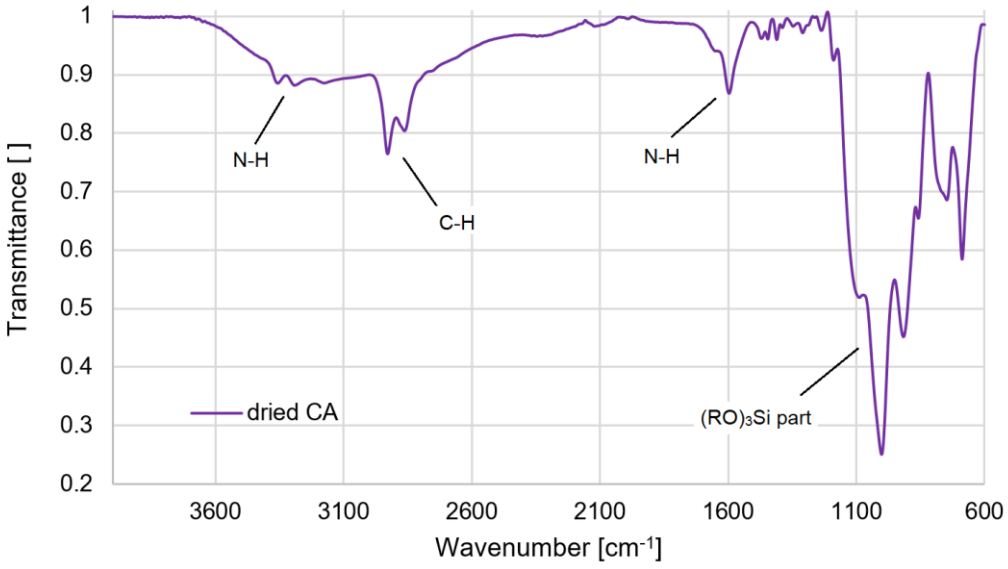

Figure 33. *FTIR spectrum of dried APTS coupling agent.*

The ‘mixed solution’ was made in order to understand the thermal behaviour of the components mixed together. Again, TGA results of dried and solution samples differed from each other. In figure 34, the TGA curve of the solution is presented. Two mass loss steps were detected, starting around 90 °C and around 420 °C. Comparing it with the TGA curves of FF and CA, it is possible to assume that the first step is associated to thermal degradation of the CA and moisture or solvent from the FF solution and the second step is due to the thermal degradation of the FF.

Figure 35 shows the TGA curve for the dried solution. As the liquid content was practically all removed, significant decrease in mass loss occurred on the curve at temperatures below 200 °C. Comparing the curves from figures 28, 32 and 35 it is possible to verify that what happened up to 300 °C is related to the desorption of CA and at temperatures above 300 °C, the FF and the remaining CA degrades. As already discussed, the difference in the curves can be related to the formation of bonds and surface modification originated from the probable interaction between the solution and the glass substrate due to the presence of the CA.

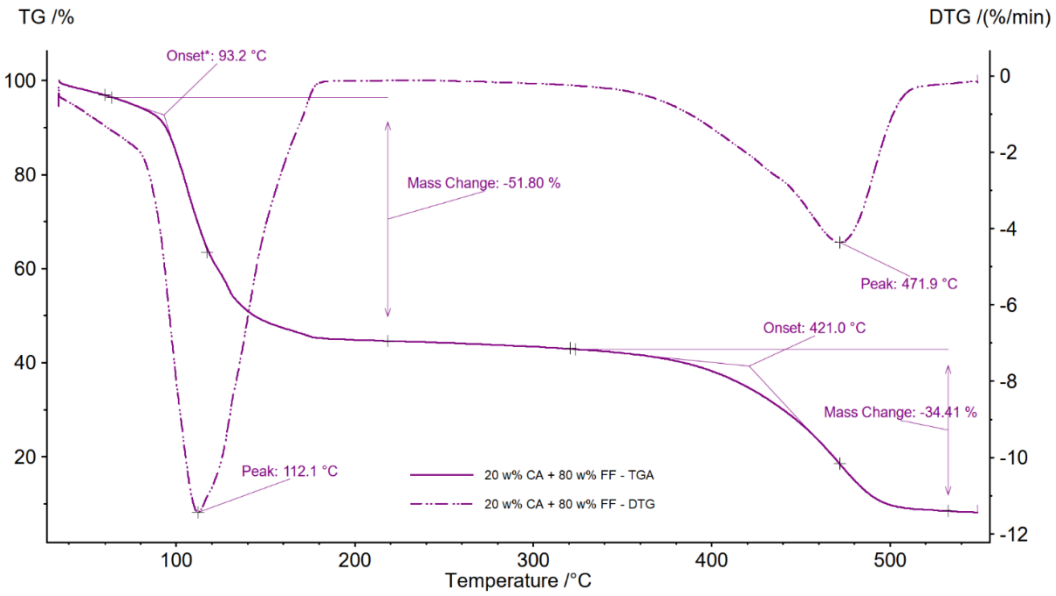

Figure 34. *TGA curve of the ‘mixed solution’.*

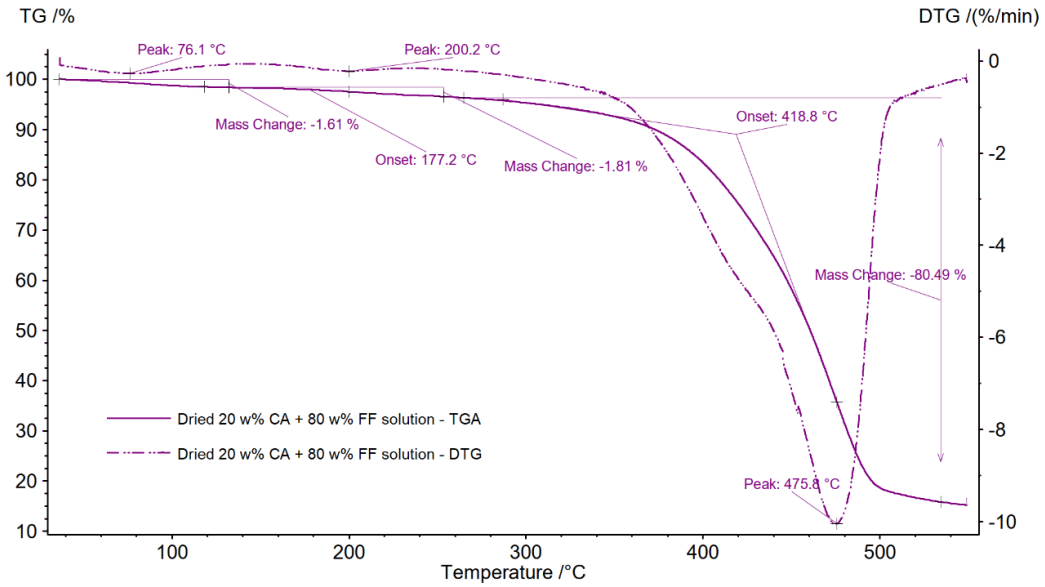

Figure 35. *TGA curve of the dried 'mixed solution'.*

For this work, an understanding of how the ATPS and MAPP interacts with the fiber's surface was also important. According to Petersen (2017), in the case of rGF, the CA is the only component on the sizing formulation that is expected to establish covalent bonds with the fiber's surface. Figure 36 shows the possible ways the CA can interact with it.

Because of the presence of three ethoxy reactive sites in each molecule, the bonding of ATPS can occur as presented in figure 36(a), (b) and (c). Furthermore, due to their reactivity in water, the ethoxy groups can hydrolyze still during storage or during the synthesis of the sizing solution, being converted into silanol groups. As a result, horizontal polymerization reaction and premature siloxane bonds can happen (Mittal & Pizzi 2002). This way, siloxanes can form before or during the silane interaction with the surface, the last alternative presented in figure 36(d) and already discussed in section 3.2. If formed before, they deposit vertically on top the fiber's surface forming multilayers that can impair the establishment of an adequate sizing layer (Mittal & Pizzi 2002; Acres et al. 2012).

Besides the influence of the ethoxy groups, the amine groups can catalyze inter and intra molecular reactions to establish the bonds with the surface. They also can form hydrogen bonds with the fiber's surface groups as seen in figure 36(e), resulting in low grafting densities and weak attachment of the CA molecules (Smith & Chen 2008).

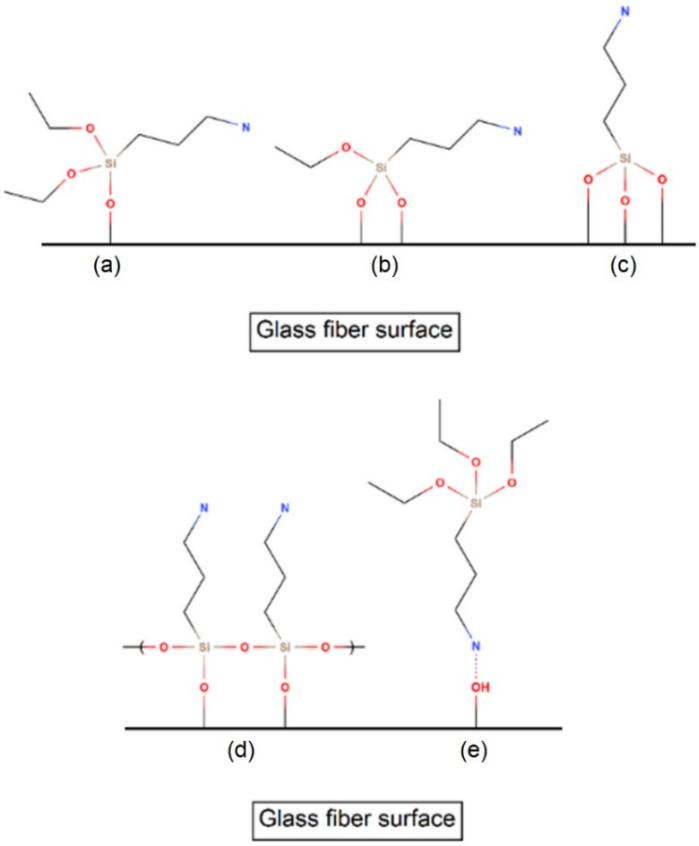

Figure 36. *Possible ways of ATPS molecule to bond with the rGF surface. Adapted from Acres et al. 2012.*

In the case of rCF, as the FF is the only constituent of sizing formulation, if there is any bonds it has to involve the FF and the active groups on the rCF. The establishment of chemical bonds between the FF and the surface can be achieved by interactions of the hydroxyl groups and maleic anhydride groups (Bikiaris et al. 2005). The resultant bonds established between those components is presented in figure 37. It was concluded that MAPP improves the interface bonding by chain entanglement with PP matrix, providing mechanical integrity, and maleic anhydride (MA) groups interact with the functional groups on the fibre surface forming covalent bonds (Wong et al. 2012).

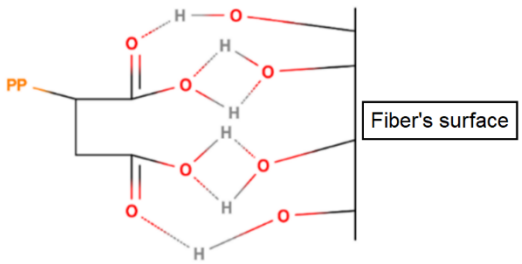

Figure 37. *Chemical interactions established between activated groups on the rCF surface and the FF. Adapted from Bikiaris et al. 2005.*

6.2 Characterization of recycled glass fibers

From FTIR and TGA of unsized rGF, it was possible to assume that fibers obtained from composite recycling were sufficiently clean to be subsequently resized without prior surface cleaning. TGA was performed in nitrogen at 10 K/min and resultant curve presented in figure 38 was obtained after blank curve subtraction. The rGF was thermally stable until the maximum temperature applied on the measurement and, consequently, it is possible to attribute the events on TGA curve to the sizing on the fibre's surface. Therefore, because no thermal degradation of organic components was detected between 30 °C to 550 °C, it indicated the absence of significant amount of sizing that could be detected by the equipment.

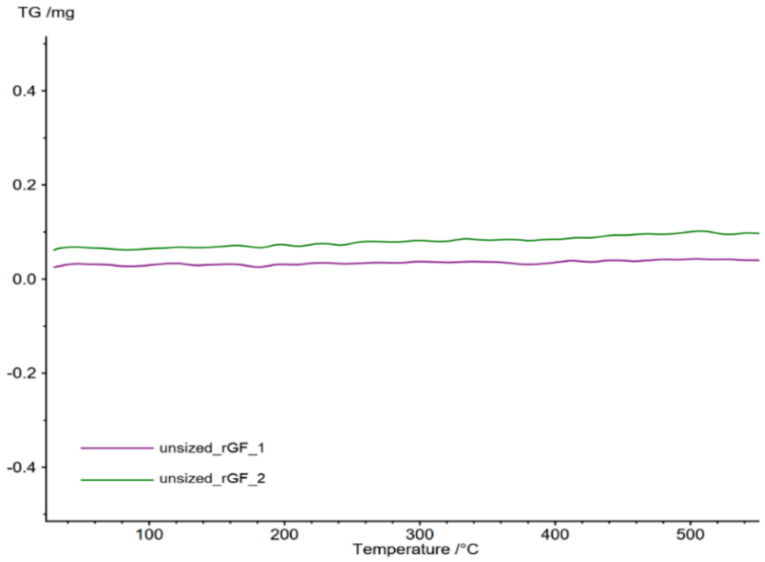

Figure 38. *TGA curves of two measurements done with unsized rGF.*

The FTIR spectrum of unsized rGF is presented in figure 39. The shoulder type region between 600 and 1200 cm^{-1} is the main noticeable event of the spectrum, this predominant area is associated to different vibrational modes of Si-O-Si bonds in the glass fiber. The medium intensity peak at 1400 cm^{-1} is related to stretching vibrations of BO_3 groups that are present in the E-glass structure. The lack of other bands on the spectrum is an indication that sizing and resin residues where completely removed or reduced to an undetectable amount after the recycling process of glass fibers. (Laurikainen 2017; Petersen 2017)

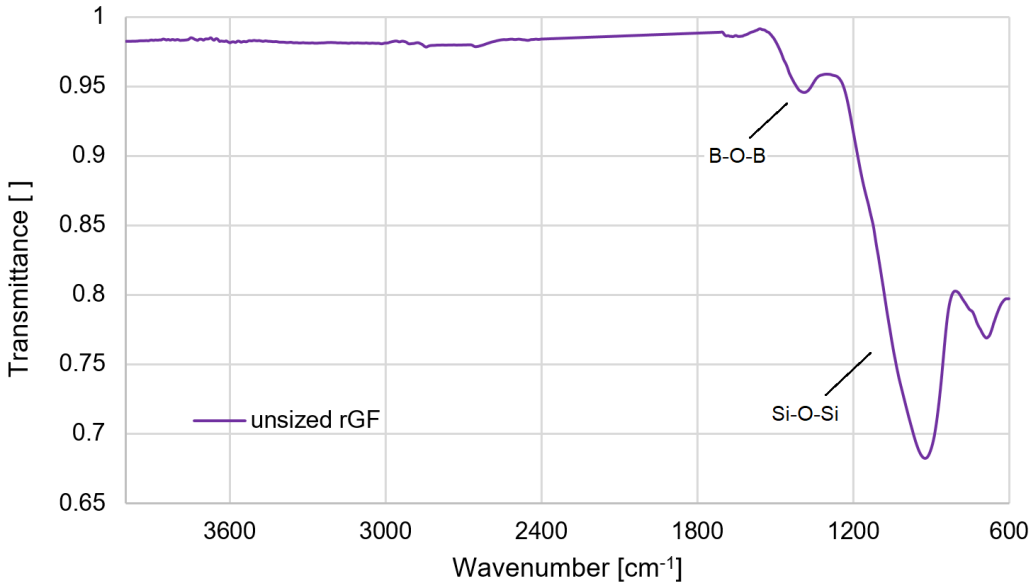

Figure 39. *FTIR spectrum of unsized rGF.*

Figure 40 shows the FTIR spectrum of fibers resized with the 5 w% absolute concentration solutions. The thickness of sizing layer on fiber surface is much smaller than the depth of penetration of the IR, which is around 1 μm in case of diamond ATR. Therefore, the IR also travels throughout the crushed bulk fibers and most of the signal captured comes from this region and not from the sizing layer itself. This is why, for rGF samples, the most pronounced peak is related to Si-O-Si vibrations of the fiber. However, comparing the spectra of sized samples to the spectrum of unsized rGF, some changes are noticeable at 2700 – 3100 cm^{-1} 1200 – 1700 cm^{-1} and 600 – 1200 cm^{-1}, the regions indicated with the dashed square in figure 40. For 1 and 3 w% absolute concentrations, the same changes are noticed as in 5 w% absolute concentration, their whole spectra are collected in Appendix A (figures 51 and 52). Because those indicated regions are the ones with relevant change in peak intensity, the wavenumber was limited to them for easier observation (figure 41, figure 42, and figure 43).

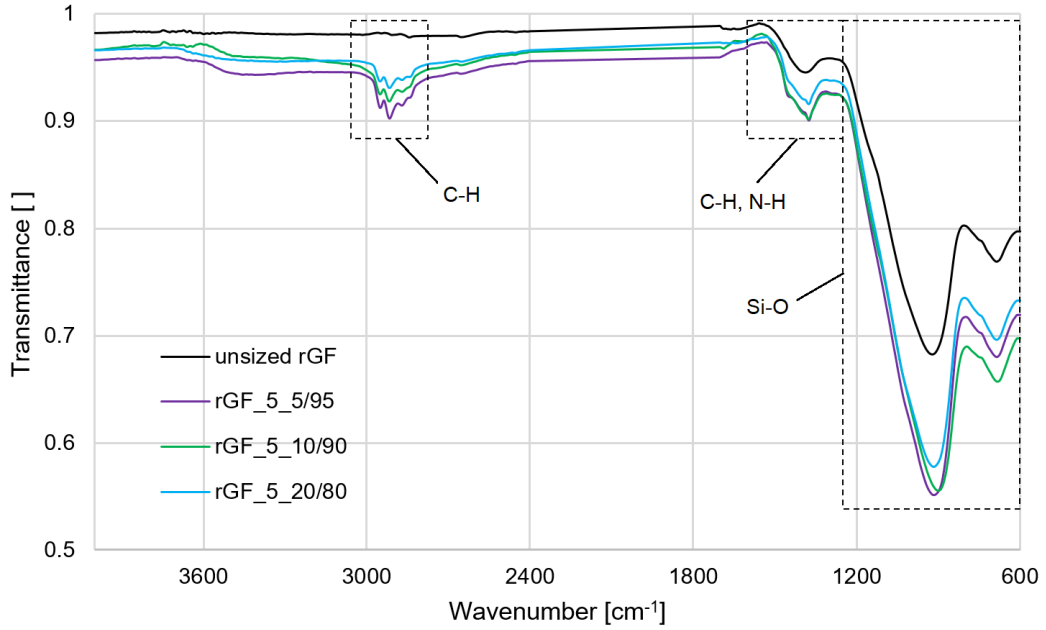

Figure 40. *FTIR spectrum of unsized rGF and rGF samples resized with 5 w% absolute concentration solution.*

The region of the spectrum between 2800 and 3000 cm^{-1}, presented in figure 41, is assigned to the stretching vibration of C-H bond in CH_2 and CH_3. Although the peak intensity is weak, it can be attributed to the presence of FF, due to its PP backbone (Liu et al. 2015), and also of CA, due to its aminopropyl segment (Sándor et al. 2016). Therefore, it is an evidence that the fiber's surface is sized. By comparing the spectrum of unsized rGF and sized samples on figure 41, while in the first one no peak is detected, the change in the C-H vibration's intensity is noticeable in most of the sized samples.

For 1 w% absolute concentration, samples with 90 and 95 w% FF did not present significant change in the peak intensity, it can indicate that the amount of sizing deposited was not sufficient and able to either cause changes in the fiber's surface composition or be detected by the IR. Sample with 80 w% FF, peaks were detected and it can be due to the higher amount of CA in the solution which could have improved the bonding of sizing and retention of FF and CA on the surface.

For 3 w% absolute concentration, the sample with the lowest amount of CA presented very weak peak intensity. An increase in the peak intensity could be noticed with the increase in the amount of CA from 10 w% to 20 w%, although the difference between them is slight. It can indicate better deposition of sizing on the fiber's surface when there is more CA in the sizing solution.

For 5 w% absolute concentration, it was visible that the higher the amount of FF the more intense was the peak. This is the contrary of what happened with the previous ones, in which the peak intensity increased with the increase in CA concentration.

From another perspective, it was also noticeable that the peak intensity increased with the increase of the absolute concentration when the relative concentration of FF and CA were kept constant. Since higher the concentration the more FF and CA was available in the solution, it was expected more of these constituents on the fiber's surface.

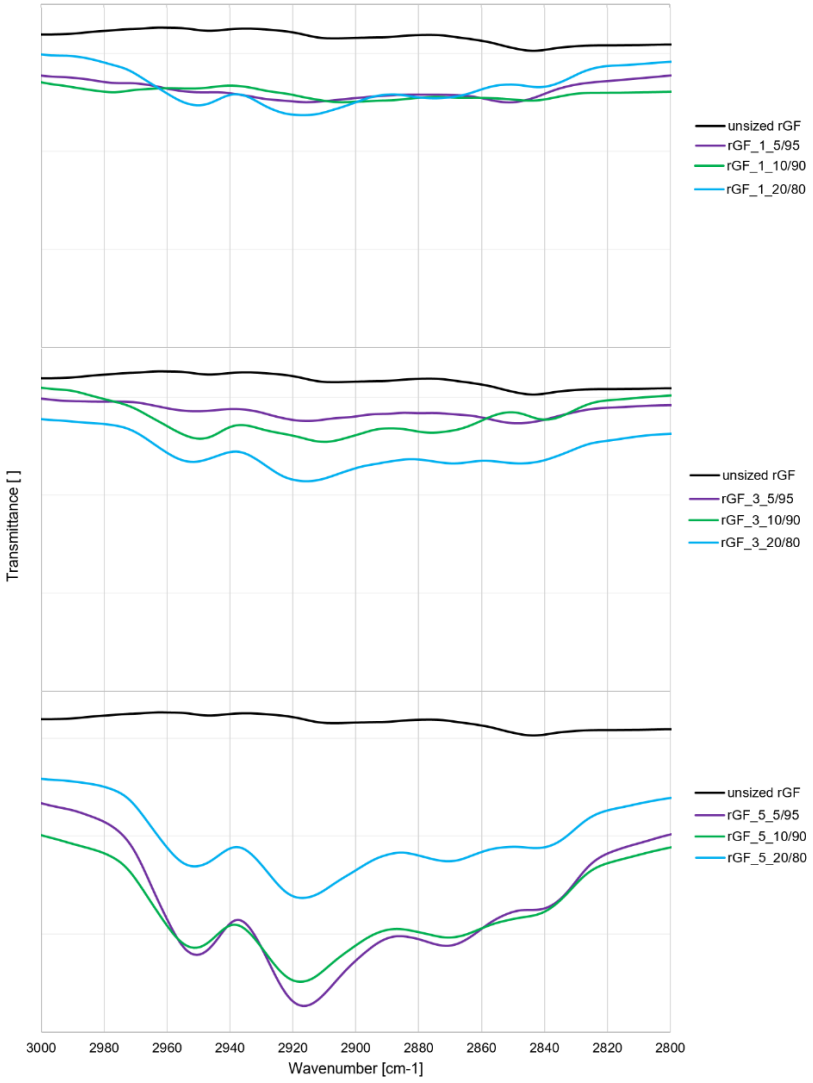

Figure 41. *FTIR spectrum between 2800 and 3000 cm^{-1} of unsized rGF and all resized rGF samples.*

The peaks in the range of 1300 to 1500 cm^{-1}, presented in figure 42, can be assigned to the bending vibrational mode of C-H of the PP backbone in MAPP (Liu et al. 2015) and of N-H in the amine group of ATPS (Sándor et al. 2016). Considering all sized samples, the peak intensity in this region was slightly stronger than the unsized samples, as seen in figure 42. This is another evidence of the presence of sizing in the fiber's surface. However, any correlation between the peak intensity and absolute and relative concentrations could be established, since the peak intensity of all samples seemed to be in a

similar magnitude. What was noticed, though, are the prominences around 1380 cm^{-1} and 1480 cm^{-1} on the rGF_5_5/95 and rGF_5_10/90.

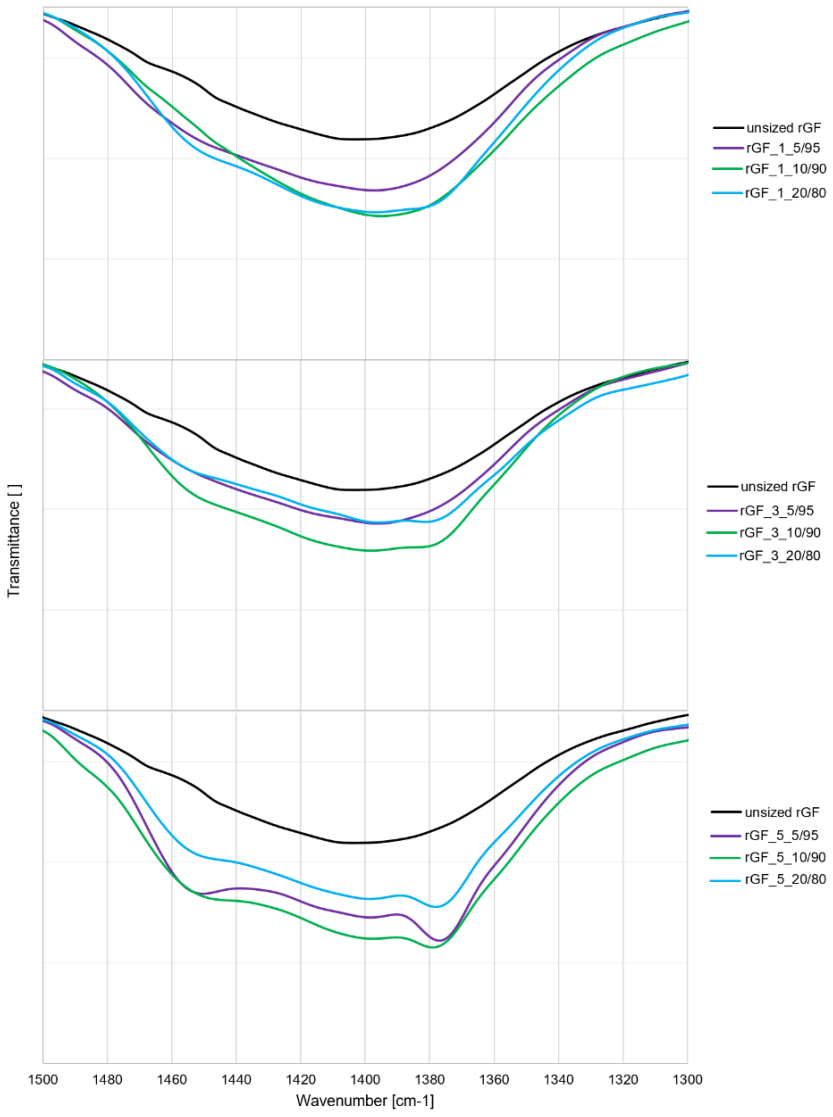

Figure 42. *Peaks in the range of 1300 to 1500 cm^{-1} of unsized rGF and all resized rGF samples.*

As discussed previously, the region between 600 and 1200 cm^{-1} is associated to different vibrational modes of Si-O-Si bonds from the glass fiber, but also from the CA groups. For the sized samples, as seen in figure 43, the peak intensity in this region is stronger comparing to the unsized fiber. Although it is not possible to differentiate between Si bonds coming from rGF or CA, this increase can be attributed to the presence of sizing in the fiber's surface, because bulk fiber remains unchanged during the resizing process. Therefore, besides the vibrations detected from the rGF, after resizing, vibrations from CA groups were detected as well. Again, any correlation between the peak intensity and

absolute and relative concentration could be established as the peak intensity of all samples seemed to be in a similar magnitude.

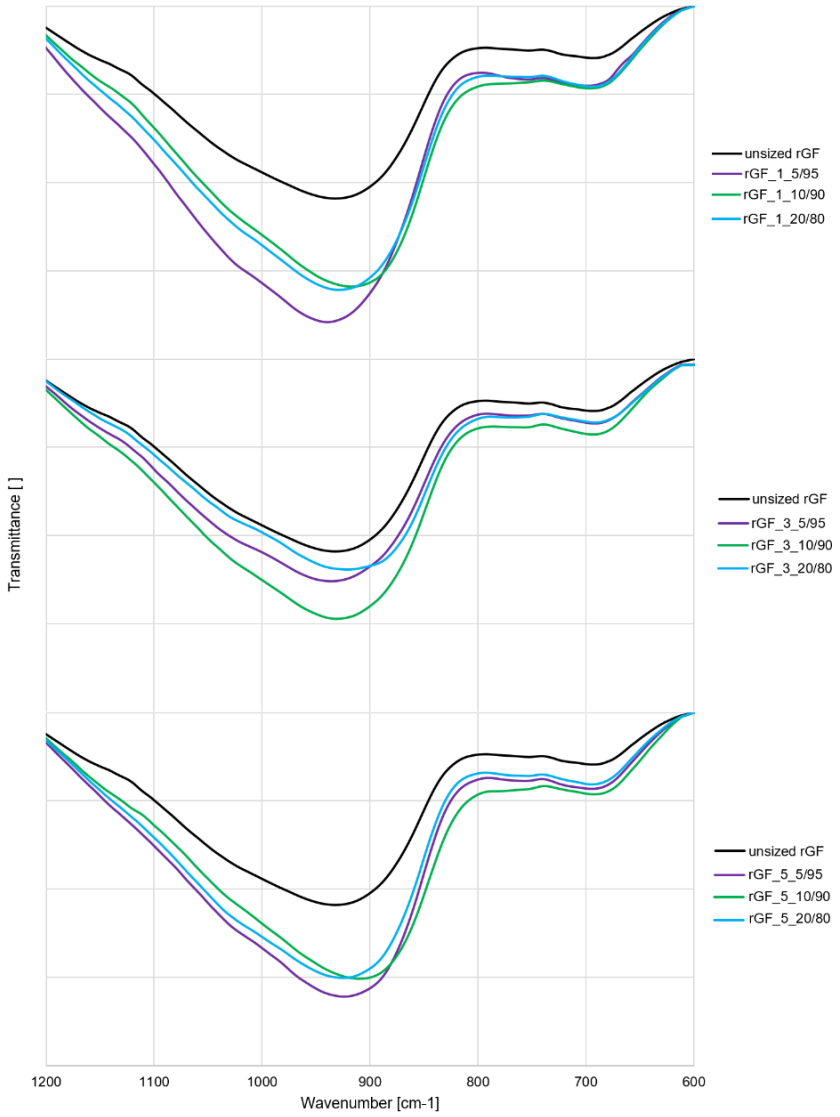

Figure 43. *FTIR spectrum between 600 and 1200 cm^{-1} of unsized rGF and all resized rGF samples.*

Because the rGF is considered stable at the temperature range of the experiment, the mass change steps presented on the curves are caused by the degradation of organic materials of the sizing on the fiber (Thomason et al. 2019). This could be further confirmed by comparing the TGA curves of the samples and the TGA curves of FF, CA and 'mixed solution', the degradation of the samples is compatible with their thermal behaviour discussed previously.

To verify the influence of heating rate on the results of the TGA of sized fibers, the samples with 5 w% absolute concentration were submitted to measurements at 5 and 10 K/min (Appendix B – figure 55 to 57). The lowest heating rate did not result in better

separation of overlapping events, on the other hand the curve shape was similar to the curves obtained from 10 K/min. Therefore, the use of 5 K/min showed unnecessary, because it did not reveal any other thermal events and the measurement time was too long. This way, the heating rate of 10 K/min was selected to proceed to the rest of measurements.

TGA graphs for samples heated in nitrogen atmosphere at 10 K/min are exhibited in Appendix B (figure 58 to 60). The curves follow similar shape in terms of mass loss in function of temperature, it was detected mainly two steps, in the range of 180 to 230 °C and of 360 to 405 °C. Thus, the measurements for all samples accused the presence of sizing as seen in table 5.

Results of mass loss are graphically illustrated in figure 44. For 1 w% absolute concentration, for samples with 90 and 95% FF the total mass loss at each step were similar, while for 80 w% FF it was two times bigger. The same trend was noticed for 3 w% absolute concentration. Therefore, in these cases, the higher the amount of CA the higher was the amount of sizing desorption detected by TGA, an indication of more sizing deposited on the surface.

On the other hand, the same did not happen to 5 w% absolute concentration. Samples containing 5 and 20 w% CA showed similar total mass loss while for 10 w% CA, it was around two and a half times bigger. Thus, the higher amount of CA did not lead to more sizing on the surface and the sample with 10 w% CA showed as the most successful resizing trial among all trials, in terms of the amount of sizing deposited. The reason sample rGF_5_20/80 did not presented the biggest mass loss, as was expected, can be that the high concentration of silane could have led to more self-polymerisation reaction due to the reactivity of the ethoxy groups in water instead of silane reaction with the reactive sites at the fiber's surface (Palimi et al. 2014). As a consequence, more resizing solution could have been removed from the fiber's surface during the rinsing stage of the resizing process, since the interaction with the surface was not strong enough.

Table 5. *Results obtained from TGA measurements of resized rGF.*

Sample	1st step		2nd step		Total mass loss (%)
	Mass loss (%)	Onset temperature (°C)	Mass loss (%)	Onset temperature (°C)	
rGF_1_5/95	0.08	204.2	0.05	367.8	0.13
rGF_1_10/90	0.08	193.1	0.06	374.9	0.14
rGF_1_20/80	0.09	225.7	0.17	402.0	0.26
rGF_3_5/95	0.11	212.4	0.11	394.1	0.23
rGF_3_10/90	0.09	201.6	0.11	378.8	0.20
rGF_3_20/80	0.11	211.3	0.30	398.3	0.42
rGF_5_5/95	0.07	201.1	0.24	401.3	0.31
rGF_5_10/90	0.16	185.9	0.54	392.5	0.70
rGF_5_20/80	0.04	194.8	0.26	386.6	0.29

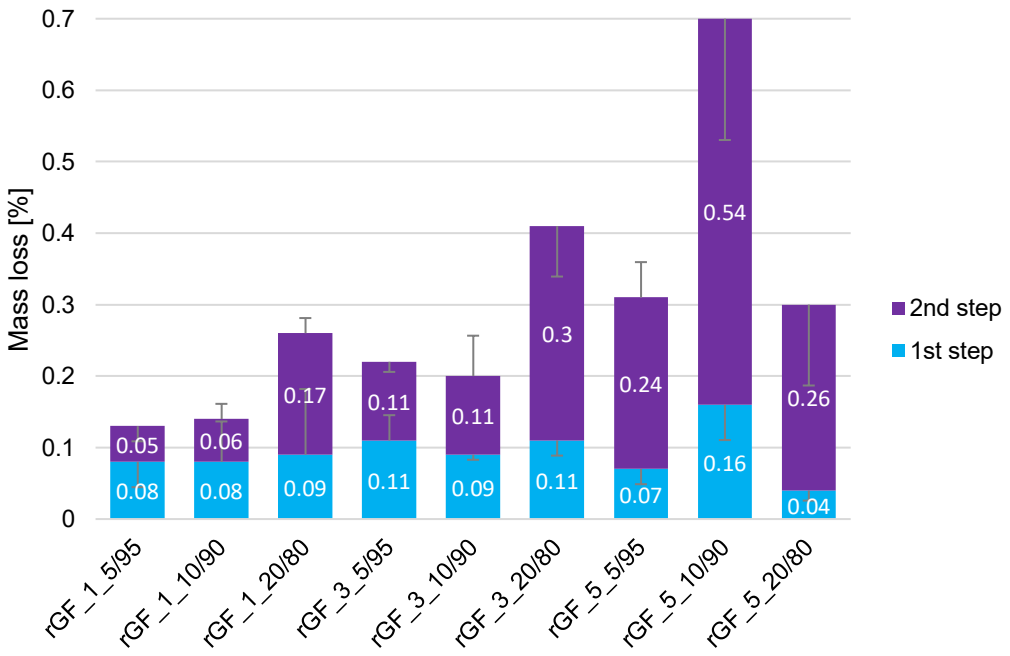

Figure 44. *The mass loss percentage on each degradation step of resized rGF samples obtained from TGA measurements.*

The first mass loss can be associated to the desorption of part of the sizing. Some authors, for example, attributed the mass loss in this region to the elimination of water from the condensation of Si-OH caused by the decomposition of surface bonded CA and desorption of carbon dioxide from carbamate originated from the interaction with silane amine group (Lee et al. 2017; Thomason et al. 2019).

Up to the beginning of the second step, the TGA curves for resized rGF samples are not a straight line similarly to the TGA curve of the dried ‘mixed solution’ presented in figure 35. This is because it should be considered that the sizing is interacting with the fiber’s surface, CA and FF are not just mixed together (as in the case of the ‘mixed solution’ in figure 34). From the literature, it is known that thermal desorption on the surface involves the breaking of bonds and the initiation of the process occurs at the weakest bonds (Beyler & Hirschler 2002). It is also stated in the literature, that the rate of mass loss on TGA measurements can be assumed to be proportional to the rate of bond scission (Anderson & Garcia 2011). In the case of the sizing, its multiple ways to interact with the fiber’s surface, as seen previously, may lead to the establishment of bonds of dissimilar energies. This way, the activation energy required to rupture them changes and, subsequently, desorption occurred in longer time span in this region. Moreover, with the increasing of the temperature, as the bonds of the sizing layer break, smaller molecular fragments are formed and volatilized, resulting in the sample’s mass loss. The lighter fragments volatilize immediately after being created and the heavier ones remain on the surface in the solid or liquid phase for some time until their volatilization (Beyler & Hirschler 2002).

The second mass loss step can be related to the desorption of the sizing fraction that was more strongly bonded to the surface (Petersen 2017). Considering the discussions in section 6.1, CA is the only component meant to establish covalent bonds with the fiber’s surface, however, because at this step the mass loss amount exceeds what was expected to originate from the CA, it can be assumed that also FF degraded at this stage (Petersen 2017). As seen in figure 28, this is the region the dried FF presented the single mass loss step.

However, comparing to the onset temperature of the dried ‘mixed solution’ in figure 35, the onset temperature of resized samples are shifted 15 to 50 °C lower, approximately. It can be explained by the difference in the surface to volume ration (SRV), sample size and concentration. The material’s degradation usually is accelerated with higher SRV, the fibers have very small diameter and the sizing coating thickness is also very small, in the order of micrometers, and the SRV should be higher comparing to the solid particles in the dried ‘mixed solution’, when turned into a powder (Thomason 2019).

The resultant TGA curves were clearly different depending on the selected atmosphere. When heated in air, the majority of the sizing layer degraded in the range of 180 to 220 °C. Curves of measurements preformed in air atmosphere at 10 K/min are presented in Appendix B (figure 61 to 63). As can be seen in figure 45, the introduction of oxygen as the purge gas led to a decrease in the start temperature of the main mass loss step, in

other words, the thermal changes on the sample were accelerated by the presence of oxygen. Therefore, the sizing is more thermally stable in nitrogen atmosphere and the major degradation in air has thermos-oxidative nature (Thomason et al. 2019).

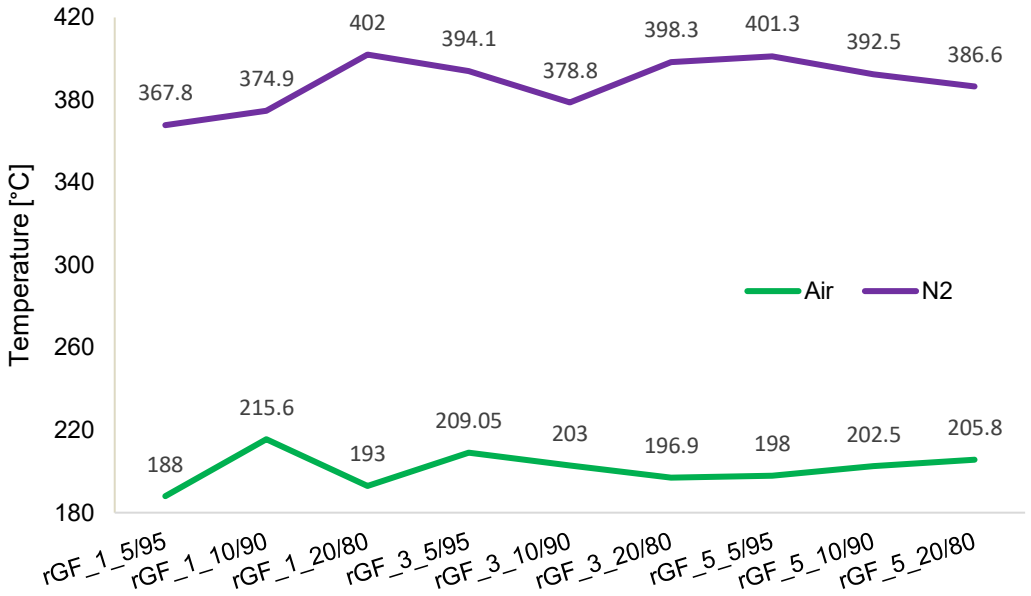

Figure 45. *The onset temperature of the main mass loss step detected on the TGA curves of resized rGF samples according to the atmosphere used on the experiment.*

For TGA measurements performed both in nitrogen or air, results regarding to the temperatures in which the main degradation steps occurred were in accordance with the study conducted by Thomason et al. (2019) about the thermal degradation of polypropylene compatible glass fiber sizing. In the study, it was assumed that MAPP and APTS were, respectively, the FF and CA in the sizing composition.

6.3 Characterization of recycled carbon fibers

From TGA of unsized rCF, it was also possible to conclude that they were sufficiently clean to be resized without previous cleaning. Again, TGA measurements were performed in nitrogen and at a heating rate of 10 K/min. After blank curve subtraction the TGA curves presented in figure 46 were obtained. The rCF presented a mass loss between 30 °C and 150 °C, that is associated to the desorption of volatile species such as water, carbon monoxide and carbon dioxide (Bascom & Drzal 1987), and was stable up to 500 °C. After this temperature, the mass loss occurred due to the pyrolysis of the material. Except from those two changes observed, it is possible to attribute the events on TGA curve to the sizing on the fibre's surface. Therefore, because no thermal degradation of organic components was detected between 150 °C to 500 °C, it indicates the absence of significant amount of sizing that could be detected by the equipment.

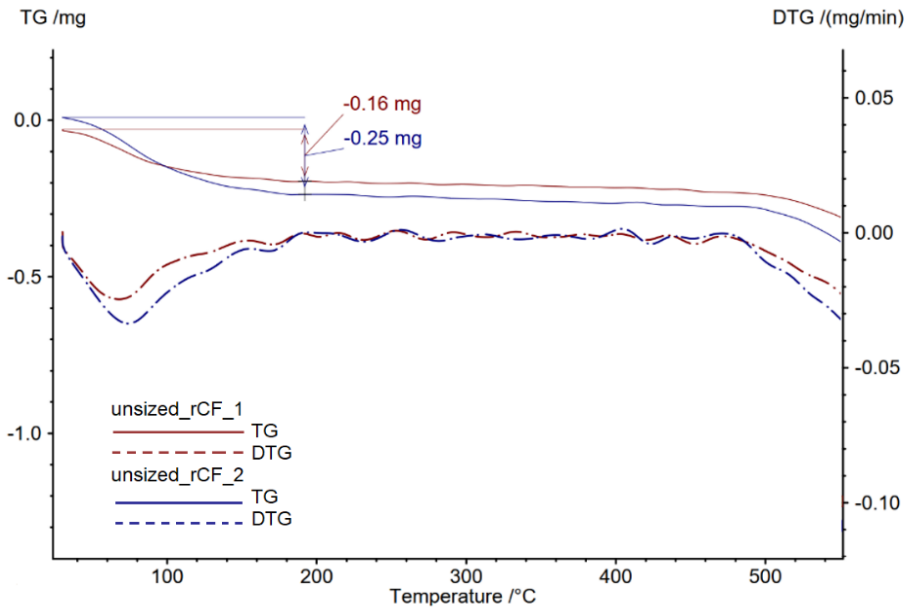

Figure 46. *TGA curves of two measurements done with unsized rCF.*

For unsized rCF, and also for the resized rCF, the FTIR-ATR diamond technique was not a reliable method. Only polar bonds are IR active, which means that only polar bonds display bands in the IR spectrum. Therefore, carbon – carbon bonds are not detectable and considered 'invisible' in IR. Results were not repeatable and signals were highly absorbed and scattered, suggesting that the IR bean was not interacting properly with the sample. In addition, it could not detect functional groups on the surface. Therefore, it cannot be said that any spectrum in fact belongs to the sample (examples of rCF spectra obtained from FTIR-ATR in Appendix A – figure 53).

Because ATR germanium is known to be more effective with black samples and to have lower depth of penetration, what would be advantageous on the analysis of the thin resizing layer, it was also tested to verify if it would generate better spectra. As seen in figure 54 in Appendix A, the measurement of the unsized rCF with germanium crystal also did not resulted in clean peaks on the spectra that would correspond to the material. Still a lot of the signal were absorbed and scattered.

Considering that the TGA measurement at 5 K/min was not advantageous for resized rGF samples, it was assumed that the same would happen with resized rCF samples, thus only measurements at 10 K/min were performed. The results of TGA measurements are presented in table 6. From the analysis of the curves collected in Appendix C (figure 73), it was possible to highlight three mass loss steps in all samples. They occurred in the following temperature intervals: 155-175 °C, 285-320 °C, 415-455 °C.

The first mass loss step was related to the significant presence of physisorbed materials on the surface, similarly to the unsized rCF discussed previously. Next detected mass loss steps were associated to the desorption of the chemisorbed constituents (Bascom & Drzal 1987). Thus, as the sizing formulation for rCF resizing contains only FF and because it was assumed that signals detected on TGA up to 500 °C come from the sizing layer only, it is reasonable to conclude that the second and third steps are related to FF thermal degradation.

Table 6. *Results obtained from TGA measurements of resized rCF.*

	1st step		2nd step		3rd step		Total mass loss (%)
Sample	Mass loss (%)	Onset temp. (°C)	Mass loss (%)	Onset temp. (°C)	Mass loss (%)	Onset temp. (°C)	
rCF_1_ar	0.34	175.9	0.57	316.9	0.10	419.6	1.01
rCF_1_pt	0.43	168.6	0.78	292.4	0.10	454.6	1.31
rCF_5_ar	0.40	164.1	1.21	299.8	0.47	431.1	2.08
rCF_5_pt	0.23	158.0	0.54	287.6	0.11	440.2	0.88

As seen in figure 47 obtained from table 6, the second step was the one with the most pronounced mass loss, accounting for more than 50% of the total mass loss. Comparing to the TGA curve of dried FF (figure 28), this main mass loss step was shifted to even lower temperatures, around 90 to 120 °C decrease. The more pronounced shift to lower temperature can be associated once more to the SRV and as the diameter of CF is even smaller than the diameter of GF, the SRV was higher in this case. The third mass loss step can be also related to thermal degradation of the FF. In this case, it can be associated to other components of the FF solution. Because the exact formulation of it was unknown, it could consist of a mixture of different polymers (Petersen 2017).

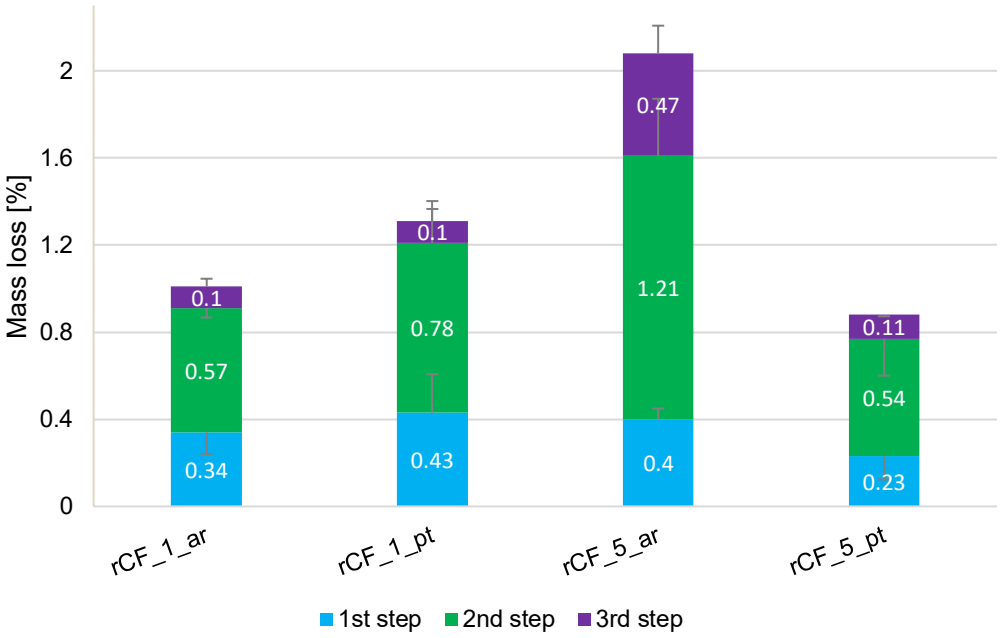

Figure 47. *The mass loss percentage on each degradation step of resized rCF samples obtained from TGA measurements.*

Mass loss steps were not sharp as seen on the TGA curve of dried FF (figure 28), but mass loss occurred more smooth along the temperature range of the measurement. Similarly to what was discussed in the case of resized rGF in section 6.2, it can be considered that FF interacts with the fiber's surface at different intensities, thus the activation energy required to desorb the sizing was varying.

Considering the 1 w% concentration samples, the pre-treatment resulted in a mass loss around 30% bigger comparing to the untreated sample. For the 5 w% concentration samples, the untreated sample had a total mass loss almost two and a half times bigger than the pre-treated sample. The 5 w% concentration sample resized as received had a more pronounce mass loss comparing to the other resizing trials. It can be considered that the bigger the total mass loss the bigger the amount of sizing deposited on the fiber's surface. However, it is uncertain to draw conclusions if it might or not indicate that the resizing was successful in terms of quality and level of interaction with the surface.

As discussed in section 3.3, the increasing on the oxidation degree of the fibers, that is considered to be achieved with the HNO_3 treatment, for example, lead to an improvement of the wettability and, thus, better interaction between the sizing and the fiber's surface. According to Moosburger-Will et al. (2018), the better the wetting the thinner the sizing layer on the fiber's surface, therefore the lower the amount of sizing on the fibers, resulting in a smaller mass loss on TGA analysis. From this point of view, the better resizing trial would be sample rCF_5_pt. Nevertheless, based on the same authors, the low

amount of sizing on sample rCF_5_pt could also indicate not homogeneous fiber coverage caused by insufficient or inadequate wetting of the fiber and not high activation of the surface.

The thermal behaviour of the sizing considerably changed depending on the atmosphere selected for the measurement. When heated in air, one main mass loss step was detected in the range of 260 to 275 °C, as seen in figure 48. Curves of the measurements preformed in air atmosphere at 10 K/min are presented in Appendix C (figure 74). Similarly to what happened to resized rGF samples, the sizing is more thermally stable in nitrogen atmosphere. It is known that PP is sensitive to the presence oxygen, thus its introduction as the purge gas accelerated the degradation process and lowered starting temperature of the mass loss (Beyler & Hirschler 2002). Furthermore, the beginning of the degradation of the rCF itself started at lower temperature and at a higher rate, what was expected in the presence of oxygen.

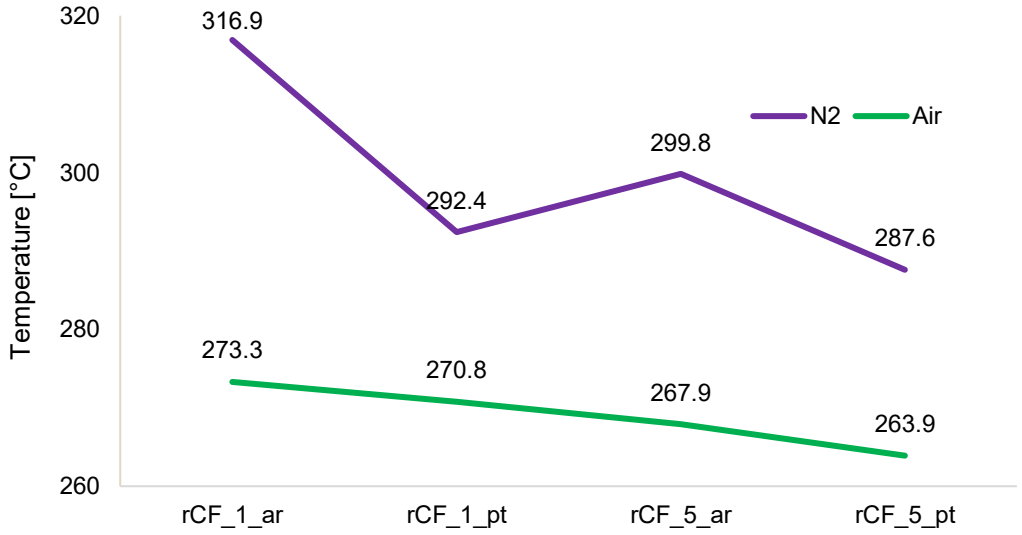

Figure 48. *The onset temperature of the main mass loss step detected on the TGA curves of resized rCF samples according to the atmosphere used on the experiment.*

6.4 Extraction of physisorbed and chemisorbed sizing

6.4.1 Resized rGF

The results for extraction followed by burning process for resized rGF are presented in figure 49. The amount of sizing removed by extraction and burning were both in the range of 35-65% of the total mass loss.

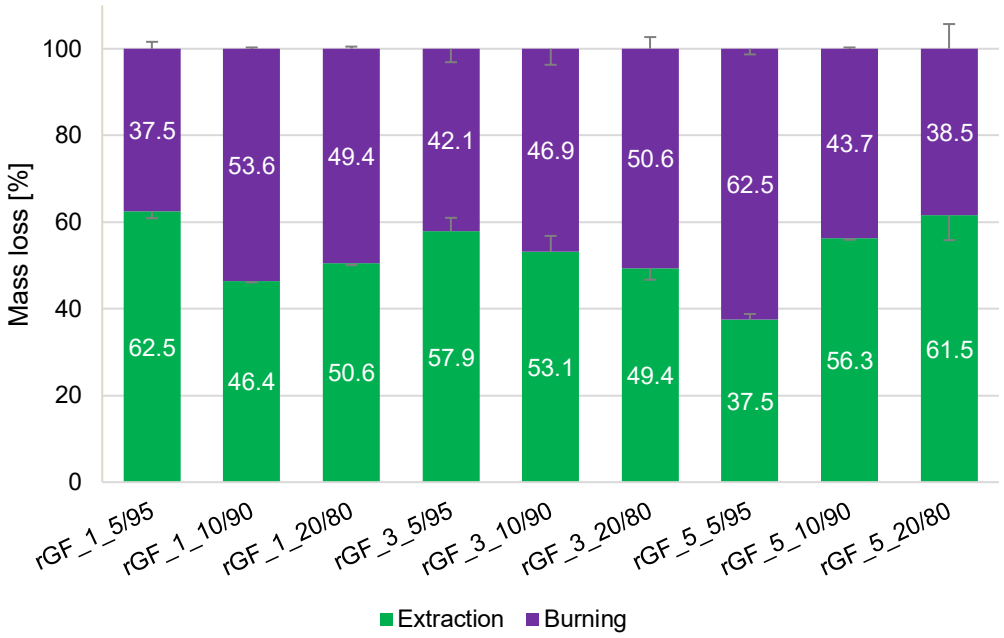

Figure 49. *Normalized mass loss of resized rGF samples after solvent extraction and burning.*

Petersen (2017) defined that the sizing on the GF can be divided as follows: FF, organic and inorganic part of bonded CA, organic and inorganic part of free CA. In soxhlet extraction, the FF and the organic and inorganic part of free CA would be removed. During the additional burning step, also the organic part of the bonded CA would be removed. The inorganic part of the bonded silane is supposed to stay on the fiber's surface.

For the samples resized with 3 w% absolute concentration solution, the higher the amount of CA the higher was the chemisorbed portion of the sizing. Therefore, it can be supposed that more substantial sizing layer was formed onto the surface, in terms of level of interaction between these components (Mittal & Pizzi 2002). On the other hand, for the samples resized with 5 w% absolute concentration solution, the opposite happened. Even though the concentration was higher, it did not bring considerable improvement in terms of bond formation between the sizing and the surface. This can be attributed to the probable higher degree of polymerization of the silanol groups leading to siloxane formation before any interaction with the fiber's surface, as discussed in section

6.1. It would cause the formation of multiple physisorbed layers on top of the surface (Acres et al 2012; Palimi et al. 2014). It could also be attributed to a significant amount of CA interacting with the fiber's surface through hydrogen bonds, resulting in low grafting onto it (Smith & Chen 2008). Considering that higher chemisorbed portion suggests better resizing process, sample rGF_5_5/95 was the most successful trial.

According to literature, the extractable part is mostly FF, therefore it could be considered that the mass loss percentage on this step should be similar to the portion of FF on the resizing solution. However, the mass loss on the extraction is not correlated to the amount of FF in the resizing solutions, which are 80, 90 and 95 w%. Possible explanations for this are (1) the rising step of the resizing process could have removed relatively more FF than CA. The rising step has important influence on the quality of the sizing deposited on the surface. Because FF is not bonded to the surface, rising could mechanically displace it away from the surface (Smith & Chen 2008); (2) the FF could also have established chemical bonds with the fiber's surface so then part of it would be removed just by burning. This hypothesis can be weakened by the fact that the dried FF was released easily from the glass watch and also, in literature, Petersen (2017) stated that CA is the only component that bonds to the surface; and (3) the different ways that the CA interacts with the fiber's surface could influence also the way the FF interacts with the CA. Therefore, different parts of not bonded sizing would still be left at the surface. Depending on the crosslink density of the polysiloxane network at the surface, the FF chains would be more or less entangled to it (Karger-Kocsis et al 2015).

Consistent indications that could supports the last two assumptions and the presence of FF on the fibers even after solvent extraction. First one is the fact that the rGF still had a smooth texture after extraction similar to resized fibers. On the other hand, after burning, fibers were very brittle as the unsized rGF. Those same characteristics were also noticed by Petersen et al. in their study about characterization of glass fiber (Petersen et al. 2013). Second, from the TGA curves collected in Appendix B (figures 64 to 72), it was verifyied that after extraction there was still sizing on the surface of the samples, only rGF_1_10/90 and rGF_1_20/80 the mass loss step was not clearly visible but still present. And, after burning, no mass loss was detected, indicating no organic portion of the sizing on the fiber's surface anymore.

6.4.2 Resized rCF

As rCF was resized only with FF, the intention of the procedure was to evaluate if the FF established chemical bonds with the fiber's surface. Results for extraction and burning performed on rCF samples are presented in figure 50. Normalized results for the weight loss after the first one and after the second one were in the range of 45 to 65% and 35 to 55%, respectively.

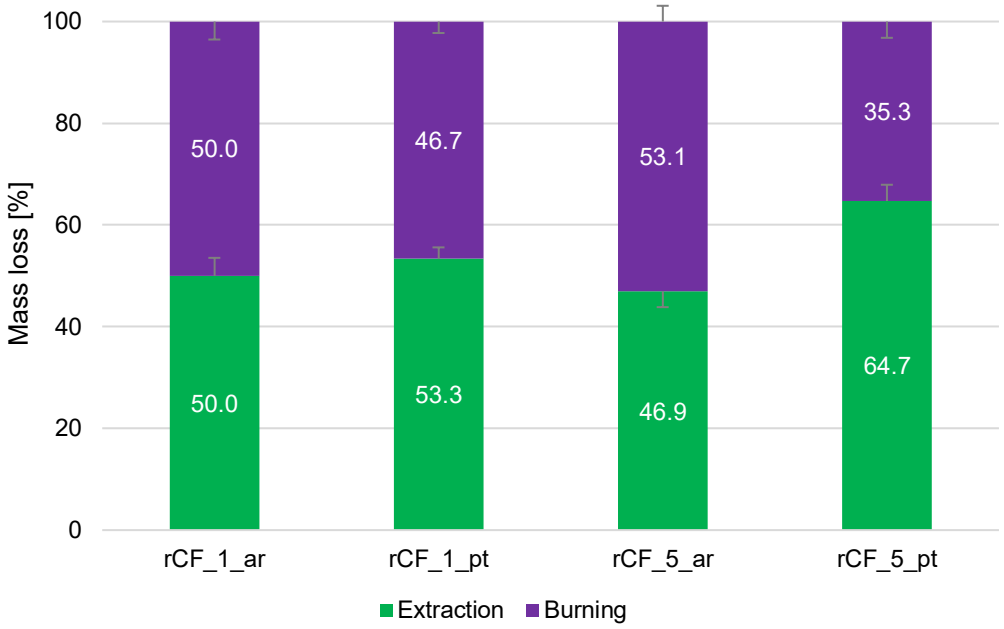

Figure 50. *Normalized mass loss of resized rCF samples after solvent extraction and burning.*

This way, it was concluded that, in all samples, a portion of the sizing formed chemical bonds with the fiber's surface. The fact that certain amount of sizing was still present on the surface after acetone extraction, and could be removed just by burning, is further confirmed after mass loss steps were detected on the TGA curves of the fibers still after solvent extraction. Furthermore, from the curves after burning, it was possible to validate that all the sizing was removed from the fiber's surface. Graphs are collected in Appendix C (figure 75 to 78).

Samples resized in the 1 w% resizing solution behaved similarly considering the percentage in mass loss they had. The sample resized as received in the 5 w% sizing solution had the biggest mass loss in the burning. According to what was discussed previously in section 6.3, based on a study done by Moosburger-Will et al. (2018), higher amount of sizing removed by solvent extraction would indicate lower activation degree and ability of the fibers to establish interactions with the sizing. Therefore, it can be assumed that sample rCF_5_ar was the most successful resizing trial in terms of quality of

interaction between the sizing layer and the fiber's surface. On the other hand, the pre-treated sample resized as received in the 5 w% sizing solution presented the biggest mass loss in the solvent extraction. Thus, the hypothesis that this trial would be the most successful considering that its low mass loss is related to better surface/sizing interaction is not true.

In the literature, it is stated that the type of sizing solution, in terms of concentration, do not influence significantly on how much of the sizing could chemically bond to the surface. The establishment of those bonds is constrained by the amount of reactive oxygen groups on the surface. Thus, what in fact affects this aspect is the degree of surface activation (Moosburger-Will et al. 2018). However, there is an inconsistency between this present work and the literature since it was not noticed a significant increase of chemically bonded sizing portion on the fiber's surface with the addition of the activation pre-treatment. For both concentrations, pre-treated samples exhibited greater mass loss with solvent extraction.

7. CONCLUSIONS

The present work had the purpose to characterize the recycled glass (rGF) and carbon fibers (rCF) that were resized with a solution containing coupling agent and film former, for rGF, and film former, for rCF. The characterization was mainly performed by thermogravimetric analysis (TGA), but Fourier-transform infrared analysis and extraction and burning process were implemented as well. The main points of interest were the determination of the amount and composition of the sizing layer on the fibers after the resizing process and the evaluation of the accuracy of the TGA method in sizing characterization. The conclusions of the work are presented in the following paragraphs.

Considering the TG analysis, lower heating hate was not advantageous, because it did not reveal any thermal events. Furthermore, the thermal stability of the sizing was different depending on the atmosphere used on the measurement. In the temperature range of the measurements in nitrogen atmosphere, it was concluded that the total mass loss, in case of rGF, and most of the mass loss, in case of rCF, derived from the sizing layer. Therefore, it was possible to determine the amount of sizing on the fiber's surface by localizing the steps on the TGA curves of the samples and quantifying their mass loss percentages with the aid of the equipment's software. Utilizing this approach, sizing was detected in all resized samples.

Regarding to the composition of the recycled and resized fibers, TGA was a suitable method, but also FTIR-ATR, for rGF. Based on the TGA measurements performed on samples containing only the CA, only the FF and the 'mixed solution', it was possible to recognize the presence of CA and FF on the thermal desorption curves of the resized samples of either rGF or rCF. On FTIR, functional groups from the film former and silane coupling agent could be identified on the resized rGF. In this case, FTIR was a quick measurement that could confirm the presence of the sizing on the fibers and indicate the nature of these existing components. The FTIR-ATR method, however, was not able to provide consistent results on the analysis of the resized rCF.

For resized rGF, higher mass loss on TGA measurement was not directly related to higher absolute concentration of the resizing solution. Besides, even the increasing on the relative concentration of CA did not lead to an increase in the total amount of sizing on the surface in every case. From the results of the physisorbed and chemisorbed extraction, although the sizing on the fibers correspond to the resizing solution, the amount of FF that was expected on the surface of rGF, based on the relative concentration of

this component on the resizing solution, may not have been reached. This assumption was made considering that, for all samples, the physisorbed fraction, composed mainly by FF, was much lower than 80, 90 or 95 w%.

For the resized rCF, the higher the resizing solution concentration the higher the mass loss on TGA measurement. However it did not necessarily mean that the sizing layer had quality in terms of the amount of bonded sizing. For this reason, the extraction study was advantageous to verify which trial resulted in the best deposition of sizing layer, once it indicated the amount of bonded sizing. Furthermore, it also showed that the HNO_3 pre-treatment did not bring considerable advantage in terms of improvement on the reactivity of the rCF surface and the fraction of chemisorbed sizing.

It can be assuredly concluded that TGA, which was the characterization method this work focused, provided rich information on the study and characterization of the recycled and resized fibers. The determination of the nature and amount of sizing on the fiber's surface was possible. However TGA technique had its sources of uncertainty and its drawbacks.

On TGA measurement, as the sizing on the surface is minor comparing to the quantity of fibers on the samples, TGA signals could have scattered and, then, the detection of the degraded material could be inaccurate or inexistent. There were uncertainties regarding to very small mass loss steps, because it was challenging to evaluate if they were associated to a change on the sample itself or if they originated from fluctuations during the measurement. Moreover, representativeness of the curves could be questionable due to sizing's uneven distribution or chemical micro-heterogeneities that could exist along the fibers. As a consequence, samples prepared for analysis could present differences in the sizing layer even coming from the same resizing batch. Finally, it was not so clear to distinguish which mass loss steps were due to the FF desorption and which ones were due to CA desorption.

Therefore, it is also concluded that no single technique can itself give a complete characterisation of the resized fibers in terms of chemical and compositional information and quality of the resizing process. The combination of techniques is the strategy to achieve more solid understanding about the material. This way, the FTIR and the physisorbed and chemisorbed extraction process were significant to establish better conclusions about the analysed samples.

From the findings of this work and considering that the main objective of resizing recycled fibers is to make them efficient on a new composite, it is reasonable to ponder about the scalability of the resizing process on the industrial level. The resizing process in large

scale should be designed in a way to avoid possible inhomogeneity on the fibers. As seen, depending on the parameters, such as rinsing step, degree of surface activation, selected solvent, drying time, concentration of CA or FF, the quality of the resizing layer regarding to its uniformity, coverage and level of interaction with the surface is affected. The issues that could arise from the resizing method is resolvable, for example, by trial and error testing in a small scale plant and by consistent research to achieve the optimum process. The challenge in the process that would be problematic to overcome, however, is the existent chemical heterogeneity of the fibers from manufacturer to manufacturer and also caused by the fiber's history, such as how it was cooled and stored. Therefore, fibers from different sources may respond to recycling process in a different way and this would result in a wide range of recycled and resized fibers with different properties. As a consequence, it is not possible to ensure that all recycled fibers would have same properties after resizing.

For further research on the subject, the recommendations would include:

- Using a crucible of higher volume, if the sample holder of the TGA device is compatible to it. More material added on the crucible would intensify the signals coming from the sizing layer;
- The application FTIR technique was not effective using either ATR diamond or ATR germanium, in case of rCF. Therefore an alternative to enable the measurement of rCF on FTIR would be coupling an integrating sphere on the equipment. The integrating sphere is an accessory that provides the ability to collect the transmission spectrum of highly scattering and highly absorbing samples;
- TG-FTIR coupled analysis provided elucidating data for the thermal behaviour of the FF. Therefore, it should be performed also on the CA only, the 'mixed solution' and even on the resized fibers;
- Considering the resizing process, there is the chance that the rinsing step could have removed part of the weakly bonded sizing deposited on the fiber's surface by mechanic action. Changing the rinsing method or use a dry solvent on the resizing solution could be alternatives to be tested in order to reduce the multilayers of physisorbed sizing. Dry solvents would avoid the extensive hydrolysis of the silanes before their interaction with the glass surface. Then, surface adsorption of the sizing is meant to happen more efficiently and controlled;

- Other characterization methods should be applied in order to have even more consistent information about the chemistry of the sizing layer and quality of the wetting of the fibers. For example, X-ray photoelectron spectroscopy for the compositional analysis of the microscopic surface, or scanning electron microscopy for morphological information of the sizing layer's surface.

REFERENCES

Acres, R.G., Ellis, A.V., Alvino, J., Lenahan, C.E., Khodakov, D.A., Metha, G.F., & Andersson, G.G. (2012). Molecular structure of 3-aminopropyltriethoxysilane layers formed on silanol-terminated silicon surfaces, The Journal of Physical Chemistry C, Vol. 116(10), pp. 6289-6297.

Anderson, B. J., & Garcia, J. P. (2011). Thermal stability of high temperature epoxy adhesives as measured by accelerated TGA DMA and adhesive strength. Paper presented at the retrieved from https://www.osti.gov/servlets/purl/1120656.

Akonda, M.H., Lawrence, C.A. & Weager, B.M. (2012). Recycled carbon fibre-reinforced polypropylene thermoplastic composites, Composites Part A, Vol. 43(1), pp. 79-86.

Bascom, W. D., & Drzal, L. T. (1987). The surface properties of carbon fibers and their adhesion to organic polymers, NASA Contractor report 4084.

Bashir, S.T., Yang, L., Anderson, R., Tang, P.L., Liggat, J.J. & Thomason, J.L. (2017). A simple chemical approach to regenerating the strength of thermally damaged glass fibre, Composites Part A, Vol. 102 pp. 76-87.

Bassetti, S. (2017). Fiber Sizing Fundamentals and Emerging Technologies, Michelman, SPE Automotive.

Beyler, C.L., Hirschel, M.M. (2002), Thermal decomposition of polymers. In: DiNenno, P.J., Drysdale, D., Beyler, C.L., Walton, W.D.W., Custer, R.L.P., Hall, J.R., Watts, J.M. (Eds.), *SFPE handbook of fire protection engineering, 3rd ed., section 1, chapter 7* (pp. 110-131). USA: National Fire Protection Association.

Bikiaris, D.N., Vassiliou, A., Pavlidou, E. & Karayannidis, G.P. (2005). Compatibilisation effect of PP-g-MA copolymer on iPP/SiO2 nanocomposites prepared by melt mixing, European Polymer Journal, Vol. 41(9), pp. 1965-1978.

Burn, D., Harper, L., Johnson, M., Warrior, N., Nagel, U., Yang, L. & Thomason, J. (2016). The usability of recycled carbon fibres in short fibre thermoplastics: interfacial properties, Journal of Materials Science, Vol. 51(16), pp. 7699-7715.

Connor M, Allen B, Heil J. (2006). Recycled carbon fiber analysis: mechanical properties. In: SAMPE Fall technical conference proceedings: global advances in materials and process engineering, Dallas.

Dai, Z., Shi, F., Zhang, B., Zhang, Z. & Li, M. (2011). Effect of sizing on carbon fiber surface properties and fibers/epoxy interfacial adhesion, Applied Surface Science, Vol. 257(15), pp. 6980-6985.

Downey, M.A. & Drzal, L.T. (2016). Toughening of carbon fiber-reinforced epoxy polymer composites utilizing fiber surface treatment and sizing, Composites Part A, Vol. 90 pp. 687-698.

Durai Prabhakaran, R. T., Thomason, J., Yang, L. (2018). Recycled glass fibre/polyester resin system – interface characterization. In: 4th Brazilian Conference on Composite Materials, Rio de Janeiro.

Feng, N., Wang, X. & Wu, D. (2013). Surface modification of recycled carbon fiber and its reinforcement effect on nylon 6 composites: Mechanical properties, morphology and crystallization behaviors, Current Applied Physics, Vol. 13(9), pp. 2038-2050.

Feresenbet, E., Raghavan, D. & Holmes, G.A. (2003). The influence of silane coupling agent composition on the surface characterization of fiber and on fiber-matrix interfacial shear strength, The Journal of Adhesion, Vol. 79(7), pp. 643-665.

Gran View Research. (2017). Carbon fiber market analysis by raw material (PAN, pitch), by tow size, by application (automotive, aerospace & defense, wind turbines, sport equipment, construction, pressure vessels), and segment forecasts, 2018 - 2025. (). United States: Grand View Research, Inc., 169 pp.

Holmes, M. (2018). Recycled carbon fiber composites become a reality, Reinforced Plastics, Vol. 62(3), pp. 148-153.

Jenkins, P., Yang, L., Thomason, J., Chen, X., Watts, J. & Hinder, S. (2019). Investigation of Chemical and Physical Surface Changes of Thermally Conditioned Glass Fibres, Fibers, Vol. 7(1), pp. 7.

Jiang, L., Ulven, C.A., Gutschmidt, D., Anderson, M., Balo, S., Lee, M. & Vigness, J. (2015). Recycling carbon fiber composites using microwave irradiation: Reinforcement study of the recycled fiber in new composites, Journal of Applied Polymer Science, Vol. 132(41), pp. 1-9.

Job, S., Leeke, G., Mativenga, P.T., Oliveux, G., Pickering, S., Shuaib, N.A. (2016). Composites recycling: Where are we now?, Composites UK.

Jones, F.R. (2010). A Review of Interphase Formation and Design in Fibre-Reinforced Composites, Journal of Adhesion Science and Technology, Vol. 24(1), pp. 171-202.

Kanemasu, M., Nishimura, W., Yoshikawa, A., Yamamori, T., Kobayashi, R. (2018). Reduction on environmental impact by recycling waste composite materials for aircraft, Mitsubishi Heavy Industries Technical Review, Vol. 55 (2).

Kao, C.C., Thomason, J. (2014) Regeneration of thermally recycled glass fibre for cost-effective composite recycling: performance of fibre recyclates from thermoset composites and with subsequent ReCoVer treatments. In: 16th European Conference on Composite Materials, Seville.

Karger-Kocsis, J., Mahmood, H. & Pegoretti, A. (2015). Recent advances in fiber/matrix interphase engineering for polymer composites, Progress in Materials Science, Vol. 73 pp. 1-43.

Kim, J. & Mai, Y. (1998). Engineered interfaces in fiber reinforced composites, 1 ed. Elsevier, Amsterdam.

Kim, J. & Hodzic, A. (2003). Nanoscale characterisation of thickness and properties of interphase in polymer matrix composites, The Journal of Adhesion, Vol. 79(4), pp. 383-414.

Launer, P. (2013). Infrared analysis of organosilicon compounds: spectra-structure correlations, in: Arkles, B. & Larson, G.L., Silicon compounds: silanes and silicones – A survey of properties and chemistry, Gelest Inc., 3rd ed, 608 pp.

Laurikainen, P. (2017). Characterization of the Ageing of Glass Fibre-Reinforced Polymers, Tampere University of Technology.

Minchul Lee(이민철), Yeongseon Kim(김영선), Hyunjun Ryu(류현준), Sung-Hyun Baeck(백성현), & Sang Eun Shim(심상은). (2017). Effects of silane coupling agent on the mechanical and thermal properties of silica/polypropylene composites. 폴리머, Vol. 41(4), pp. 599-609.

Leroy, J. (2017). Composites and sustainability – the big picture, EuCIA blog. www.eucia.eu

Liu, Y., Zhang, X., Zhang, Y., Song, C., Fang, Y., Yang, B. & Wang, X. (2015). An effective surface modification of carbon fiber for improving the interfacial adhesion of polypropylene composites, Materials & Design, Vol. 88 pp. 810-819.

Menczel, J.D. & Prime, R.B. (2009). Thermal analysis of polymers: fundamentals and applications, Wiley, Hoboken, NJ, 688 p.

Mittal, K. and Pizzi, A. (2002). Adhesion promotion techniques. 3rd ed. New York: M. Dekker, 416 pp.

Moosburger-Will, J., Bauer, M., Laukmanis, E., Horny, R., Wetjen, D., Manske, T., Schmidt-Stein, F., Töpker, J. & Horn, S. (2018). Interaction between carbon fibers and polymer sizing: Influence of fiber surface chemistry and sizing reactivity, Applied Surface Science, Vol. 439 pp. 305-312.

Netzsch (n.d.-a). TG 209 F3 Tarsus®, Thermogravimetric Analysis – TGA: Method, Technique and Applications [Brochure]. Selb, Germany: Author.

Netzsch (n.d.-b). Coupling to Fourier Transform Infrared Spectrometers FT-IR: Concepts, Instruments and Applications from (10°C) RT to 2000°C [Brochure]. Selb, Germany: Author.

Netzsch (n.d.-c). Differential Scanning Calorimetry DSC 214 Polyma: Method, Technique, Applications [Brochure]. Selb, Germany: Author.

Oliveux, G., Dandy, L.O. & Leeke, G.A. (2015). Current status of recycling of fibre reinforced polymers: Review of technologies, reuse and resulting properties, Progress in Materials Science, Vol. 72 pp. 61-99.

Paabo, M. & Levin, B.C. (1987). A literature review of the chemical nature and toxicity of the decomposition products of polyethylenes, Fire and Materials, Vol. 11(2), pp. 55-70.

Palimi, M. J., Rostami, M., Mahdavian, M., & Ramezanzadeh, B. (2014). Surface modification of Cr2O3 nanoparticles with 3-amino propyl trimethoxy silane (APTMS). part 1: Studying the mechanical properties of polyurethane/Cr2O3 nanocomposites. Progress in Organic Coatings, Vol. 77(11), pp. 1663-1673.

Park, S. & Hey, G. (2015), Precursors and Manufacturing of Carbon Fibers, in: Park, S. (2 ed.), Carbon Fibers, Springer, Dordrecht, pp. 31-66.

Park, S. & Seo, M. (2011). Modeling of Fiber–Matrix Interface in Composite Materials, in: Park, S. & Seo, M. (volume 18), Interface Science and Technology, Elsevier Science & Technology, pp. 739-776.

Peters, L. (2018) Influence of Glass Fibre Sizing and Storage Conditions on Composite Properties. In: Davies P., Rajapakse Y. (eds) Durability of Composites in a Marine Environment 2. Solid Mechanics and Its Applications, vol 245. Springer, Cham.

Petersen, H.N. (2017). Investigation of sizing - from glass fibre surface to composite interface, Technical University of Denmark, PHD thesis, 84 p.

Petersen, H. N., Kusano, Y., Brøndsted, P., & Almdal, K. (2013). Preliminary characterization of glass fiber sizing. Proceedings of the Risø International Symposium on Materials Science, 34, 333-340.

Pimenta, S. (2013). Toughness and strength of recycled composites and their virgin precursors, ProQuest Dissertations Publishing.

Robertson, I., Lawson-Wood, K. (2017). Advanced data analysis of evolved gases from TG-IR hyphenation studies of polymers, PerkinElmer, Inc., UK.

Sáez-Rodríguez, E., Yang, L., Thomason, J. (2013). Investigation of strength recovery of recycled heat treated glass fibres through chemical treatments. In: 19th International Conference on Composite Materials, Montreal.

Sándor, M., Nistor, C. L., Szalontai, G., Stoica, R., Nicolae, C. A., Alexandrescu, E., Fazakas, J., Oancea, F. & Donescu, D. (2016). Aminopropyl-Silica Hybrid Particles as Supports for Humic Acids Immobilization, Materials, Vol. 9(1), pp. 34.

Sauer, M., Kühnel, M. (2017). The global CF- and CC-Market 2017, Carbon Composites. www.eucia.eu

Sharma, M., Sharma, H., Gao, S., Mäder, E., Wei, L.Y. & Bijwe, J. (2014). Carbon fiber surfaces and composite interphases, Composites Science and Technology, Vol. 102 pp. 35-50.

Smith, E. A., & Chen, W. (2008). How to prevent the loss of surface functionality derived from aminosilanes. Langmuir: The ACS Journal of Surfaces and Colloids, Vol. 24(21), pp. 12405-12409.

Stoeffler, K., Andjelic, S., Legros, N., Roberge, J. & Schougaard, S.B. (2013). Polyphenylene sulfide (PPS) composites reinforced with recycled carbon fiber, Composites Science and Technology, Vol. 84 pp. 65-71.

Tang, L. & Kardos, J.L. (1997). A review of methods for improving the interfacial adhesion between carbon fiber and polymer matrix, Polymer Composites, Vol. 18(1), pp. 100-113.

Tanoglu, M., Ziaee, S., Mcknight, S., Palmese, G. & Gillespie Jr, J. (2001). Investigation of properties of fiber/matrix interphase formed due to the glass fiber sizings, Journal of Materials Science, Vol. 36(12), pp. 3041-3053.

Thermo Nicolet Corporation (2001). Introduction to Fourier Transform Infrared Spectroscopy [Brochure]. Wisconsin, USA: Author.

Thomason, J. L. (2015). Glass fibre sizing: A review of size formulation patents, 244 pp.

Thomason, J.L., Nagel, U., Yang, L. & Bryce, D. (2019). A study of the thermal degradation of glass fibre sizings at composite processing temperatures, Composites Part A, Vol. 121 pp. 56-63.

Thomason, J.L., Nagel, U., Yang, L. & Sáez, E. (2016). Regenerating the strength of thermally recycled glass fibres using hot sodium hydroxide, Composites Part A, Vol. 87 pp. 220-227.

Thomason, J.L. & Adzima, L.J. (2001). Sizing up the interphase: an insider's guide to the science of sizing, Composites Part A, Vol. 32(3), pp. 313-321.

Wagner, M. (2009). Thermal analysis in practice - application handbook, Mettler Toledo, Schwerzenbach, 327 p.

Witten, E. (2017). The European GRP – market 2017, Industrievereinigung Verstärkte Kunststoffe (AVK). www.eucia.eu

Wong, K.H., Syed Mohammed, D., Pickering, S.J. & Brooks, R. (2012). Effect of coupling agents on reinforcing potential of recycled carbon fibre for polypropylene composite, Composites Science and Technology, Vol. 72(7), pp. 835-844.

Yang, L., Jenkins, P., Liggat, J., Thomason, J.(2015). Strength of thermally conditioned glass fibre degradation, retention and regeneration. In: 20th International Conference on Composite Materials, Copenhagen.

Yip, H.L.H., Pickering, S.J. & Rudd, C.D. (2002). Characterisation of carbon fibres recycled from scrap composites using fluidised bed process, Plastics, Rubber and Composites, Vol. 31(6), pp. 278-282.

Zhang, W. (2014). Modification of carbon fiber / epoxy matrix interphase in a composite material: Design of a self-healing interphase by introducing thermally reversible Diels-Alder adducts, L'Institut National des Sciences Appliquées de Lyon, 210 p.

APPENDIX A: FTIR SPECTRA

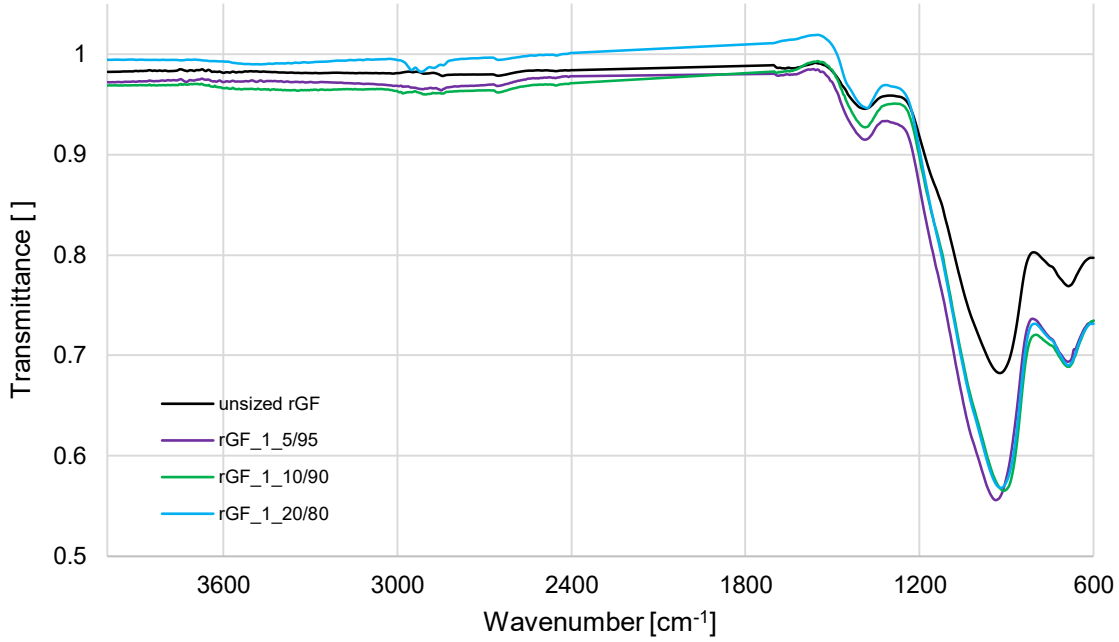

Figure 51. *FTIR spectrum of unsized rGF and rGF samples resized with 1 w% absolute concentration solution.*

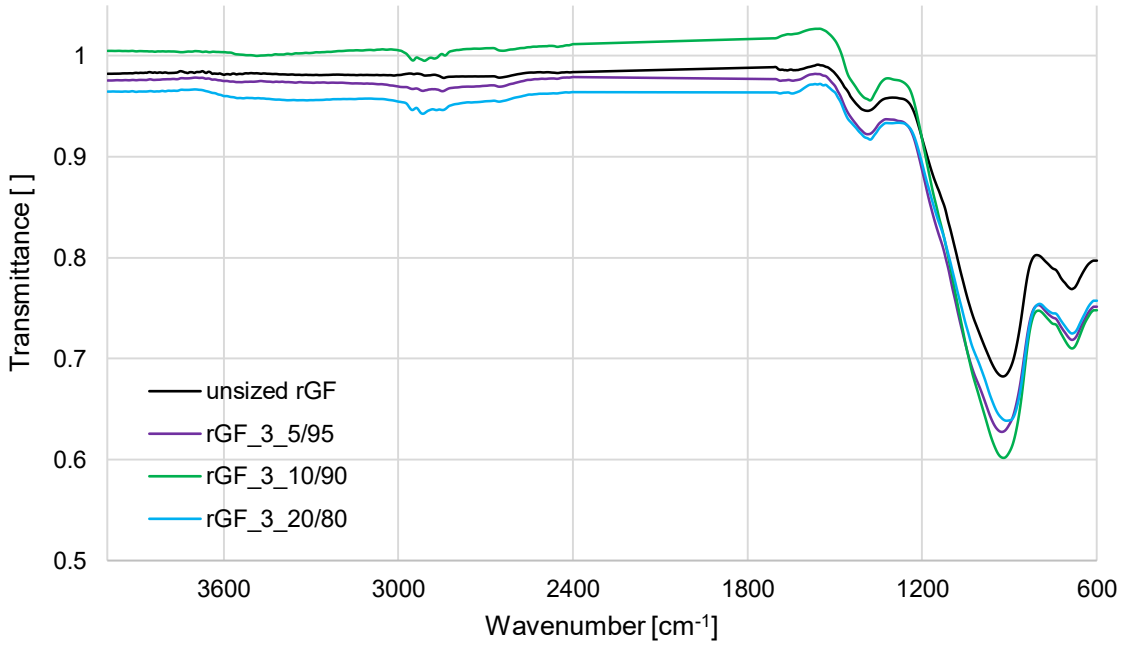

Figure 52. *FTIR spectrum of unsized rGF and rGF samples resized with 3 w% absolution concentration solution.*

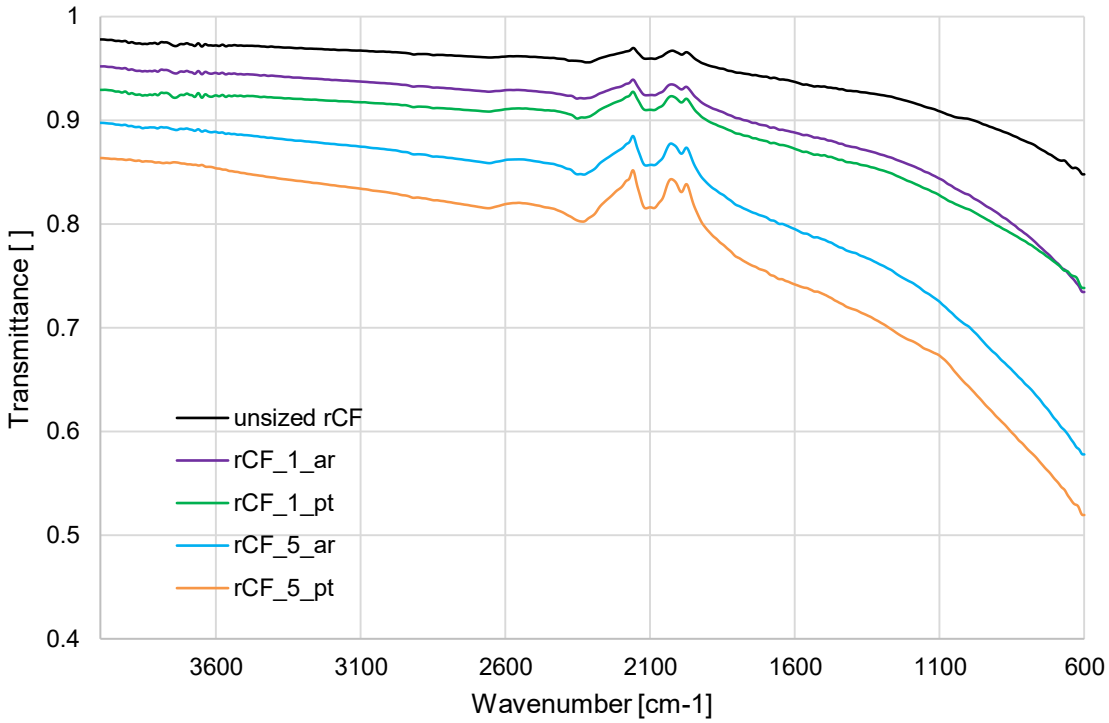

Figure 53. *FTIR-ATR diamond of unsized rCF and resized rCF, indicating that the method was not applicable for rCF.*

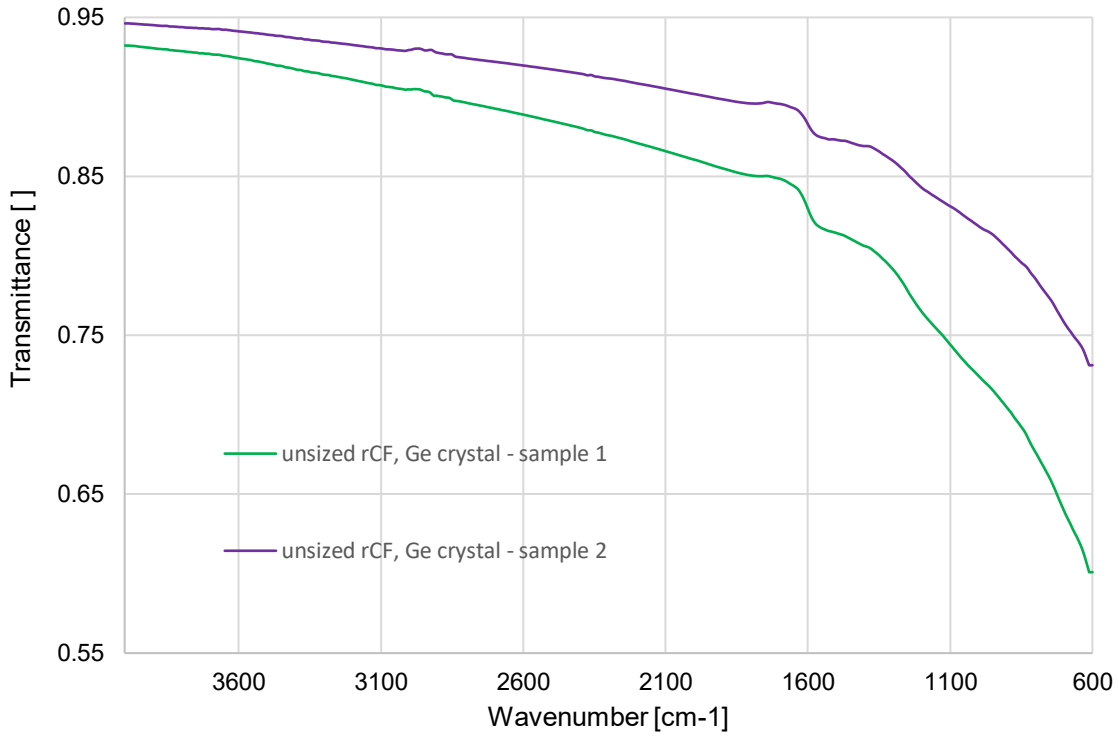

Figure 54. *FTIR-ATR germanium of unsized rCF, indicating that the method was not applicable for rCF.*

APPENDIX B: TGA CURVES OF RESIZED RGF

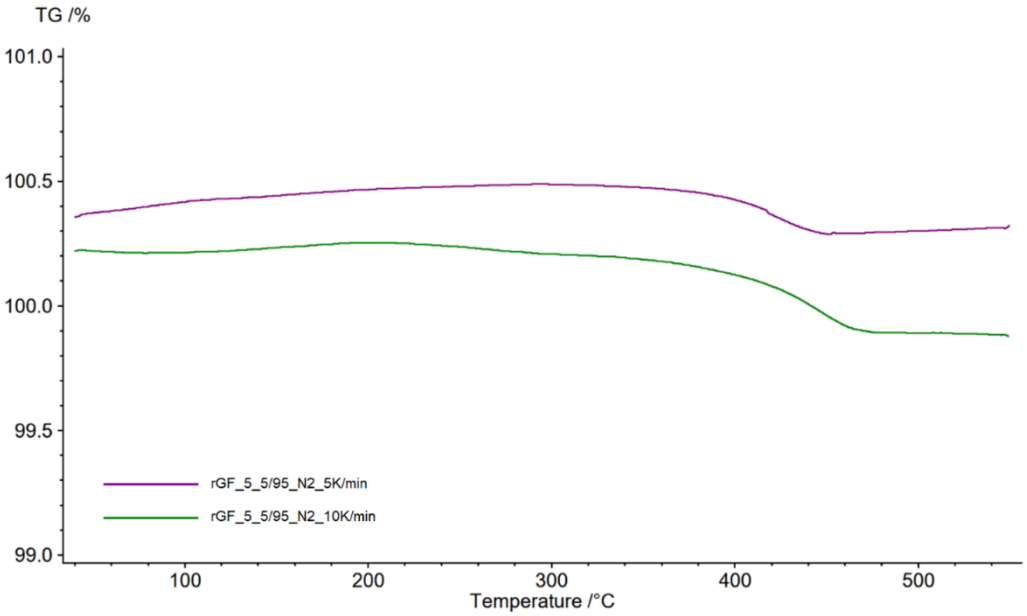

Figure 55. *TGA curves measured at 5 K/min and 10 K/min heating rates under nitrogen atmosphere of rGF samples resized in the 5 w% absolute concertation sizing solution with 5 w% CA and 95 w% FF.*

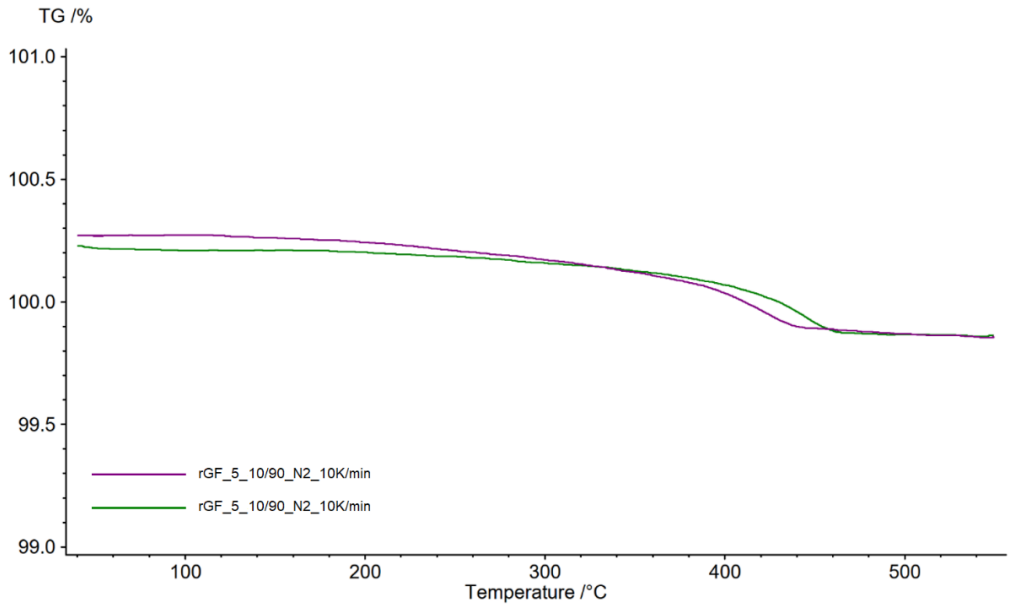

Figure 56. *TGA curves measured at 5 K/min and 10 K/min heating rates under nitrogen atmosphere of rGF samples resized in the 5 w% absolute concertation sizing solution with 10 w% CA and 90 w% FF.*

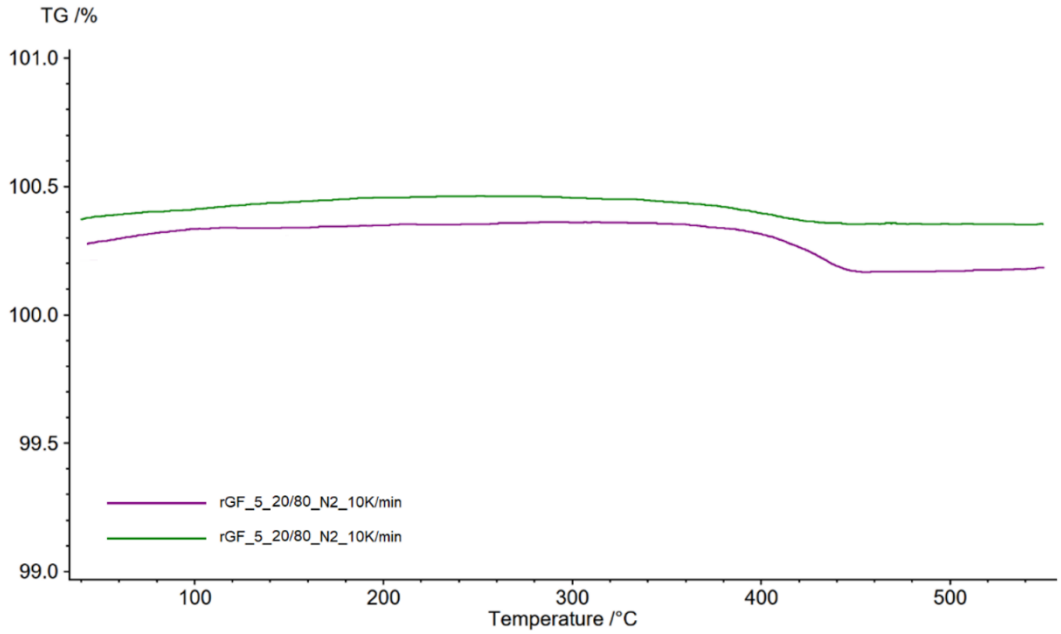

Figure 57. *TGA curves measured at 5 K/min and 10 K/min heating rates under nitrogen atmosphere of rGF samples resized in the 5 w% absolute concertation sizing solution with 20 w% CA and 80 w% FF.*

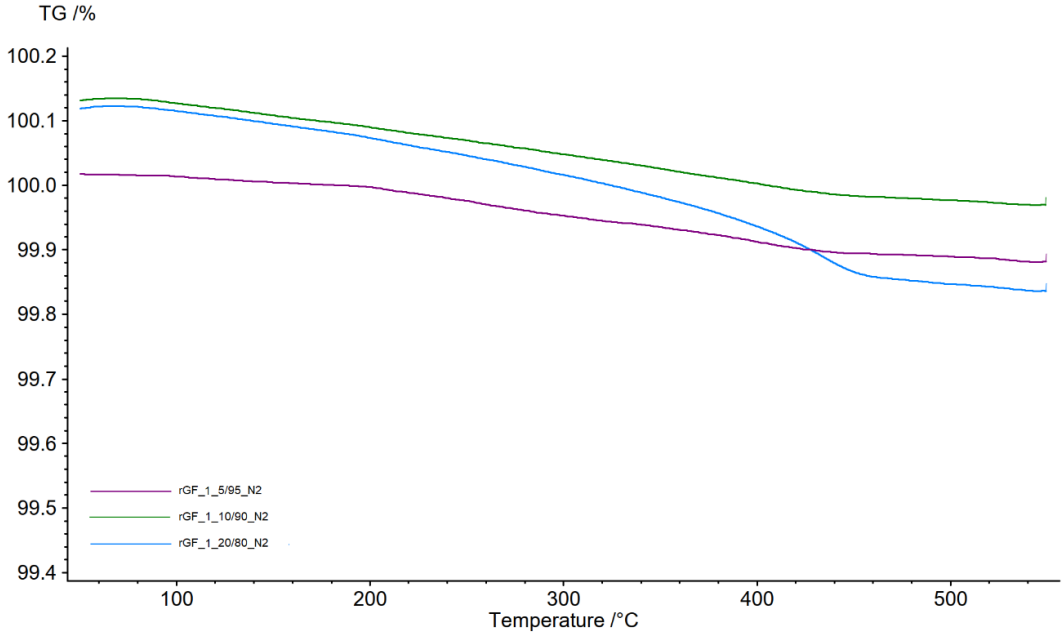

Figure 58. *The TGA curves of rGF samples resized with 1 w% absolute concertation sizing solution measured under nitrogen atmosphere at a heating rate of 10 K/min.*

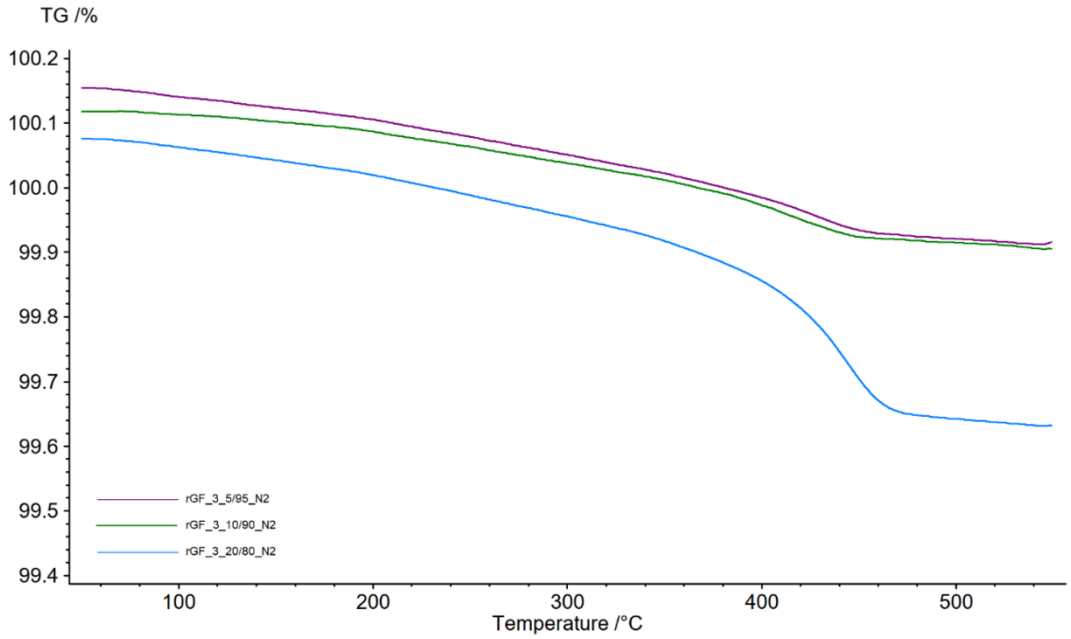

Figure 59. *The TGA curves of rGF samples resized with 3 w% absolute concertation sizing solution measured under nitrogen atmosphere at a heating rate of 10 K/min.*

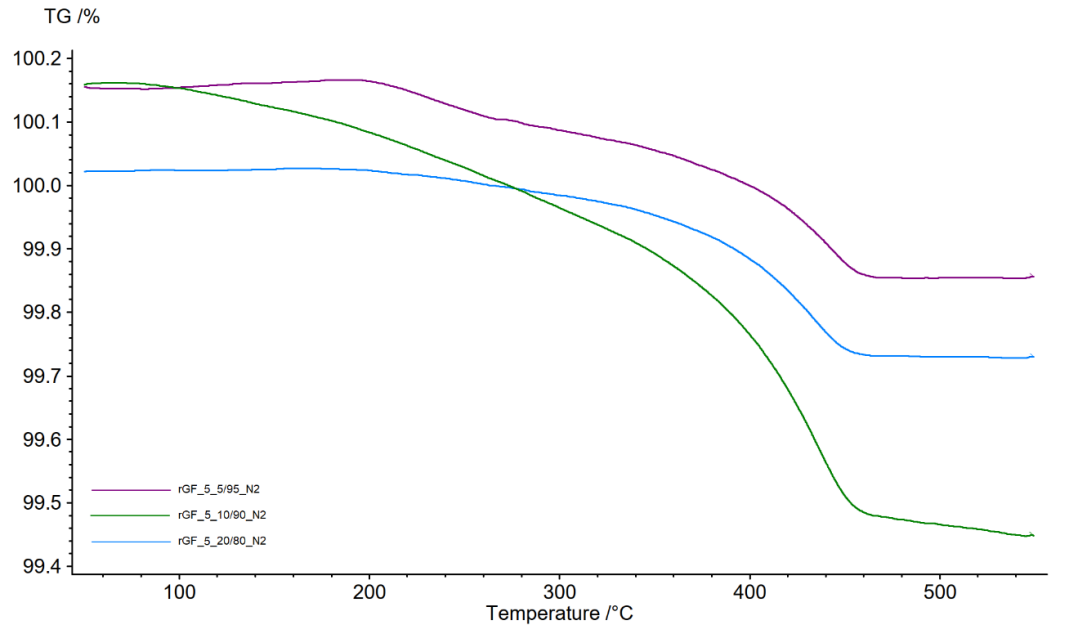

Figure 60. *The TGA curves of rGF samples resized with 5 w% absolute concertation sizing solution measured under nitrogen atmosphere at a heating rate of 10 K/min.*

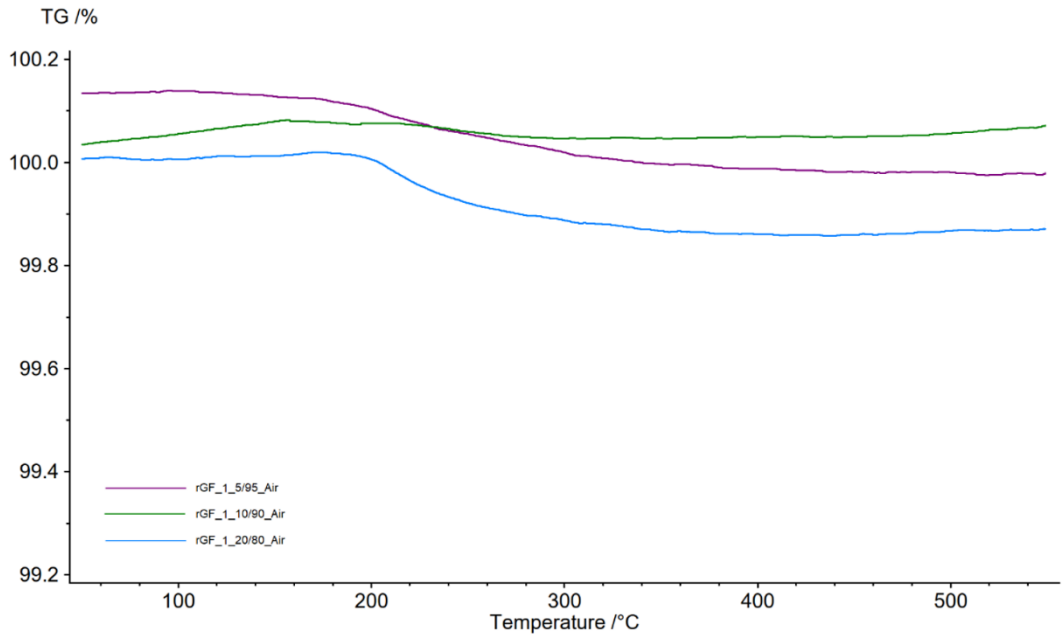

Figure 61. *The TGA curves of rGF samples resized with 1 w% absolute concertation sizing solution measured under synthetic air at a heating rate of 10 K/min.*

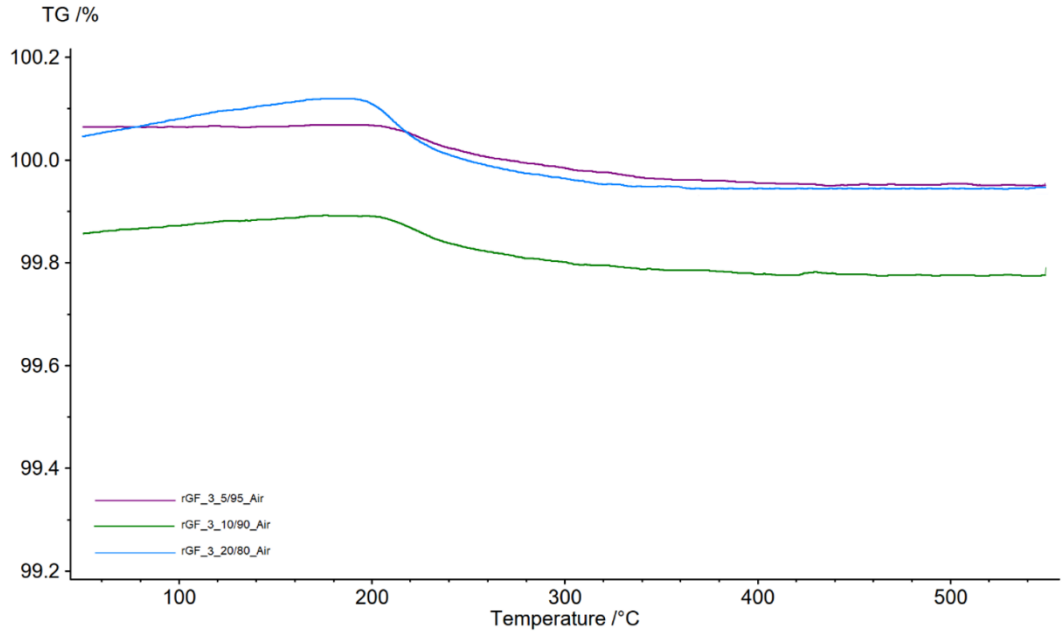

Figure 62. *The TGA curves of rGF samples resized with 3 w% absolute concertation sizing solution measured under synthetic air at a heating rate of 10 K/min.*

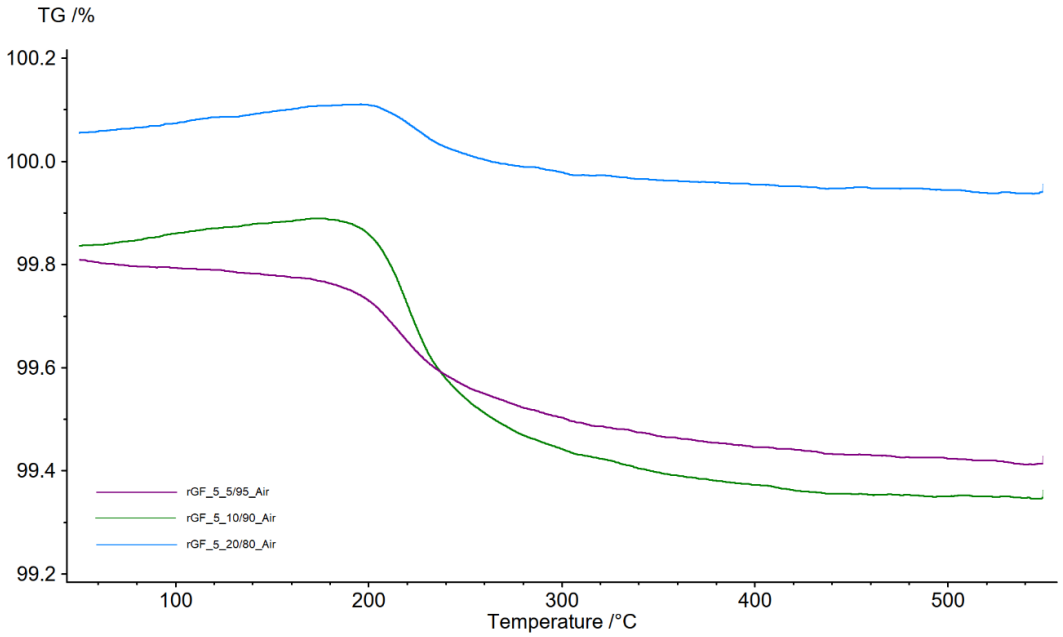

Figure 63. *The TGA curves of rGF samples resized with 5 w% absolute concertation sizing solution measured under synthetic air at a heating rate of 10 K/min.*

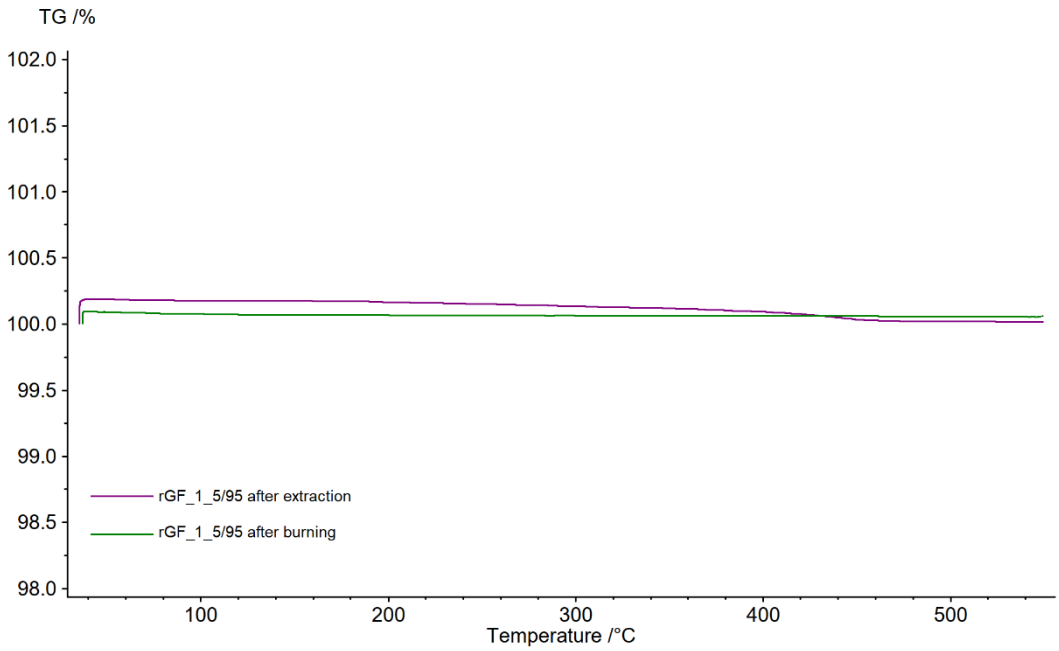

Figure 64. *TGA curves of rGF_1_5/95 after solvent extraction and after burning.*

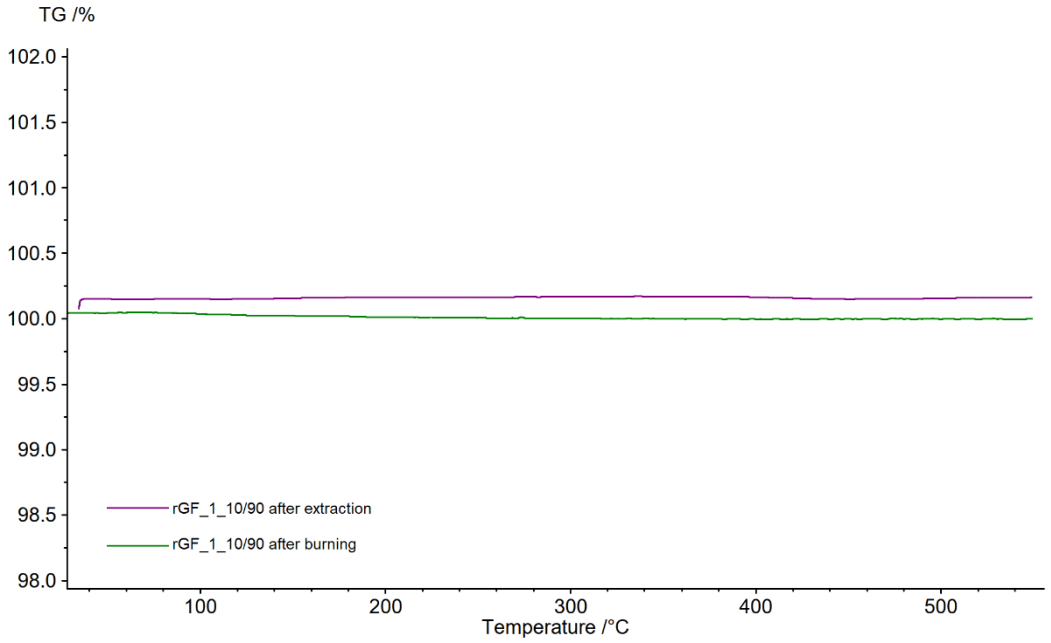

Figure 65. *TGA curves of rGF_1_10/90 after solvent extraction and after burning.*

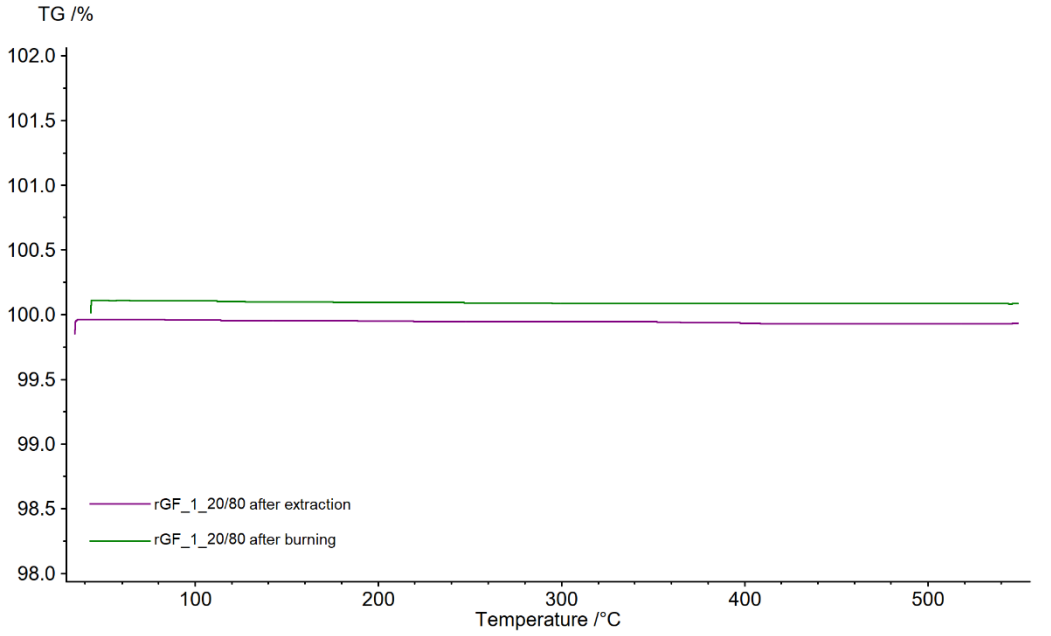

Figure 66. *TGA curves of rGF_1_20/80 after solvent extraction and after burning.*

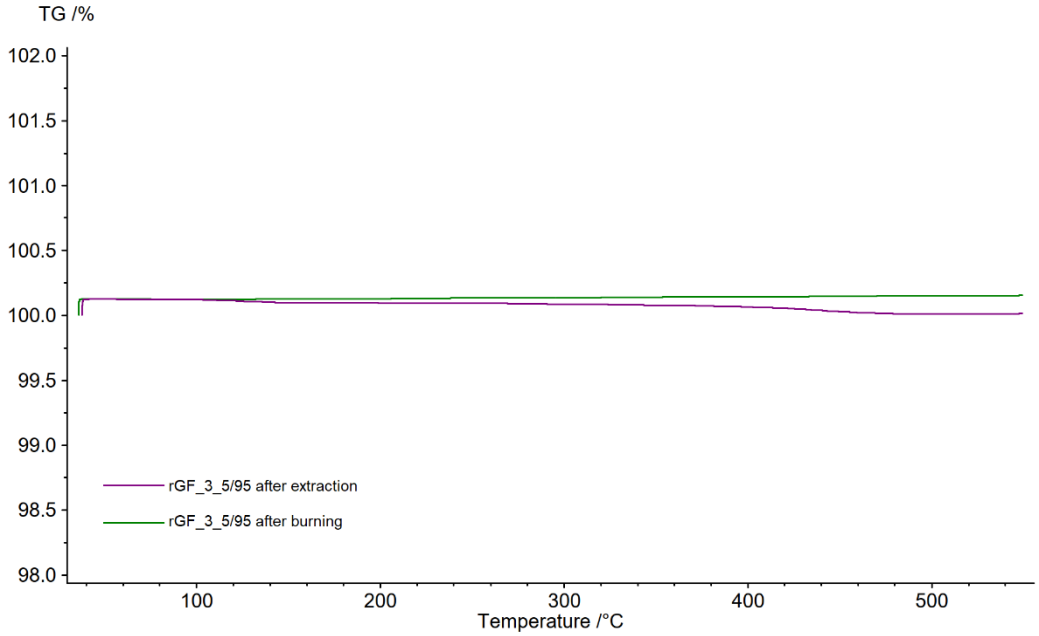

Figure 67. *TGA curves of rGF_3_5/95 after solvent extraction and after burning.*

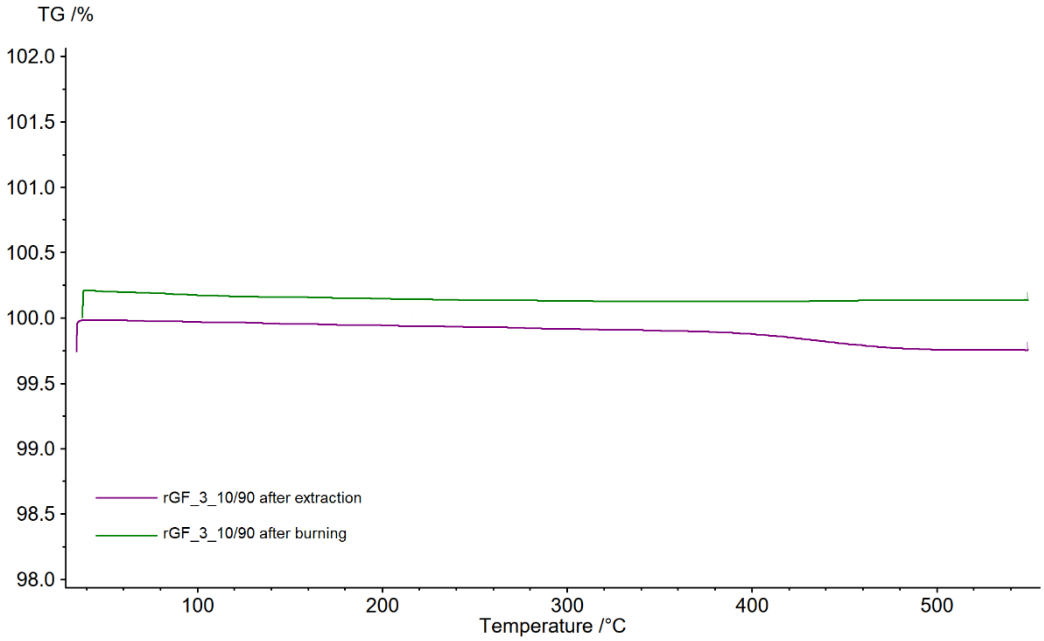

Figure 68. *TGA curves of rGF_3_10/90 after solvent extraction and after burning.*

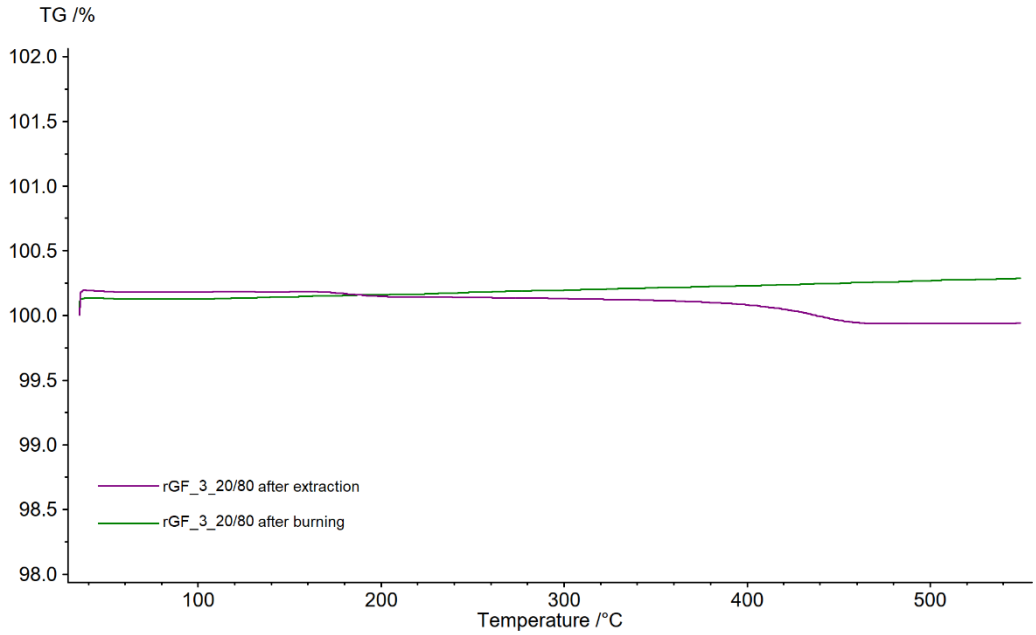

Figure 69. *TGA curves of rGF_3_20/80 after solvent extraction and after burning.*

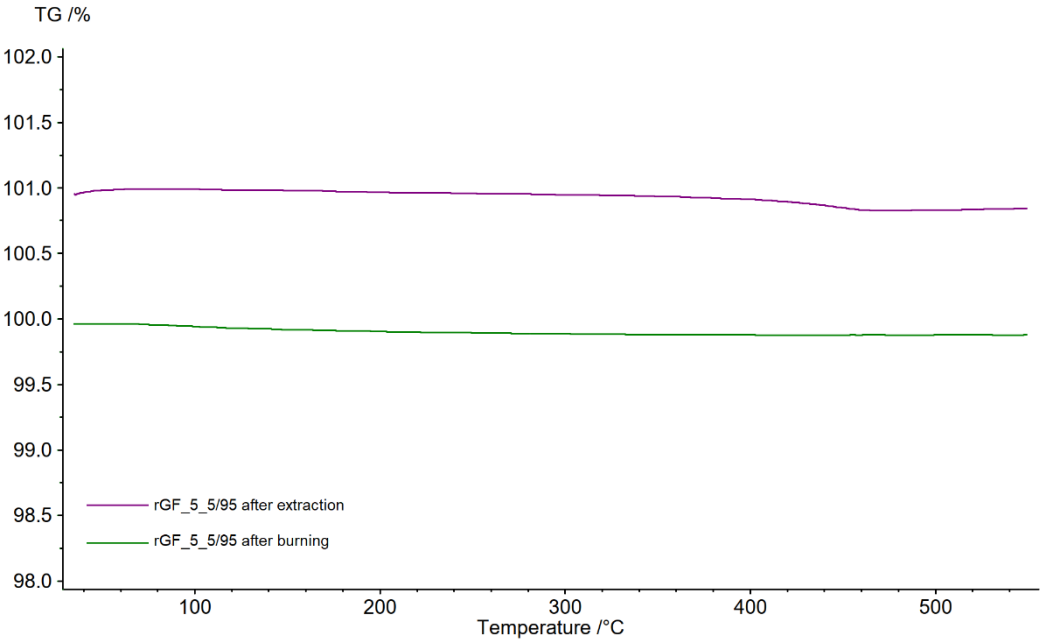

Figure 70. *TGA curves of rGF_5_5/95 after solvent extraction and after burning.*

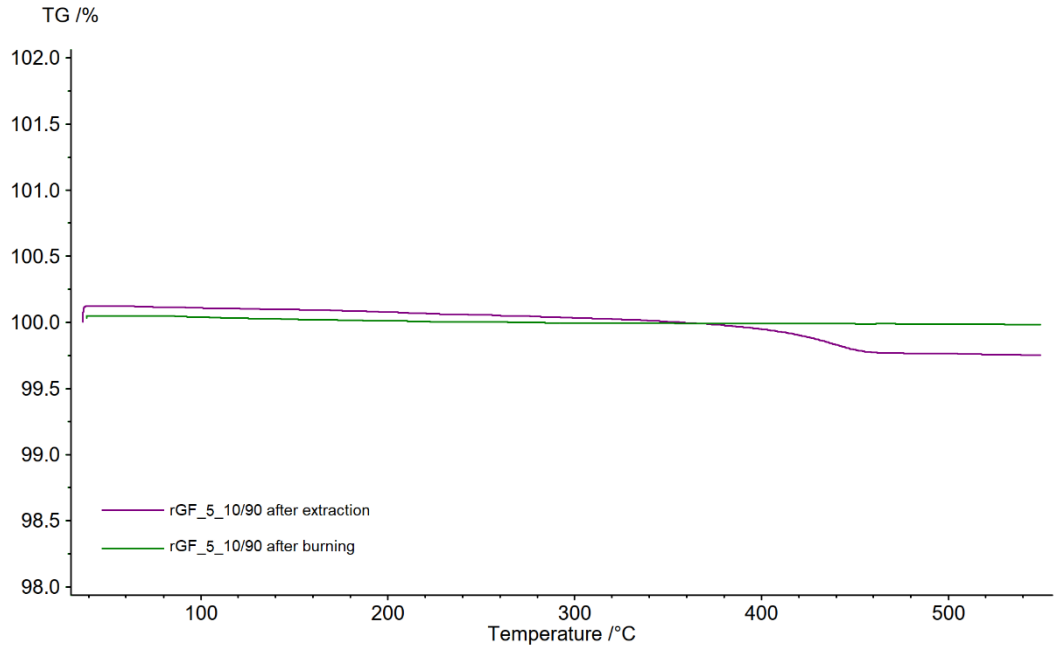

Figure 71. *TGA curves of rGF_5_10/90 after solvent extraction and after burning.*

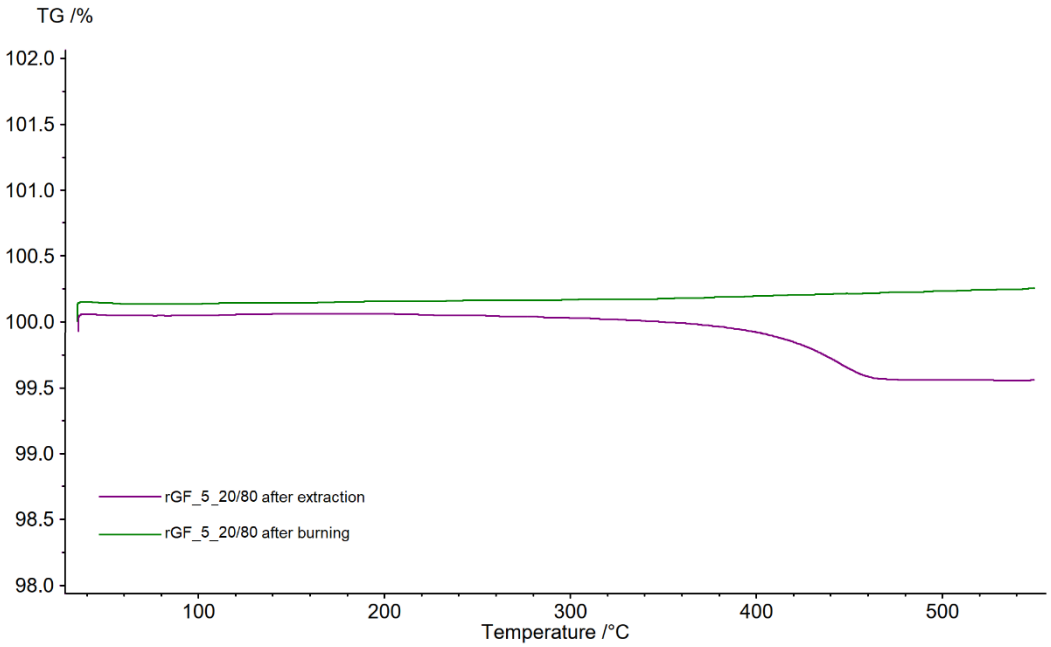

Figure 72. *TGA curves of rGF_5_20/80 after solvent extraction and after burning.*

APPENDIX C: TGA CURVES OF RESIZED RCF

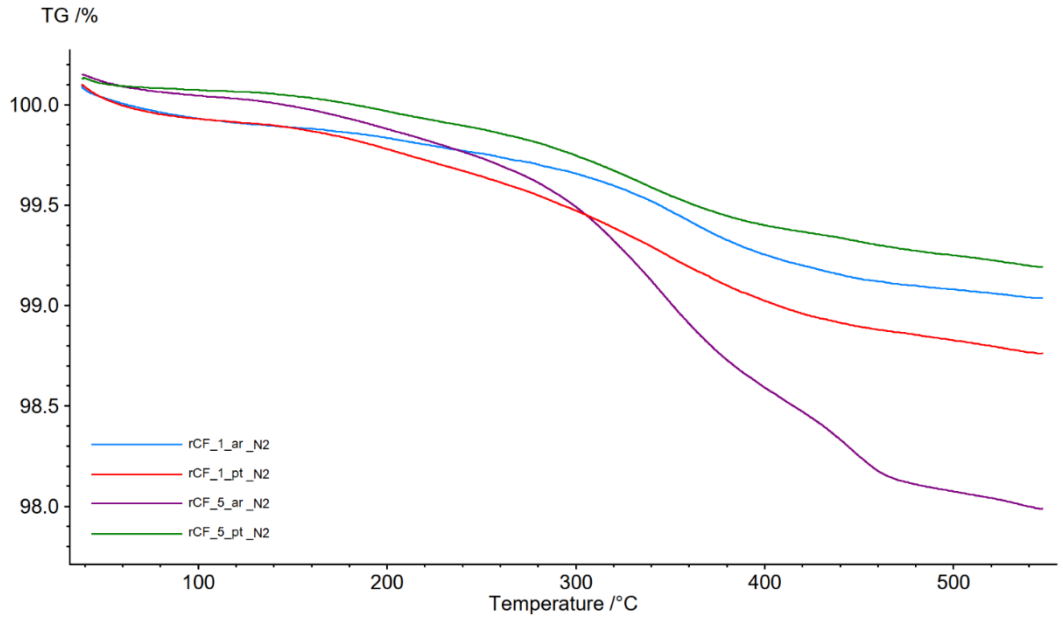

Figure 73. *The TGA curves of all resized rCF samples measured under nitrogen atmosphere at a heating rate of 10 K/min.*

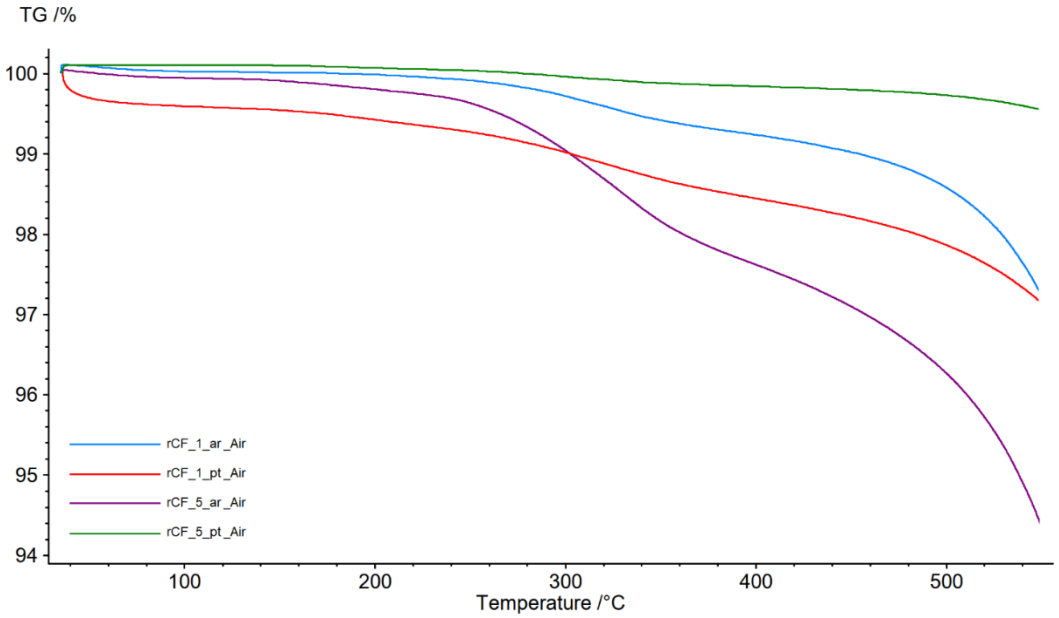

Figure 74. *The TGA curves of all resized rGF samples measured under synthetic air at a heating rate of 10 K/min.*

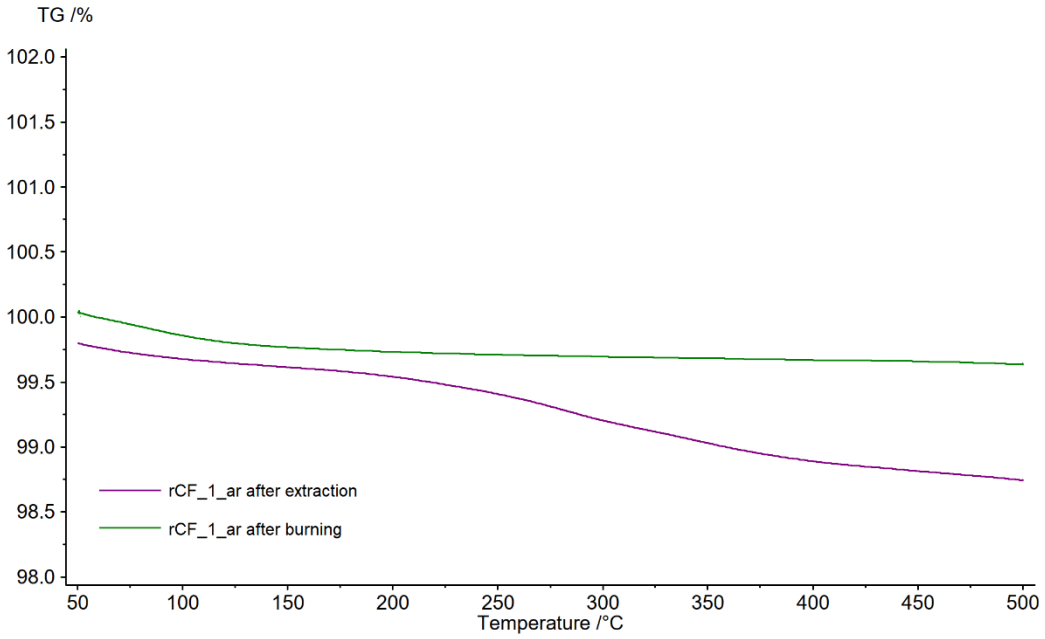

Figure 75. *TGA curves of rCF_1_ar after solvent extraction and after burning.*

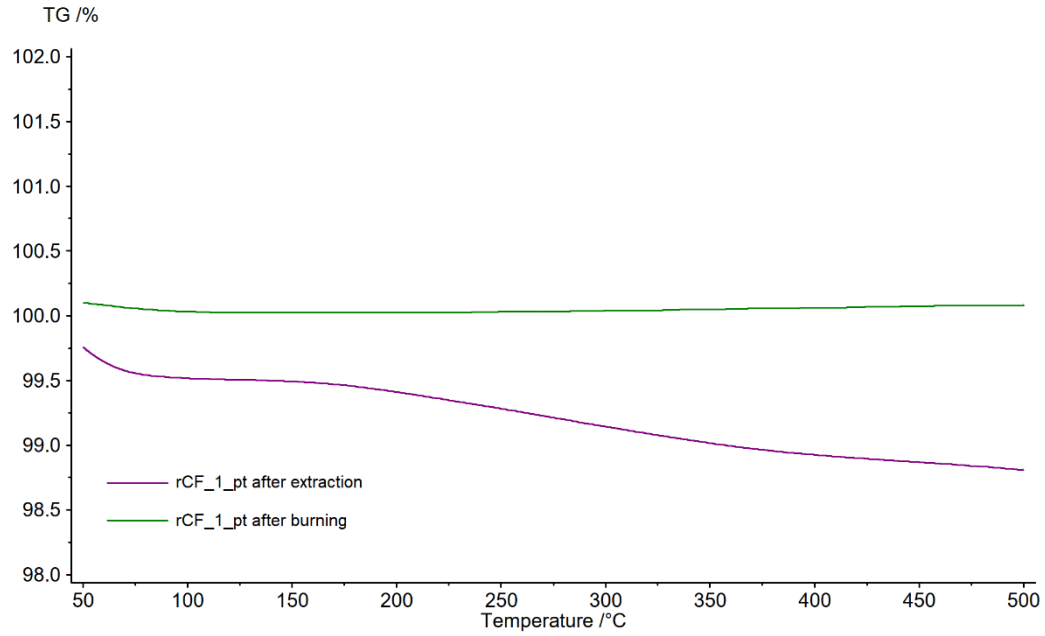

Figure 76. *TGA curves of rCF_1_pt after solvent extraction and after burning.*

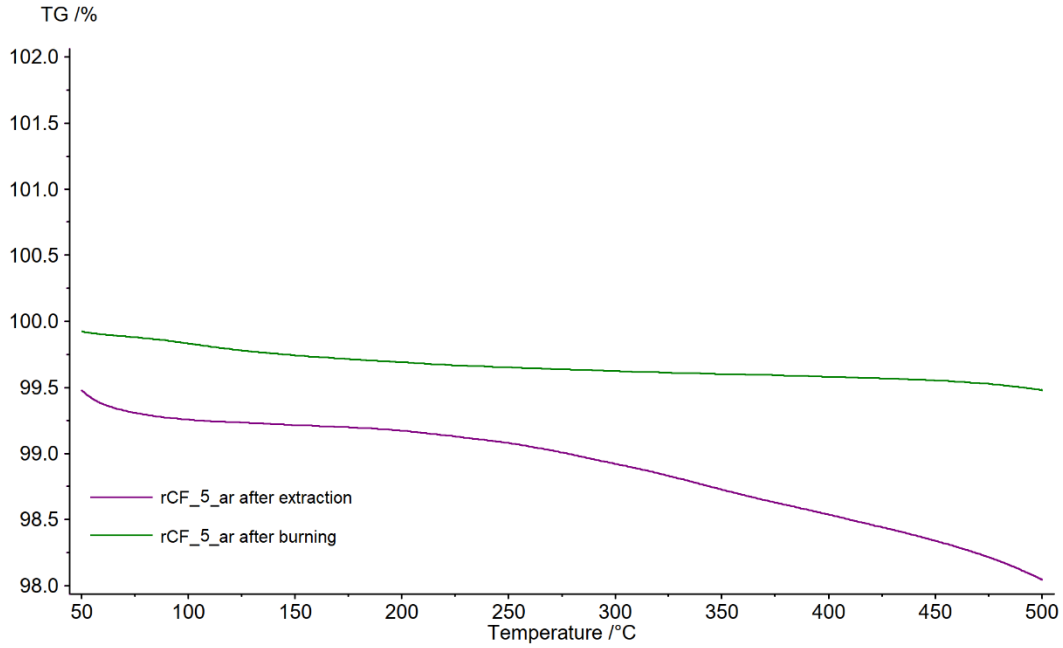

Figure 77. *TGA curves of rCF_5_ar after solvent extraction and after burning.*

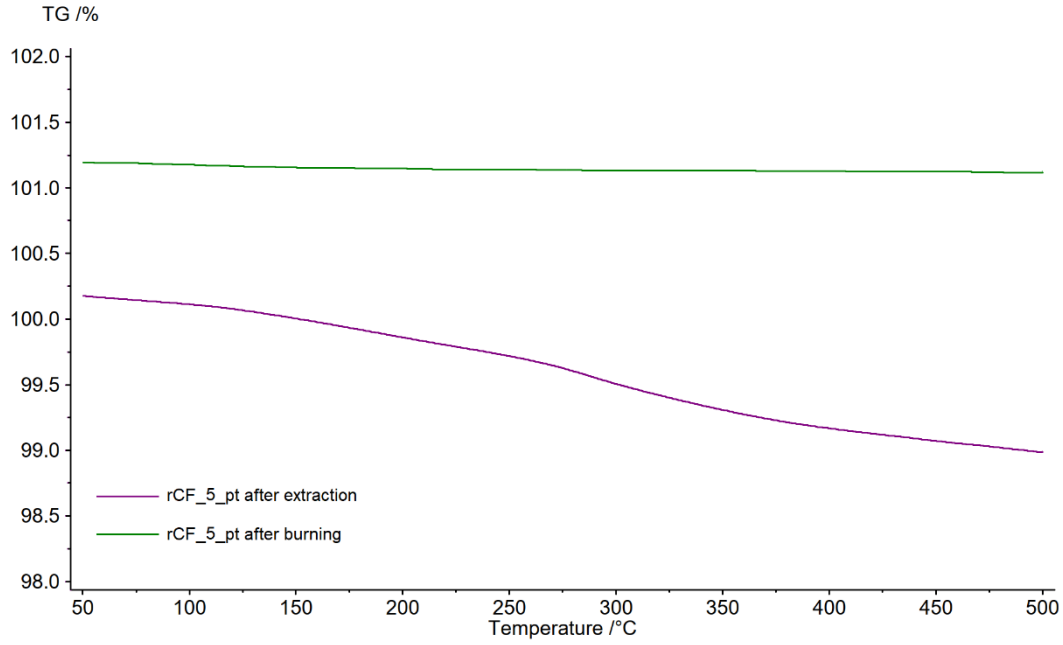

Figure 78. *TGA curves of rCF_5_pt after solvent extraction and after burning.*